Medical Library
610.5
J35352
v.3
no.2

1959 Vol. 3 No. 2

JAPANESE JOURNAL OF OPHTHALMOLOGY

THE UNIVERSITY OF MICHIGAN *
MAY 8 1969
MEDICAL LIBRARY

Contents

An Experimental Study on the Mucocutaneous-Ocular Syndrome: Clinical and Histological Studies on Suppurative Uveitis by Staphylococcus Aureus ..... *Tadashi Kato*

Effects of Vitamin B_2 on Corneal Metabolism ..... *Hidehiro Funatsu*

Studies on Color Vision deu to ERG
Report II On the Progress of Dark Adaptation under Filtered Light Stimuration ..... *Hitohiro Sakanashi*

Absorption of Fatty Soluble Vitamins into the Ocular Melanin .....
Koku Kojima & Katsuyoshi Mizuno

Optical Investigation of Limit of Visual Acuity
Report II ..... *Akira Yamamori*

Studies on Myopia by Estimating Aniseikonia and the Refractive Components of both Eyes ..... *Tomihisa Sugata*

The Periodicity in the Electromyograph of Human Extraocular Muscles ..... *Tetsuya Kuboki*

Development of Lacrimal Apparati in Japanese Fetus ..... *Takayuki Seo*

Studies on the Initial Growth of the Extraocular Muscles of Japanese ..... *Tsuneto Iwasaki*

9

Published by
Department of Ophthalmology School of Medicine
University of Tokyo Hongo Tokyo

UNIVERSITY OF MICHIGAN
MEDICAL LIBRARY

Editorial Board

Hogara HAGIWARA
Shinichi SHIKANO Seiji SUGIURA

Technical Editor

Hisaya TOKUDA

Acta Societatis Ophthalmologicae Japonicae.....Acta O. Jap.

Japanische Monatsschrift für praktische
Augenheilkunde (Ganka Rinsho Iho).....J. M. P. A.

Journal of Clinical Ophthalmology
(Rinsho Ganka).....J. C. O.

Folia Ophthalmologica Japonica.....F. O. J.

Japanese Journal of Ophthalmology is issued four times a year, appearing in February, May, August, and November. ***Subscription price:*** **six dollars per annum, including postage.**

Publication Office
Department of Ophthalmology, School of Medicine, University of Tokyo
Hongo, Tokyo, Japan

Correspondence relating to subscription should be sent to the sole agent, the **MARUZEN Co., LTD P.O. Box 605 Tokyo Central, Tokyo.**

med
med
manuscr
5-6-69
shortage

JAPANESE JOURNAL OF OPHTHALMOLOGY

VOLUME 3. April~June 1959. NUMBER 2.

Contents

An Experimental Study on the Mucocutaneous-Ocular Syndrome:
Clinical and Histological Studies on Suppurative Uveitis
by Staphylococcus Aureus ..... *Tadashi Kato* ... 83

Effect of Vitamin B_2 on Corneal Metabolism ..... *Hidehiro Funatsu* ... 99

Studies on Color Vision deu to ERG
Report II On the Progress of Dark Adaptation under Filtered
Light Stimuration ..... *Hitohiro Sakanashi* ... 111

Absorption of Fatty Soluble Vitamins into the Ocular Melanin .....
Koku Kojima & Katsuyoshi Mizuno ... 117

Optical Investigation of Limit of Visual Acuity
Report II ..... *Akira Yamamori* ... 121

Studies on Myopia by Estimating Aniseikonia and the Refractive
Components of both Eyes ..... *Tomihisa Sugata* ... 142

The Periodicity in the Electromyograph of Human Extraocular
Muscles ..... *Tetsuya Kuboki* ... 148

Development of Lacrimal Apparati in Japanese Fetus ..... *Takayuki Seo* ... 156

Studies on the Initial Growth of the Extraocular Muscles
of Japanese ..... *Tsuneto Iwasaki* ... 161

AN EXPERIMENTAL STUDY ON THE MUCOCUTANEOUS OCULAR SYNDROME: CLINICAL AND HISTOLOGICAL STUDIES ON SUPPURATIVE UVEITIS BY STAPHYLOCOCCUS AUREUS

Tadashi KATO

Department of Ophthalmology, School of Medicine, University of Tokyo

Part I. Discussion on the experimental methods.

Uveitis of Behçet's syndrome had been frequently reported in this country as shown in my previous report. Since H. Behçet, the original reporter of this syndrome, regarded this syndrome as a viral infection, F.N. Sezer, A.D. Evans and Y. Nakagawa reported to have proved the virus. On the other hand, there has deen another theory that this syndrome is a kind of bacterial allerergic reaction. Both of these theories, however, have remained mere supposition. Prior to the experiments to prove the theory of bacterial allergic reaction by means of staphylococcus aureus, the experimental methods are discussed.

Bacterial suspension of staphylococcus aureus. The Terashima strain of staphylococcus aureus cultured on a semisynthetic medium (modified Knight's medium, shown in Table I) was used. Live staphylococcal suspension was obtained from the sediment by 3 times washing with sterile physiological saline at 3000 rpm. for 15 minutes, and then diluted to proper concentrations with the saline. Killed staphylococcal suspension was obtained in a similar way, following heating of the suspension at 90°C for 30 minutes. The pathogenity of the live staphylococcal suspension gained by this way was unexpectedly high and the injection of 0.1 cc. of×10 suspension (above Mc Farland's No. 10) into the tail vein of a 20gr. mouse killed the animal within 24 hours, and by×1000 suspension (Mc Farland's No. 2-3) within 72 hours.

Table 1. Culture Solution for Staphylococcus Aureus

Z. amin	7.0g
Glucose	2.5g
Potassium sulfate, monobasic	4.5g
Sodium citrate	3.0g
Magnesium sulfate	0.04g
Vitamin B_1, hydrochloride	10mg
Nicotinamide	10mg

↓

Add 1 liter of distilled water and warm up to 40–50°C to dissolve.

↓

Adjust pH. at 7.0 with 10% Sodium carbonae.

↓

Divide the solution into 5 beakers.

↓

Sterilize 3 times at 15-minute interval at 100°C.

↓

Place it at 37°C for 48 hours.

Immunization with staphylococcus aureus and measurement of its antibody in rabbits. Immunity caused by staphylococcus aureus have been studied by A. Kihoin, H. Kawamura, K. Kondo and K. Nakamata etc. in our country; and it has been known, that the antibodies

are produced by staphylococcus aureus in rabbits and the immunized rabbits react differently from nonimmunized ones to the reinfection of the same bacteria.

Immunization: Taking after the adjuvant technique of J. Freund, which is widely used in the studies on tuberculous bacilli, 1 cc. of oily suspension with the contents shown in Table 2 was injected into the femoral muscle of rabbits.

Precipitation-Test: Antigen, 0.1% suspension of killed bacilli which were destroyed by high pressure of 20 pounds for 10 minutes keeping it at 37°C for 48 hours, was used. The sera of the immunized rabbits were diluted with 1.5% solution of Gummi arabicum, and the antibody titer was expressed by the maximum dilution which shows positive result.

Tabel 2. Method of Immunization

Killed Staphylococcus aureus
(Terashima) ×10 ..... 10.0 vol.
Paraffinum liquidum ..... 8.5 vol.
Tween 80 ..... 1.5 vol.
0.1% Merzonin ..... 5 drops
↓
stir up completely
↓
keep in dark cold place
↓
warm up to 37°C before use

Results of Immunization in Rabbits with Staphylococcus aureus: Ten healthy white rabbits weighing 1.5-2.0kg., after being confirmed to have a negative antibody by ring-test, were immunized in the above-mentioned technique once every week. The titer of the serum was measured on the 2nd, 4th and 7th day after every injection. The injection after the 2nd was done following the sampling of serum on the 7th day.) The antibody (×1-4 titer) was proved to be produced in 4 rabbits out of 10 on the 4-7th day after 3 injections.

Injection into the vorticous vein. In order to apply the bacterial suspension to the uvea, H. Ulbrich's method of injecting the suspension into the vorticous vein has been used by many investigators. The following method was used in this experiment to avoid unnessesary stimulation by manipulation.

Operation:

Cut long hair around the eye.

Instillation of 0.05% merzonin (Natrium aethylmercurithiosalicylicum).

Washing the eye with 0.05% Hydrargynum oxycyanatum and 2% boric acid.

Instillation of 3% cocaine.

(1) An incision was made on the bulbar conjunctiva 3-5 mm above the upper part of limbs. The detached conjunctiva is pulled upwards by the suture.

(2) The eye ball is rotated downwards by the suture on the insertion of the M. rectus superior.

(3) When the vorticous vein is exposep, the blood stream is stopped by cauterization and the solution or the suspension is injected at the peripheral part of the vein by the syringe with Yaoi's needle for tuberculin test. The punctual hole was cauterized after the injection.

(4) The conjunctiva is sutured back.

Injection of Indian ink: In order to prove the diffusion in the uvea, 0.1 cc. of Indian Ink was injected into the vorticous vein of the rabbit. Immediately after the injection, the root of the iris appeared black and soon the capillaries of the surface of the iris became pigmented. The fundus appeared dark by direct illumination, and no pathological change was observed by biomicroscopy. Five minutes later enucleation of the eyeball was performed. Scattering of the pigment of the Indian Ink was revealed in half the part of the uvea, especially in the ciliary body and neighboring choroid. (Figure 1.)

Injection of sterile normal saline: The clinical and histological findings were examined immediately, 2,4,6 and 8 hours after injecting 0.1 cc. of sterile normal saline into the vorticous veins of the 6 eyes of white rabbits.

Clinical findings: Immediately after the injection of sterile normal saline, in the root of the iris, where injection was given a slight edematous swelling appeared and the pupil became vertically oval and lasted 2 hours. The congestion of this part became more apparent 4-8 hours later with dilated capillaries of the surface of the iris. Sometimes several cells were seen in the anterior chamber.

Histological findings: The histological examination at the 6th and 8th hour (10% formalin fixation, paraffin embedding and hematoxylin-eosin staining) revealed a slight dilatation of the empty vessels on the injected side, and a small spotty hemorrhage on some parts of the ciliary process.

Dissemination of staphylococcus aureus injected in the vorticous vein: Dissemination of staphylococcus aureus injected in the vorticous vein was studied by the following way. Live staphylococcal suspension (0.1 cc. of×10 and×100) was injected in 14 groups of rabbits and the bacilli in the blood stream was examined 1,2,3,4,5,6 and 12 hours after the injection. Blood taken from the ear veins was cultured on media for 24 hours at 37°C. The bacilli were found one hour after the injection of×10 suspension and 3 hours after that of×1000 suspension in the venous blood as shown in Table 3. Thus injected bacilli were disseminated rather quickly after the injection.

Table 3. Results of Blood Culture

Staphylococcus injected \ Hour		1	2	3	4	5	6	12
× 10	+	2	2	2	2	1	1	1
	−	0	1	0	2	0	2	0
× 1000	+	0	0	2	2	1	0	1
	−	2	3	0	2	0	2	1

+··· Cases with bacteria in the blood stream.
−··· Cases without bacteria in the blood stream.

Discussion

It has been known by these experiments, that the injection of the bacterial suspension into the vorticous vein is a reasonable method to produce experimental suppurative uveitis in the rabbits. Compared with tfie injection of the bacilli into the anterior chamber, this method is similar to the course of endogenous uveitis in which bacilli invade the uvea through the vessel. And compared with the injection of bacilli into the carotid artery, this method causes less general influences. It should be considered, however, even in this method, that the bacilli are found in the whole blood stream one hour after the injection in the vorticous vein and the general influences may occur some hours later. On the other hand the tie or cauterization on the vorticous vein at the injection of bacilli may cause a circulatory disturbance of the uvea to some extent. According to A. Nambu, the tie of all 4 vorticous veins caused hyphaema. However in my method only one vorticous vein was cauterized with 3 others remaining free. With the presence of colateral anastomosis, the changes caused by that may be negligible.

Semisynthetic liquified media was used for the culture of staphylococcus aureus in order to avoid the antigenous substances which may be contained in the bacterial suspension. The method like the adjuvant technique used for immunization has many problems, such as increased antibody production or delayed allergy in case of tuberclous bacilli. But this method was used because it is sufficient to inject the oily suspension once a week and it is similar to the immuuization in chronic inflammatory disease due to the slow absorption of antigen.

Part II. Clinical and histological findings on suppurative uveitis

.....The difference between the immunized and nonimmunized groups

The course and finding in suppurative uveitis are modified in general in rabbits which have been immunized beforehand, as proved by S. Shikano and S. Rin by injecting E. coli into the anterior chamber of the rabbits. The modification is considered due to hypersensitivity of the anaphylactic state of A.R. Rich, since S. Shikano observed this also in rabbits which were immunized passively. As to the ocular changes due to staphylococcus aureus, on the other hand, few reports have been presented except S. Rin's and A. Urayama's. For a different purpose, suppurative uveitis has been produced by F. Shimazu, S. Makiuchi and S. Okada etc. by injecting bacilli suspension in the anterior chamber without immunological consideration.

The uveitis in the Behçet's syndrome takes mostly a form of recurrent hypopyon uveitis as to Behçet's description, but in a few cases, appears as serous or fibrinous. However, hypopyon uveitis, serous uveitis and fibrinous uveitis have no essential difference in their nature. Although A.C. Woods pathologically classified uveitis into granulomatous and non-granulomatous, the classification by clinical findings may suggest the clues for understanding the etiology of hypopyon uveitis.

The recurrent hypopyon uveitis was first described by W. Bietisch in 1879 as "In-

termittierendes Hypopyum" depending only upon the macroscopic finding of hypopyon. Biomicroscopically, it may be explained as "exudative uveitis in which only wandering cells are emphasized in the exudate in the anterior chamber" and it is rather similar to "suppurative catarrh" of the mucous membrane. It is different from simple serous inflammation because of the abundant wandering cells and from suppurative inflammation because of lack of other pus components. In hypopyon uveitis, the rapid appearance and disappearance of wandering cells in the anterior chamber suggest that these changes related somehow with antigen-antibody reaction, differing from simple inflammation. A. Urayama produced experimentally the similar ocular changes to hypopyon uveitis by means of antigen-antibody reaction using staphylococcus aureus and concluded these changes were caused by the Arthus' phenomen.

The author has investigated in this experiment on 2 points; (I) whether the rabbits which have been immunized previously with staphylococcus aureus react differently from nonimmunized rabbits to the invasion of the live or killed bacilli into the uvea instead of the infiltrate of staphylococcus aureus, and (2) if the reaction is different, what are the factors to cause these changes. The initial changes were mainly investigated, for the reactions in the later stage may be altered because the injected bacilli soon spread to the whole body and might produce the antibody, and weak antibody in the immunized rabbits might disappear in a short period. Experiments were performed under the conditions clinically similar to endogenous uveitis in the human.

Materials and methods

Materials: non-immunized group……24 healthy white rabbits. immunized group……24 healthy white rabbits immunized by staphylococcus aureus with×1-4 positive titer.

Bacterial suspension: ×10 and×1000 suspension of live and killed staphylococcus aureus.

Injection: intravenous injection of 0.1 cc. of bacterial suspension into the upper vorticous vein.

All these methods were performed according to the previously described way.

Clinical and histological examinations: Accurate macro-and biomicroscopical observations on the ocular changes were made immediately and 2,4,6 and 8 hours after the injection. Subsequent histological examinations were also performed by 10% formalin fixation, paraffin embedding, hematoxylin-eosin and Azan staining, and in case of need, other special stainings after the enucleation of the eyeballs as shown in Table 4.

Results

A) Findings in non-immunized groups

1) ×10 suspension of live bacilli.

Clinical Findings: 2 hours; The pupil contracted slightly and light reflex retarded.

Table 4. Number of Enucleated Eyeballs

Rabbits	Non-immunized				Immunized			
Staphylococcus injected	alive		killed		alive		killed	
	×10	×1000	×10	×1000	×10	×1000	×10	×1000
Hour								
2	1	1	1	1	1	1	1	1
4	1	1	1	1	1	1	1	1
6	1	1	1	1	1	1	1	1
8	3	2	2	2	2	2	2	2
8～	1				2			

In the root zone of the iris where injection was given, a slight edematous swelling and congestion appeared. The capillaries of the surface of the iris especially in the upperside, dilated. No abnormal findings were observed in the cornea, anterior chamber and lens etc.

4 hours; The pupil became mydriatic and its light reaction was lost. The swelling of the iris extended all around and surface markings of the iris were slightly disordered. Dilatation of the capillaries became intensive, appearing like a spider's web, accompanied with small spotty hemorrhages. A few wandering cells were seen in the anterior chamber and some adhered to the cornea and the lens.

6 hours; The swelling, hyperemia and hemorrhage of the iris became more marked and its markings became obscure. In the anterior chamber, prulent exudate, and red blood cells appeared.

8 hours; The turbidity of the anterior chamber, and swelling, hyperemia and turbidity of the iris became aggrevated, forming similar pictures to panophthalmia.

Histological Findings: 2 hours; Hyperemia was observed in the uvea especially in the ciliary process. Some bacilli were stained in the capillaries, which wall appeared normal without infiltration of leucocytes or any other changes.

4 hours; Some leucocytes···all polymorphonuclear···appeared around the capillaries in the uvea and the angle of the anterior chamber. No other development in changes was observed.

6 hours; The leucocytes were wandering to the tissue of the uvea, and conglomerated with bacilli between lamina vasculosa and spacium perichorioideum in the choroid. Hemorrhage was also observed sporadically in the uvea.

8 hours; Leucocytes and fibrin appeared in the anterior chamber and adhered to the surface of the iris near the angle. Many bacilli, polymorphonuclear leucocytes, red blood cells and some histiocytes were seen with fibrin nets in the choroid. In some places, these formed abscesses and projected to the vitreous body. No change of the capillary wall was observed before 8 hours.

2) ×1000 suspension of live bacilli.

Clinical Findings: 2-4 hours; Except an edematous swelling of the iris and dilatations

of the capillaries on the surface of the iris, there was no clinical finding.

6 hours; The swelling of the iris extended all around and its markings were slightly disordered. The capillaries on the surface of the iris dilated, and, in some cases, bled to the anterior chamber. In the anterior chamber of the rabbits without bleeding, cells were observed, which circulated slowly and did not adhere to the cornea or the lens.

8 hours; Swelling and capillary dilatation of the iris was more intensive. The anterior chamber became turbid with wandering cells, including red blood cells and fibrinous exudate.

Histological Findings: 6-8 hours; Polymorphonuclear leucocytes appeared in the uvea including the angle of the anterior chamber, and had a tendency to conglomerate in the choroid. Hemorrhage was also observed in the ciliary process. Fibrinous exudate with polymorphonuclear leucocytes adhered to the surface of the iris.

3) ×10 suspension of killed bacilli.

Clinical Findings: 2-4 hours; Swelling, congestion and capillary dilatation of the iris appeared. Cells were observed in the anterior chamber in about half of the cases.

6 hours; The anterior chambers of the rabbits in which cells appeared already, were turbid with increased cells, red blood cells and fibrinous exudate, and the markings of the iris became disordered. In the anterior chamber of the rest of the rabbits, the cells were seen at this stage.

8 hours; Swelling and hyperemia of the iris extended to some degree, but were not so apparent as the group injected×10 suspension of live bacilli.

Histological Findings: 2 hours; No pathological finding was observed except spotty hemorrhage in the ciliary process.

4-6 hours; The hemorrhage and infiltration of polymorphonuclear leucocytes were seen in the uvea including the angle of the anterior chamber. The polymorphonuclear leucocytes formed a conglomeration in the choroid.

8 hours; The number of the leucocytes increased.

4) ×1000 suspension of killed bacilli.

Clinical Findings: 2-4 hours; No pathological change was observed except capillary dilatation on the surface of the iris.

6-8 hours: The capillary dilatation extended to a higher degree and formed hemorrhagic spots in places. Only few wandering cells and red blood cells appeared in the anterior chamber.

Histological Findings: 6 hours; The hemorrhage and infiltration of polymorphonuclear leucocyces were seen around the vessels of the uvea.

8 hours; The cellular infiltration slightly increased and showed a tendency to form absesses in the choroid.

B) Findings in immunized groups

1) ×10 suspension of live bacilli.

Clinical Findings: 2 hours; The pupil contracted slightly and light reaction retarded. In the upper root zone of the iris, edematous swelling and congestion appeared and capi-

llary dilatation was slightly observed. A few cells were circulating already in the anterior chamber.

4 hours; The edema of the iris became aggrevated. Although capillary dilatation on the surface of the iris was not so intensive, some spotty hemorrhage appeared. The rapidly circulating cells appeared in the anterior chamber of all rabbits.

6 hours; Findings in the anterior chamber were able to be classfied into two types. 1) The speed of the circulation of the wandering cells became slow due to increase of thin fibrinous exudate. 2) The anterior chamber was turbid with purulent exudate, and red blood cells. However, disorder of the markings of the iris and the capillary dilatation were relatively slight in these cases.

8 hours; The fibrinous exudate filled up the anterior chamber of the rabbits which showed the findings of type one above. The cells were seen among the fibrin and the iris was observed obscurely. On the other hand, the turbidity due to suppuration of the anterior chamber of the rabbits which showed the findings of type two, was as much as that of the non-immunized rabbits.

Histological Findings: 2 hours; The bacilli were seen conglomerated in the capillaries. Already polymorphonuclear leucocytes appeared in the uvea and hyalin-like exudate which was homogenously stained by eosin was observed around the angle of the anterior chamber.

4 hours: The adventitia of the capillaries of the uvea swollen edematously with the findings of the so-called hyalin-thrombus were observed. In the uvea, leucocytes increased and spotty hemorrhage was also observed.

6-8 hours: The bacilli, polymorphonuclear leucocytes, red blood cells and exudate conglomerated in the choroid of the rabbits which showed clinically type one. The fibrinous exudate including the leucocytes adhered to the iris. In the choroid of the rabbits which showed clinically type two, the tissue was thick, and many bacilli, leucocytes, destroyed leucocytes and red blood cells formed abscesses.

2) $\times 1000$ suspension of live bacilli.

Clinical Findings: 2 hours; A few cells were observed in the anterior chamber as in the cases injected with the $\times 10$ suspension of live bacilli.

4 hours; The wandering cells which circulated rapidly appeared in the anterior chamber of all rabbits. The swelling of the iris and its vascular dilatation were both slighter than those of the control group.

6-8 hours; The cells in the anterior chamber increased but their circulatory speed became slower. A little fibrinous exudate appeared in some cases. The markings of the iris was not disordered. Hyphema was seen in one case.

Histological Findings: 2 hours: The conglomeration of the bacilli in the capillaries was observed. The hemorrhage in the cillary processes and infiltration of polymorphonuclear leucocytes toward the choroid were seen.

4 hours; The hyalin-like exudate appeared in the angle of the anterior chamber, and

the leucocytes increased in the uvea accompanied by thin fibrinous exudate in the spatium perichorioideum.

6-8 hours; Capillary adventitia swelled edematously. The thin fibrinous exudate with leucocyte adhered to the iris. The large hemorrhage was seen sporadically in the iris, ciliary processes and choroid.

3) ×10 suspension of killed bacilli.

Clinical Findings: 2 hours: The swelling of the upper part of the iris appeared, but the vascular dilatation was almost absent. A few cells were seen in the anterior chamber of 2 rabbits.

4 hours; Many wandering cells circulated rapidly in the anterior chamber, and the iris swelled edematously. The markings of the iris were not disordered. The spotty hemorrhage without vascular dilatation on the surface of the iris was observed in one rabbit.

6-8 hours; The findings of the anterior chamber was not aggrevated except the appearance of the thin fibrinous exudate in some cases. The anterior chamber of tne rabbit which had a hemorrhagic tendency became shallow and hyphema was observed.

Histological Findings: 2 hours; The hyalin-like exudation and a few leucocytes appeared around the angle of the anterior chamber. The polymorphonuclear leucocytes were also observed around the capillaries of the choroid.

4 hours; The number of the leucocytes increased in the uvea and the capillaries slightly swelled edematously.

6 hours; In addition to the previous findings, the hyalin-like exudate was observed in the capillary.

8 hours; The thin fibrinous exudate adhered to the iris accompanied by leucocytes, The spotty abscesses and hemorrhage were observed in the choroid. A few histiocytes appeared.

4) ×1000 suspension of killed bacilli.

Clinical Findings: 4 hours; A few cells circulated in the anterior chamber in some cases.

6 hours; The wandering cells increased without fibrin exudation and the red blood cells appeared in some cases. The vascular dilatation was absent.

8 hours; A little fibrinous exudate accompanied with wandering cells appeared in the anterior chamber, but the changes of the iris were not marked.

Histological Findings: 2-4 hours; The conglomeration of the bacilli in the capillaries of the uvea, and homogenous hyalin-like exudation around the angle of the anterior chamber were observed. The polymorphonuclear leucocytes appeared already in the ciliary bodies and choroid.

6-8 hours; Adventitia of the capillaries swelled slightly and the spotty hemorrhage was observed in the stroma of the iris. The polymorphonuclear leucocytes had a tendency to conglomerate and form the abscess.

Discussion

Summarizing these clinical and histological findings; the initial symptom was the congestion in the root zone of the iris 2 hours after the injection of the thick suspension of the live staphylococcus aureus into the vorticous vein of the non-immunized rabbits. The picture of purulent inflammation of the iris···the swelling, disordered markings and dilatation and hemorrhage of the capillaries···appeared 4 hours later. Then purulent or hemopurulent exudation appeared in the anterior chamber and developed into the findings suggestive of panophthalmia the 8 hours later.

Histological examinations revealed that the leucocytes reacted 4-6 hours after the injection, at first around the capillaries, then into the tissue of the uvea. In the choroid, chiefly between the lamina vasculosa and the spatium perichorioideum the leucocytes which caught the bacilli formed abscesses with exudate etc. In general, the leucocytes in the iris and ciliary body had a tendency to spread into the tissue, while those in the choroid had a tendency to conglomerate and form abscess. Different distribution of the bacilli may be another cause to produce this difference in the attitude of leucocytes. The hemorrhage was intense in the ciliary processes.

When the diluted suspension of the live bacilli was given, the congestion in the root zone of the iris appeared also 2 hours after the injection, but the purulent inflammation, which did not differ essentially from the former, was delayed and began at 6-8 hours in most of the cases. When the suspension of the killed bacilli was given, no development of the inflammation was observed 6-8 hours after the injection. It is considered, that difference was due to the fact, that live bacilli, provoking more intense tissue reaction by multipling than the killed bacilli do not provoke. On the other hand, when the thick suspension of the live bacilli was injected in the vorticous vein of the rabbits previously immunized, the reaction of the tissues were observed within 2 hours, The wandering cells appeared in the anterior chamber, and the infiltrations of the polymorphonuclear leucocytes into the uvea were proved histologically. After 6 hours, fibrinous exudation was clinically and histologically observed. The swellings and the vascular dilatation were slighter and more edematous compaired with those of the nonimmunized groups. Around the 8th hour the findings of the purulent inflammations developed, forming the panophthalmia-like findings in a few cases. The spotty hemorrhage on the iris or the red blood cells in the anterior chamber was observed in spite of slight vascular dilatation on the surface of the iris. This hemorrhagic tendency might be due to increased permeability of the capillary wall.

Histological examinations revealed still more specific findings. The bacilli conglomerated together in the capillaries or adhered to the intima of the capillaries 2 hours after the injection. The hyalin-like exudate which homogenously stained with eosin was seen around the angle of the anterior chamber or in the tissue of the uvea around the 4th hour. The adventitia of the capillaries swelled edematously, with findings of hyalin-thrombus 4 hours later. From 6-8 hours after the injection many polymorphonuclear leucocytes appeared

and conglomerated, forming abscesses around which a few histiocytes were observed. The above mentioned findings were observed with a similar course in all cases regardless of the concentration of the suspension or the vitality of the bacilli. Wandering cells circulated rapidly, increasing in their number without inflammatory changes of the iris were observed in the anterior chamber of the rabbits, injected with the suspension of killed bacilli, followed with the fibrinous exudation 6-8 hours after the injection. It is interesting, that the findings were similar to those of the hypopyon iritis.

The differences in the clinical and histological findings between the immunized and non-immunized rabbits were……in immunized groups, (1) appearance of the wandering cells in the anterior chamber began sooner. (2) The fiindings of the purulent inflammation in the anterior chamber and the iris of the immunized rabbits were certainly slighter. In the anterior chamber of the immunized rabbits, only wandering cells were the picture of inflammation before the appearance of the fibrinous exudation, while the anterior chamber of the non-immunized rabbits showed purulent turbidity from the early stage. In the immunized groups, the disorder of the iris and its vascular dilatation was also slighter than those of non-immunized groups. (3) The hemorrhagic tendency of the capillaries of the immunized rabbits was more marked. Moreover, histological examinations revealed: (4) The injected bacilli had a tendency to conglomerate with each other in the capillaries of the immunized rabbits. (5) The adventitia of the capillaries in the immunized groups slightly swelled edematously. (6) Hyalin-like exudate was observed around the angle of the anterior chamber and in the tissue of the uvea of the immunized rabbits.

These differences in the findings remind us of the Arthus' phenomenon. Since found by M. Arthus in 1903, this phenomenon has been studied well as an antigen-antibody reaction manifested in the tissue. The essential differences in the tissue reaction in the ordinary inflammatory changes and in the Arthus' phenomenon have been discussed frequently. Recently Arthus' phenomenon has been treated as a localized anaphylaxis which is characterized by the changes in the mesenchymal tissues, mainly of the vessels. In the initial stage, hemostasis, hemorrhage, edema, transudation, polymorphonuclear leucocyte infiltration, swelling of the vascular wall, softening and sometimes, fibrinous thrombosis are seen. Granuloma formation and cicatrization occur subsequently, These changes may be produced by intravascular injection of antigen as well as by the original intradermal method. In my experiment, the changes occured by injection of bacilli suspension into the vorticous vein. Therefore, they are not the classical Arthus' phenomenon, but belong to the "simple Arthus' phenomenon" of A. Okabayashi. Similarly, K. Takahashi produced uveitis by the injection into the vorticous vein of horse serum and concluded, that the changes had allergic properties suggestive of the Arthus' phenomenon.

Pictures similar to the characteristic "recurrent hypopyon iritis" were observed in both immunized and non-immunized groups. They were seen in the very short period before the appearance of suppurative exudate in the anterior chamber in the non-immunized groups, while they lasted for a comparatively long time in the immunized groups. Especially, when

the killed bacilli were injected, wandering cells alone occupied the anterior chamber in 4-6 hours before the fibrinous exudation. The significantly rapid appearance of the clinical and histological changes in the immunized groups, compared with that in the non-immunized groups, suggests that the changes are the allergic reaction similar to the Arthus' phenomenon, rather than the bacterial type reaction which is characterized with slow onset and cellular degeneration and necrosis. It is also of interest, that the injection of the bacterial suspension from semi-synthetic liquid media caused the allergic reaction suggestive of Arthus' phenomenon. Moreover, the mode of immunization was made similar to chronic focal infection. Intravenous injection of bacilli suspension used in this experiment presents thc possibility that a similar reaction may be caused by the antigen reaching endogenously to the eye region. T. Ogatas observed that the serum precipitin titer and the degree of the tissue changes in the Arthus' phenomenon were in parallel relation. Accordingly, it is suggested, that the immunization and low antibody titer may be one of the factors which produce reversible mild tissue changes similar to the initial findings of hypopyon iritis.

Conclusion

1. Clinical and histological findings and courses of suppurative inflammation of the uvea were studied. In the rabbit which had been previously immunized with staphylococcus aureus, those findings and courses were modified as compared with those in the control group.

2. The difference seems to be due to Arthus' type of hypersensitivity of the immunized rabbits,

3. On this basis, etiology of recurrent hypopyon iritis, which is considered as the main ophthalmological manifestation of the Behçets' syndrome, was discussed.

(Published in Acta Ophth. Jap. 62: 1176, 1958 in Japanese.)

Fig. 1. Injection of Indian Ink into tne vorticous vein.

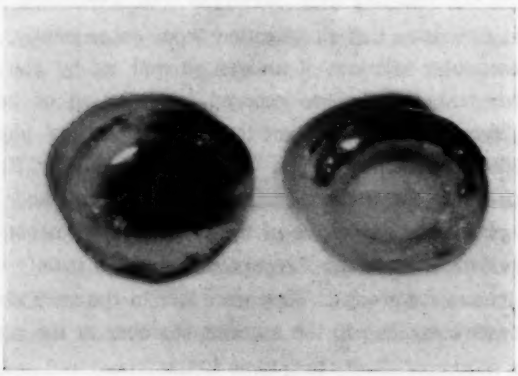

Fig. 2. Fibrinous exudate on the surface of the iris. (×10 suspension of killed bacilli, 8 hours later, in immunized rabbit.)

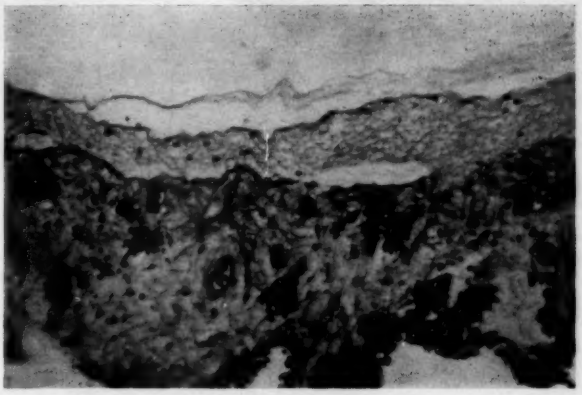

Fig. 3. Polymorphonuclear lueccoyte infiltration into the choroid. (×10 suspension of live bacilli, 8 hours later, in non-immunized rabbit.)

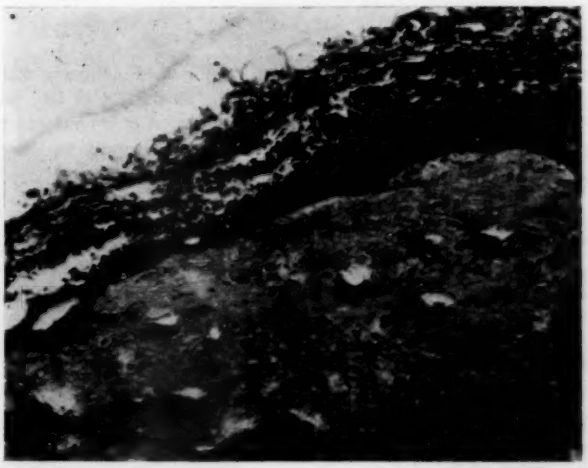

Fig. 4. High magnification of Fig. 3.

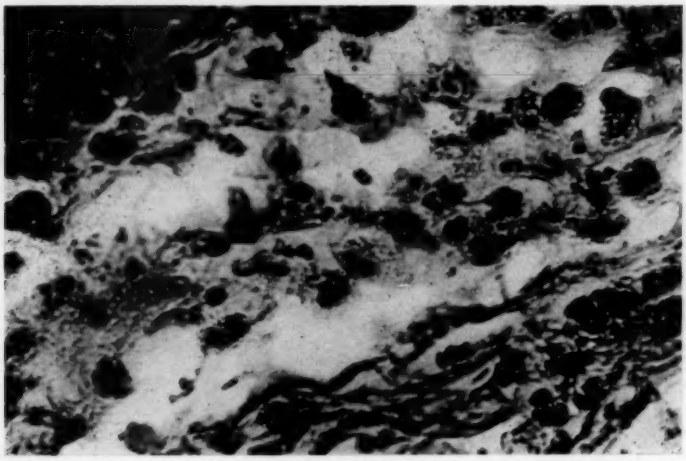

Fig. 5. Findings of the iris. (×1000 suspension of live bacilli, 6 hours later, in non-immunized rabbit).

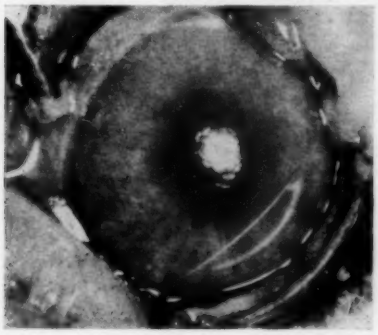

Fig. 6. Findings of the iris. (×1000 suspension of live bacilli, 6 hours later, in immunized rabbit.)

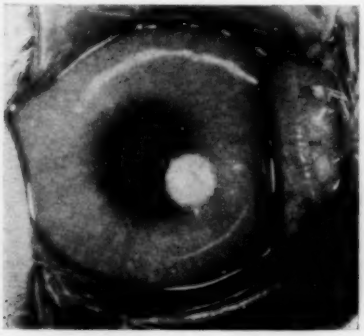

Fig. 7. Bacilli-conglomeration in the capillary of the iris. (×10 suspension of live bacilli, 2 hours later, in immunized rabbit.)

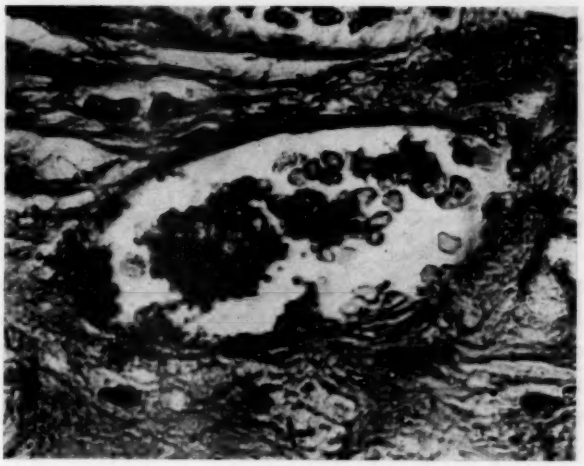

Fig. 8. and 9. Edema in the vascular adventitia of the iris. (×10 suspelnsion of live bacili, 4 hours later, in immunized rabbit)

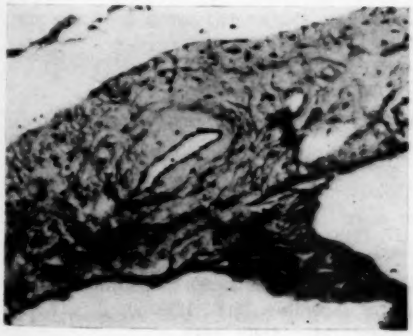

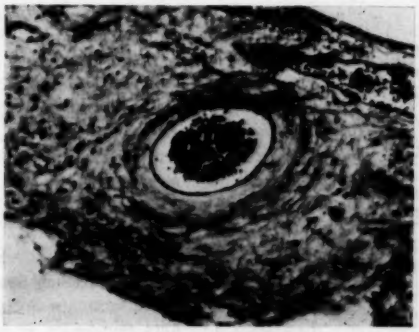

Fig. 10. Hyalin-like exudate around the angle of the anterior chamber. (×100 suspension of live bacili, 4 hours later, in immunized rabbit.)

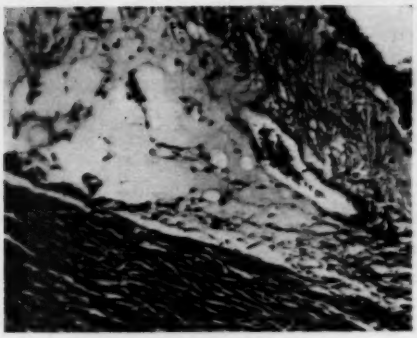

REFERENCES

1) Kato, T.: Acta Ophth. Jap. 62:37, 1958.
2) Behçet, H.: Derm. Wochenschrift. 36:1152, 1937. etc.
3) Sezer, F.N.: Am. J. Ophth. 36:301, 1953.: 41:41, 1956.
4) Evans, A.D. etc.: The Lancet. 6991:349, 1957.
5) Nakagawa Y. etc.: The Journal of the Japanese Association for infectious diseases. 32:270, 1958.
6) Kihoin, A. etc.: Journal of Kyoto Prefectural Medical University. 15:1047, 1935.
7) Kawamura, H.: Japanische Zeitschrift für Mikrobiologie und Pathologie. 30:62, 1936.: 30:1520, 1936.
8) Kondo, K.: Journal of the Nagoya Medical Association. 48:579, 1938.
9) Nakamata, K.: Nagasaki Medical Journal. 20:735, 1942; 20:762, 1942.
10) Ulbrich, H.: Klin. Monatsbl. f. Augenh. 48:159, 1910.
11) Niimi, Y.: Acta Ophth. Jap. 40:1333, 1935.
12) Takahashi, K.: Acta Ophth. Jap. 45:1214, 1941;45:1236, 1941;46:641, 1942.
13) Sakuma, M.: Acta Ophth. Jap. 59:889, 1955.
14) Nambu, M.: Acta Ophth. Jap. 60:962, 1956.
15) Sikano, S.: The Tokyo Journal of Medical Science. 60:167, 1952,
16) Rin, S.: Transactiones Societatis Pathologicae Japonicae. 27:372, 1937.
17) Rich, A.R. The Pathogenesis of Tuberculosis. 2nd Ed. 1951.
18) Urayama, A.: Acta Ophth. Jap. 55:375, 1951.
19) Shimazu, F.: Acta Ophth. Jap. 23:601, 1919.
20) Makiuchi, S.: Acta Ophth. Jap. 54:440, 1950.
21) Okada, S.: Acta Ophth. Jap. 59:16, 1955.
22) Woods, A.C.: Am. J. Ophth. 30:257, 1947; 32:1457, 1949. etc.
23) Bietisch, W.: Klin. Monatsbl. f. Augenh. 17:56, 1879.
24) Okabayashi, A.: Transactiones Societatis Pathologicae Japonicae. 42:99, 1953.
25) Muro, M. etc.: Transactiones Societatis Pathologicae Japonicae. 45:32, 1956.
26) Kitamura, I.: Acta Serologica et Immunologica 3:389, 1942; 3:401, 1942.

EFFECT OF VITAMIN B_2 ON CORNEAL METABOLISM

Hidehiro FUNATSU

Department of Ophthalmology, School of Medicine, University of Tokyo

Some amount of VB_2 which is absorbed from the small intestine with foods is phosphorilated and converts into Flavin Mononucleotide (FMN) in the mucous membrane and some amount emigrates into the blood stream as free type riboflavin. The greater part becomes Flavin Adenine Dinuclectide (FAD) mainly in the liver with cooperation of ATP and Mg ion. This bound form of riboflavin combines with enzyme protein and is utilized to oxidize and reduce metabolites in the living tissues. That is to say, flavoproteins act as oxygen carriers between dehydrogenases and coenzymes and the cytochrome system.

Respiration and glycolysis of cornea have been studies by Herrmann, Jaeger, deRoetth and Kinoshita. Philpot and Pirie reported that riboflavin was present throughout the bovine cornea with highest concentration in the epithelium. Studying the oxygen uptake of the cornea of riboflavin deficient rats, Lee and Hart found, that before vascularization took place, the oxygen uptake of the corneal epithelium was low compared to the normal, but that of the corneal stroma was unchanged. However after vascularization took place, the oxygen uptake of the stroma was found to be raised.

The present studies were undertaken in an attempt to discuss the effects of vitamin B_2 on the corneal metabolism and the clinical significance of its local application.

The experiments consist of

1. The measurement of the oxygen uptake and aerobic carbon dioxide output of the normal rabbit cornea.
2. The oxygen uptake and aerobic carbon dioxide output of the rabbit cornea in addition of FAD, FMN or free type riboflavin into solution.
3. The oxygen uptake and aerobic carbon dioxide output of the rabbit cornea which was removed from the rabbit after the subconjunctival injection of FAD or FMN.

Method

1. Normal rabbits weighing between 1.5 and 2.0kg. were used for the experiments. Warburg's indirect manometric method was used to measure the corneal respiration and aerobic glycolysis.

Special flasks (content 9ml) were employed. A fresh rabbit cornea was cut into half and each was placed into the flask containing 2.0ml. or 4.0ml., of the Krebs-Ringer's bicarbonate solution respectively with addition of glucose in 0.2%. The flasks was gassed with a mixture of 5% carbon dioxide and 95% oxygen. The frequency was seventy five in a minute and the experiment was conducted at 37.5°C for one hour, reading being taken every ten minutes. Thereafter the cornea was dried at 90°C for about fourteen hours and weighed.

The results were expressed in Qo_2 unit, i.e., microliter of oxygen absorbed per milligram

dry weight cornea per hour and $Q_M^{O_2}$ unit, i.e., microliter of carbon dioxide produced per milligram dry weight cornea per hour.

2. In order to study the effects of the addition of vitamin B_2, 1.2×10^{-5} M FAD, 1.2×10^{-5} M FMN or 1.2×10^{-5} M riboflavin was added as a final concentration into the solution in the flasks.

The procedure used was the same as above mentioned. Control study was performed without vitamin B_2.

The Krebs-Ringer's bicarbonate solution without glucose was also used in the experiment of the addition of FAD.

3. In another series of the experiment, FAD (30γ or 300γ) or FMN (300 γ) was injected into the upper subconjunctiva of one eye and 0.7% NaCl was injected into the other eye as a control, because the solvent of FAD or FMN was 0.7% NaCl. Then the cornea was removed after various time intervals and Warburg's method was used.

Results

Respiration and aerobic glycolysis of the normal half corneal slice

There were reports in literature concerning the corneal respiration of several animals by Kohra, Shimoyama, Langham. Herrmann, deRoetth and Lee.

Table 1. O_2 Uptake and Aerobic CO_2 Output of Normal Rabbit Cornea

body weight gr.	dry tissue mg.	Q_{O_2}	$Q_M^{O_2}$
1480	16.0	−1.13	+1.20
	15.2	−1.08	+1.11
1700	19.3	−0.57	+0.75
	19.5	−0.71	+0.87
1790	17.8	−0.83	+1.22
	17.7	−0.68	+0.99
1840	18.2	−0.76	+0.81
	18.5	−0.77	+0.86
1500	14.7	−0.75	+1.07
	14.5	−0.60	+0.88
1550	16.9	−0.60	+0.76
	18.0	−0.86	+0.89
1600	18.2	−0.91	+1.07
	18.4	−1.00	+0.90
1750	13.1	−0.80	+0.86
	13.9	−0.55	+0.79
1730	17.1	−0.46	+0.56
	18.0	−0.73	+0.58
1930	19.0	−0.57	+0.82
	19.3	−0.89	+0.68
1500	13.7	−1.20	+0.92
	13.1	−1.01	+0.99
1850	16.2	−0.94	+1.02
	16.4	−0.76	+0.88
average		−0.80	+0.89

The author measured the oxygen uptake and aerobic carbon dioxide output of normal rabbit cornea. Table 1 showed corneal respiration and aerobic glycolysis. The average Qo_2 was—0.80 and $Q_M^{O_2}$ was+0.89.

Effect of an addition of FAD, FMN or free type riboflavin on the corneal respiration and aerobic glycolysis

When 1.2×10^{-5} M FAD as a final concentration was added into the Krebs-Ringes's bicarbonate solution containing glucose, the average corneal Qo_2 was—1.59. The increase of Qo_2 was 123.9% and significant at the 1% level as compared with those in the control group (Table 2).

The average corneal $Q_M^{O_2}$ was+1.09, but did not show any significant difference as compared with those in the control group, which showed+0.93.

On the other hand, when $1.2\times^{-5}$ M FAD was added into the solution without glucose, as

Table 2. O_2 Uptake and Aerobic CO_2 Output of Cornea in Krebs-Ringer's Bicarbonate Solution containing Glucose with 1.2×10^{-5}M FAD

body weight	Control			FAD added		
gr.	dry tissue mg	Qo_2	$Q_M^{O_2}$	dry tissue mg	Qo_2	$Q_M^{O_2}$
1560	15.0	−0.51	+0.72	15.7	−1.64	+1.31
1680	17.8	−0.70	+0.89	17.2	−1.48	+1.03
1700	16.0	−0.80	+0.75	15.8	−1.97	+1.08
1400	11.2	−0.66	+1.03	11.9	−1.20	+0.90
1530	15.8	−0.73	+1.17	14.8	−1.59	+1.13
1920	18.6	−0.87	+1.01	18.8	−1.64	+1.10
average		−0.71	+0.93		−1.59**	+1.09
increase					+0.88	+0.16
rate of increase					+123.9%	+17.2%

** significant difference of 1% level

shown in Table 3 the average corneal Qo_2 was—0.85 and the rate of increase was 19.4%, but Qo_2 did not show any significant difference as compared with that in the control group. The average corneal $Q_M^{O_2}$ was+0.06 and an equal equivalent to that in the control group.

As a result of this experiment, it was observed, that added FAD increased the corneal oxygen uptake and the local use of the instillation seemed to be beneficial for the corneal respiration.

Table 4 showed, that the average corneal Qo_2 with added 1.2×10^{-5} M FMN was—0.80 and almost equivalent to that in the control which was—0.81. The cornea had a $Q_M^{O_2}$ of+0.90 and a rate of increase of 3.4% with no significant difference.

It could not be observed that the addition of FMN into the solution increased the corneal respiration and aerobic glycolysis.

Table 3. O_2 Uptake and Aerobic CO_2 Output of Cornea in Krebs-Ringer's Bicarbonate Solution with 1.2×10^{-5}M FAD

body weight	Control			FAD added		
gr	dry tissue mg	Qo_2	$Q_M^{O_2}$	dry tissue mg	Qo_2	$Q_M^{O_2}$
1610	17.7	−0.51	0	17.5	−0.58	0
1900	14.6	−0.82	+0.08	14.4	−0.79	+0.04
1760	13.6	−0.99	+0.13	13.6	−1.18	+.018
2000	13.7	−0.53	+0.02	14.2	−0.67	+0.01
1740	15.3	−0.76	+0.08	14.9	−0.84	+0.06
1530	13.1	−0.73	+0.02	13.6	−0.96	+0.07
average		−0.72	+0.06		−0.85	+0.06
increase					+0.13	0
rate of increase					+19.4%	

Table 4. O_2 Uptake and Aerobic CO_2 Output of Cornea in Krebs-Ringer's Bicarbonate Solution Containing Glucose with 1.2×10^{-5} M FMN

body weight	Control			FMN added		
gr	dry tissue mg	Qo_2	$Q_M^{O_2}$	dry tissue mg	Qo_2	$Q_M^{O_2}$
1700	16.6	−0.83	+0.95	15.8	−1.03	+1.02
2010	14.4	−0.69	+0.93	13.5	−0.70	+0.88
1830	12.0	−0.90	+0.94	13.8	−0.76	+0.75
1770	15.5	−0.85	+0.77	15.7	−0.96	+0.94
1700	14.7	−0.60	+0.71	14.0	−0.40	+0.75
1920	15.8	−0.96	+0.91	15.3	−0.92	+1.06
average		−0.81	+0.87		−0.80	+0.90
increase					−0.01	+0.03
rate of increase					− 1.2%	+ 3.4%

When 1.2×10^{-5} M free type riboflavin was added to the solution, as shown in Table 5 the average corneal Qo_2 was—0.67 and equivalent to that in the control group. The average $Q_M^{O_2}$ showed a decrease of 2.2%, but which was not significant in difference as compared with that in the control. It will be concluded that free type riboflavin does not increase the corneal respiration.

Effect of subconjunctival injection of FAD or FMN on the corneal respiration and aerobic glycolysis

Table 5. O_2 Uptake and Aerobic CO_2 Output of Cornea in Krebs-Ringer's Bicarbonate Solution Containing Glucose with 1.2×10^{-5} Riboflavin

body weight	Control			Free added		
gr.	dry tissue mg	Qo_2	$Q_M^{O_2}$	dry tissve mg	Qo_2	$Q_M^{O_2}$
1620	14.4	−0.58	+0.89	14.8	−0.60	+0.81
1630	15.1	−0.57	+0.71	15.7	−0.66	+0.82
1730	15.6	−0.75	+0.96	14.8	−0.81	+0.86
1800	16.3	−0.77	+1.15	16.2	−0.61	+1.16
average		−0.67	+0.93		−0.67	+0.91
increase					± 0	−0.02
rate of increase					0 %	−2.2%

Table 6 and Fig. 1 showed a result of the subconjunctival injection of FAD in a dosis of 300γ. A significant increase of the average corneal Qo_2 was found between one hour and fifteen hours after the injection, and the rate of increase of Qo_2 was 70.7% five hours later and—16,3% twenty four hours later as compared with those in the subconjunctival injection of 0.7% NaCl.

It was also found that the corneal Qo_2 increased with the significant difference of 1% level between one hour and fifteen hours after the injection as compared with normal rabbit cornea (Table 1).

Fig. 1. Diagram showing relationship between rate of increase of corneal Qo_2 and $Q_M^{O_2}$ and time intervals after subconjunctival injection of 300γ of FAD.

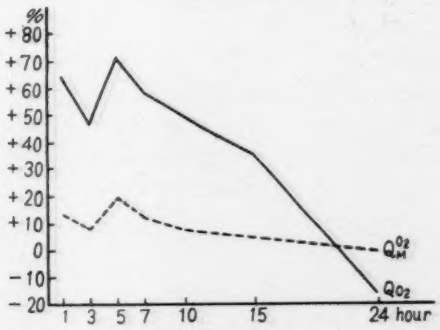

In conclusion, the subconjunctival injection of FAD in a dosis of 300γ, increases the corneal respiration between one hour and fifteen hours later. The maximum Q_{O_2} was—1.40 five hours later.

The average corneal $Q_M^{O_2}$ in the injection of FAD showed a slight increase between one hour and fifteen hours later, but a significant difference compared with that in the control group was observed only five hours later. And $Q_M^{O_2}$ showed a slight increase only five hours later as compared with those in the normal rabbit cornea (Table 1), but without

Table 6. O_2 Uptake and Aerobic CO_2 Output of Cornea after Subconjunctival Injection of 300γ of FAD

hour after injection	body weight gr	Control			FAD injected		
		dry tissue mg	Q_{O_2}	$Q_M^{O_2}$	dry tissue mg	Q_{O_2}	$Q_M^{O_2}$
1	1900	16.7	−0.59	+0.81	17.7	−0.99	+0.88
	1800	18.8	−0.85	+1.14	18.5	−1.34	+1.14
	1920	16.9	−0.56	+0.81	15.7	−0.93	+0.90
	1510	14.7	−0.61	+0.71	13.0	−1.09	+0.84
	1590	14.4	−0.47	+0.67	15.3	−1.18	+0.96
	1500	12.6	−0.82	+0.78	12.8	−0.86	+0.88
	average		−0.65	+0.82		−1.07**	+0.93
	increase					+0.42	+0.11
	rate of increase					+64.6%	+13.4%
3	1900	16.0	−0.91	+0.90	15.7	−1.27	+1.08
	1520	18.9	−0.54	+0.77	19.5	−0.99	+0.98
	1520	15.4	−0.98	+1.10	15.8	−1.33	+1.08
	1670	14.4	−0.93	+0.81	15.0	−1.33	+0.81
	1880	12.9	−0.85	+0.87	13.2	−1.30	+0.91
	1790	17.8	−0.84	+0.89	17.7	−1.18	+0.90
	average		−0.84	+0.89		−1.23**	+0.96
	increase					+0.39	+0.07
	rate of increase					+46.4%	+ 7.9%
5	1580	16.8	−0.90	+0.91	16.6	−1.83	+1.15
	1820	15.5	−0.97	+0.99	15.0	−1.52	+1.09
	1400	12.3	−0.50	+0.71	13.4	−1.11	+0.99
	1600	18.0	−0.76	+0.82	18.7	−1.33	+1.08
	1600	15.9	−0.91	+0.92	16.8	−1.35	+0.97
	1760	14.6	−0.87	+0.92	14.2	−1.27	+1.02
	average		−0.82	+0.88		−1.40**	+1.05**
	increase					+0.58	+0.17
	rate of increase					+70.7%	+19.3%

7	1850	15.8	−0.81	+0.81	15.8	−1.67	+1.15
	1300	15.8	−0.97	+1.00	15.6	−1.47	+1.05
	1700	14.2	−0.52	+0.81	14.7	−0.93	+0.91
	1630	14.6	−1.02	+1.24	14.6	−1.56	+1.30
	1420	16.7	−0.65	+0.80	15.8	−0.91	+1.09
	1600	16.7	−1.21	+1.20	14.5	−1.60	+1.10
	average		−0.86	+0.98		−1.36**	+1.10
	increase					+0.50	+0.12
	rate of increase					+58.1%	+12.2%
10	1600	15.5	−0.47	+0.89	16.5	−0.98	+0.93
	1420	16.9	−0.67	+1.01	15.0	−1.34	+1.16
	1600	14.7	−0.87	+0.78	13.0	−1.10	+0.86
	1710	15.3	−0.63	+0.80	15.1	−0.86	+0.95
	1480	14.3	−0.89	+1.02	14.0	−1.10	+1.01
	1620	16.2	−0.89	+0.95	16.6	−1.03	+0.97
	average		−0.72	+0.91		−1.07**	+0.98
	increase					+0.35	+0.07
	rate of increase					+48.6%	+7.7%
15	1590	14.7	−0.88	+0.95	15.2	−0.82	+1.07
	1600	15.2	−0.62	+1.05	15.6	−0.94	+1.08
	1620	18.6	−0.60	+0.97	19.5	−1.13	+0.97
	1510	15.6	−0.61	+0.98	16.0	−0.90	+1.02
	1470	12.7	−0.93	+0.97	12.5	−1.14	+0.99
	1800	18.5	−0.60	+0.72	18.2	−0.18	+0.76
	average		−0.71	+0.94		−0.96*	+0.98
	increase					+0.25	+0.04
	rate of increase					+35.2%	+ 4.3%
24	1580	13.9	−0.88	+0.82	14.3	−0.72	+0.90
	1710	15.3	−1.12	+1.08	15.1	−0.63	+0.76
	1510	14.0	−0.68	+0.82	14.3	−0.61	+0.91
	1820	16.8	−0.93	+0.93	16.8	−0.89	+0.91
	1500	17.3	−0.73	+1.02	17.4	−0.71	+1.04
	1630	17.2	−0.84	+1.03	16.8	−0.74	+1.09
	average		−0.86	+0.95		−0.72	+0.94
	increase					−0.14	−0.01
	rate of increase					−16.3%	−1.1%

* significant difference of 5% level
** significant difference of 1% level

significant difference.

The result suggests that the subconjunctival injection of FAD in a dosis of 300γ may not affect corneal aerobic glycolysis.

Table 7 and Fig. 2 showed a result of the subconjunctival injection of FAD in a dosis of 30γ. A significant increase of the average corneal Qo_2 was found only one hour later as compared with those in the control group. But there was no significant difference

Table 7. O_2 Uptake and Aerobic CO_2 Output of Cornea after Subconjunctival injection of 30γ of FAD

hour after injection	body weight	Control			FAD injected		
	gr	dry tissue mg	Qo_2	$Q_M^{O_2}$	dry tissue mg	Qo_2	$Q_M^{O_2}$
1	1800	16.5	−0.71	+0.82	16.2	−0.89	+0.92
	1510	17.8	−0.71	+0.72	19.0	−0.74	+0.98
	1500	19.5	−0.52	+0.77	19.8	−0.77	+0.77
	1550	16.1	−0.68	+0.79	16.4	−0.84	+0.99
	1500	16.8	−0.73	+0.82	16.8	−0.94	+0.98
	1300	13.7	−0.71	+0.82	17.0	−0.85	+0.93
	average		−0.68	+0.79		−0.84**	+0.93**
	increase					+0.16	+0.14
	rate of increase					+23.5%	+17.7%
3	1600	18.9	−0.86	+0.81	17.8	−0.77	+0.78
	1600	16.4	−0.80	+0.85	17.0	−0.92	+0.91
	1920	20.2	−0.97	+0.99	18.5	−0.92	+0.85
	1300	17.2	−1.17	+1.17	16.1	−1.20	+1.06
	1400	16.0	−0.86	+1.05	20.0	−0.85	+0.82
	1390	13.0	−0.71	+0.81	12.9	−0.82	+0.91
	average		−0.89	+0.95		−0.91	+0.89
	increase					+0.02	−0.06
	rate of incease					+2.2%	−6.3%
5	1400	18.8	−1.01	+1.01	17.8	−0.75	+0.83
	1400	17.5	−0.75	+0.79	17.0	−0.79	+0.97
	1620	17.8	−0.85	+0.89	18.5	−0.78	+0.78
	1540	16.2	−0.83	+1.03	16.1	−1.17	+1.00
	1600	19.6	−0.75	+0.79	20.0	−0.90	+0.92
	1830	18.7	−0.87	+0.86	18.9	−0.78	+0.87
	average		−0.84	+0.90		−0.86	+0.90
	increase					−0.02	0
	rate of increase					+2.4%	0%

7	1300	13.9	−0.94	+1.06	14.9	−0.80	+1.08
	1500	15.8	−1.06	+0.93	15.2	−1.03	+1.00
	1680	14.2	−0.92	+1.18	14.0	−0.91	+1.17
	1900	16.2	−1.02	+0.89	16.0	−0.90	+0.93
	1300	13.9	−0.84	+0.96	14.9	−0.81	+1.08
	1500	11.9	−0.76	+0.83	13.0	−0.86	+1.01
	average		−0.92	+0.98		−0.89	+1.05
	increase					−0.03	+0.07
	rate of increase					−3.2%	+7.1%
10	1560	15.6	−0.69	+0.97	14.9	−0.78	+1.06
	1580	16.0	−0.71	+0.71	15.0	−0.82	+0.92
	1300	17.9	−0.45	+0.86	18.0	−0.55	+0.87
	1510	16.1	−0.93	+1.03	16.0	−1.01	+1.20
	1820	17.7	−0.71	+0.72	16.9	−0.79	+0.88
	1400	17.0	−0.77	+0.96	17.3	−0.72	+0.98
	average		−0.71	+0.88		−0.78	+0.99
	increase					+0.07	+0.11
	rate of increase					+9.9%	+12.5%
15	1440	14.4	−0.56	+0.79	13.8	−0.66	+0.85
	1390	13.7	−0.91	+0.99	14.0	−1.00	+1.21
	1770	16.3	−0.71	+0.80	16.2	−0.73	+0.79
	1440	14.4	−0.68	+0.99	13.8	−0.71	+1.10
	average		−0.72	+0.89		−0.78	+0.99
	increase					+0.06	+0.10
	rate of increase					+8.3%	+11.2%

** significant difference of 1% level

between one hour and fifteen hours, compared with that in the normal rabbit cornea (Table 1).

The average corneal $Q_M^{O_2}$ did not show a significant difference as compared with that in the control to which 0.7% NaCl was injected and that in the normal rabbit cornea.

Fig. 2. Diagram showing relationship between rate of increase of corneal Qo_2 and $Q_M^{O_2}$ and time intervals after subconjunctival injection of 30γ of FAD.

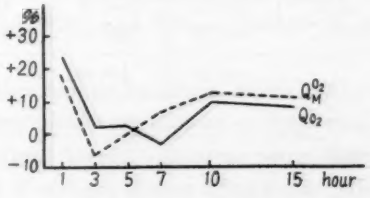

As a conclusion, it does not appear, that the injection of 30γ of FAD into the subconjunctiva has an effect on the corneal respiration and aerobic glycolysis.

When FMN was injected into the subconjunctiva in a dosis of 300γ, the average Qo_2 and $Q_M^{O_2}$ showed to be almost the same as that in the control group to which 0.7% NaCl was injected, and also showed a little increase, compared with that in the normal rabbit cornea, (Table 1), but a significant difference could not be obtained. (Table 8 and Fig. 3.)

Table 8. O_2 Uptake and Aerobic CO_2 Output of Cornea after Subconjunctival Injection of 300γ of FMN

hour	body weight	control			FMN injected		
	gr	dry tissue mg	Qo_2	$Q_M^{O_2}$	dry tissue mg	Qo_2	$Q_M^{O_2}$
1	1780	14.4	−0.62	+0.97	15.1	−0.96	+1.22
	1630	14.6	−0.92	+0.62	13.6	−0.53	+0.63
	1580	15.4	−0.63	+0.72	14.7	−0.73	+0.47
	2020	12.6	−0.71	+0.83	13.6	−0.71	+1.04
	1900	15.9	−1.07	+0.95	16.5	−0.77	+0.85
	1630	17.2	−0.37	+0.85	17.1	−0.54	+0.62
	average		−0.72	+0.83		−0.71	+0.81
	increase					−0.01	−0.02
	rate of increase					−1.3%	−2.4%
3	1200	15.5	−1.25	+1.07	15.9	−0.71	+0.75
	1730	15.2	−1.19	+1.05	15.3	−0.85	+0.68
	1790	15.5	−1.03	+0.88	14.4	−1.19	+0.99
	1950	15.4	−0.82	+0.67	16.8	−1.32	+0.92
	1950	19.2	−1.07	+1.04	21.3	−0.82	+0.91
	1740	16.8	−1.07	+0.82	19.3	−0.99	+0.60
	average		−1.06	+0.92		−0.98	+0.81
	increase					−0.08	−0.11
	rate of increase					−7.5%	−12.0%
5	1900	15.1	−1.36	+1.02	15.0	−0.92	+0.85
	1900	14.6	−0.69	+0.58	14.3	−0.67	+0.68
	2000	11.6	−1.32	+1.38	12.6	−1.22	+1.11
	1650	14.9	−1.21	+0.96	15.2	−0.85	+0.75
	1800	16.2	−0.62	+0.72	16.7	−1.13	+0.78
	1500	14.5	−0.61	+0.62	14.7	−0.72	+0.83
	average		−0.97	+0.88		−0.92	−0.83
	increase					−0.05	−0.05
	rate of increase					−5.2%	−5.7%

10	1700	17.9	−0.73	+0.64	18.5	−0.97	+0.73
	1500	14.8	−1.36	+1.04	14.7	−1.00	+1.15
	1800	15.9	−0.73	+1.13	16.8	−0.69	+0.66
	1410	14.9	−1.04	+0.65	16.0	−1.17	+0.81
	1400	15.0	−0.86	+0.99	15.0	−0.90	+1.02
	1150	11.2	−0.50	+0.53	11.7	−1.12	+0.75
	average		−0.87	+0.83		−0.98	+0.85
	increase					+0.11	+0.02
	rate of increase					+12.7%	+2.4%
15	1630	15.0	−1.01	+0.85	15.0	−0.67	+0.81
	1900	17.7	−0.52	+0.71	17.1	−0.61	+0.80
	1500	14.4	−0.98	+0.86	14.9	−1.21	+1.01
	1650	14.9	−0.73	+0.90	14.6	−0.99	+0.77
	average		−0.81	+0.83		−0.88	+0.85
	increase					+0.07	+0.22
	rate of increase					+8.6%	+2.4%

Fig. 3. Diagram showing relationship between rate of increase of corneal Qo_2 and $Q_M^{O_2}$ and time intervals after subconjunctival injection of 300γ of FMN.

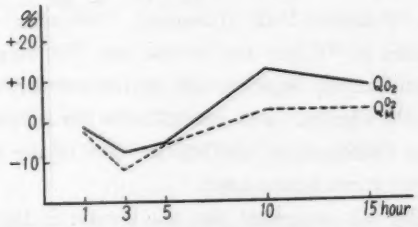

Therefor the subconjunctival injection of FMN seemed to have no effect on the normal corneal respiration and aerobic glycolysis.

Discussion

In the experiments in addition of 1.2×10^{-5} M FAD, FMN or free type riboflavin respectively, only FAD increased the corneal oxygen uptake when the solution contained glucose. This fact means, that FAD may be used directly in the corneal tissue, not passing through the liver.

The activity of flavoprotein enzyme is gained, when FAD combines with enzyme protein, so the increase of oxygen uptake by addition of FAD may mean, that FAD combines with the protein in the corneal tissue. However when FAD was added to the solution without glucose, the increase of corneal oxygen uptake was minimal and did not show a

significant difference compared with the control.

There are D-amino-acid oxidase and xanthine oxidase which have been found in the living tissues, which are flavoprotein enzymes containing FAD. However the results suggest, that FAD added to the cornea may not affect the oxidation of D-amino-acid and xanthine in the cornea.

No influence of FAD on the aerobic glycolysis was found regardless whether glucose was added or not. But further investigation is needed to solve the question, whether carbon dioxide results from lactic acid only or not.

In the experiments of the addition of FMN or free type riboflavin, no increase of the corneal oxygen uptake and aerobic carbon dioxide output was found. There are yellow ferment, TPN-cytochrome *c* reductase and L-amino-acid oxidase which are flavoprotien enzymes containing FMN.

In these flavoprotein enzymes, only TPN-cytochrome *c* reductase play a small role in the glycolysis of the living tissues, but this enzyme has not been confirmed in the cornea. The author considers, that FMN may not have been converted into FAD in the cornea.

In the next approach, it was found that the subconjunctival injection of FAD in a dosis of 30γ did not affect the corneal respiration, but the subconjunctival injection of FAD in a dosis of 300γ increased the corneal respiration between one hour and fifteen hours later. However the subconjunctival injection of FMN in a dosis of 300γ did not increase the corneal respiration.

Hishiki reported the emigration of FAD and FMN which were injected into the subconjunctiva. He injected ^{32}P-labeled FAD (1.5mg/ml, 7100cpm/g) into the subconjunctiva of the rabbit, the emigration of ^{32}P into the cornea was 778cpm/g at the injected side of the eye and 164cpm/g at the non injected side of the eye three hours later. When ^{32}P-labeled FMN (2mg/ml, 10479cpm/g) was injected into the subconjunctiva, the emigration of ^{32}P into the cornea was 2962cpm/g at the injected side of the eye and 241cpm/g at the non injected side of the eye three hours later.

It is a problem whether ^{32}P emigrated into the cornea in the form of FAD or FMN, but a large difference is found in the injected eye and non injected eye, so the fact of the emigration of FAD or FMN running through the blood stream may be disregarded.

The increase of the corneal respiration by means of the subconjunctival injection of 300γ of FAD may depend upon the direct emigration into the cornea.

Summary

In the present report, the effect of vitamin B_2 on the rabbit corneal metabolism were studied by means of the Warburg's indirect manometric method.

1. When FAD, FMN or free type riboflavin was added into the solution, only the addition of FAD showed a more significant increase of the respiration of the corneal slice as compared with that in the control group.

2. In the second approach, FAD (300γ) was injected into the upper subconjunctiva of one eye and 0.7% NaCl was injected into the other eye as a control, and rabbits were sacrificed after various time intervals up to twenty four hours, and then corneal Qo_2 and $Q_M^{O_2}$ were measured. A significant effect of FAD on the corneal oxygen uptake was observed between one hour and fifteen hours after the injection.

3. But when FAD (30γ) or FMN (300γ) was injected by the same method, not any signficant effect could be found in the corneal respiration and aerobic glycolysis between one hour and fifteen hours after the injection.

It may be concluded that only a local use of FAD seems to be worth while of clinical application and the subconjunctival injection of FAD appears to have a clinical significance as far as the corneal metabolism is concerned.

(Published in Acta O. Jap. 62:1668, 1958 and Acta O. Jap. 63:461, 1959 in Japanese.)

REFERENCES

1) Herrmann, H., Moses, S.G., and Friedenwald, J.S.: Arch. Ophth. 28;1381, 1942.
2) Jaeger, W.: Arch. f. Ophth. 154:142, 1953.
3) de Roetth, A.: Arch. Ophth. 44:666, 1950.
4) de Roetth, A.: Arch. Ophth. 45:139, 1951.
5) Kinoshita, J.H., Masurat, T., and Helfant, M.: Science, 72:122, 1955.
6) Philpot, F.J., and Pirie, A.: Biochem. J. 37:250, 1943.
7) Kohra, T.: Acta O. Jap. 39:1429, 1935.
8) Shimoyama, K.: Acta O. Jap. 43:1694, 1939.
9) Lee, O.S., and Hart, W.A.: Amer. J. Ophth., 27:488, 1944.
10) Langham, M.E.: J. Physiol., 126:396, 1954.
11) Hishiki, T.: Acta O. Jap. 62:1653, 1958.

STUDIES ON COLOUR VISION DUE TO ERG
REPORT II ON THE PROGRESS OF DARK-ADAPTATION UNDER FILTERED LIGHT STIMULATION

Hitohiro SAKANASHI

Department of Ophthalmology, Tokyo Medical College

In the previous paper, the author reported of his observation on the course of dark adaptation of the human being by electroretinogram (E.R.G.) using the monochromatic light of 420mμ, 470mμ, 520mμ, and 580mμ with equal energy as stimuli. In the initial stage of dark adaptation, the cones reacted mainly and the sensibility to the light of the longer wave was high, but later the rods reacted mainly and the sensibility to the light of the shorter wave was high. As for the curve of dark adaptation to each chromatic light, it was gentler to the light of the shorter wave and was steeper to the light of the longer wave. In the previous experiment, however, only the b-wave in the broad sense from which the x-wave was not separated was recorded, because of the weakness of the stimulating light. In the present study, the author performed a similar experiment with a stronger illuminant and recording not only the b-wave but also the a-and x-waves which were considered to have strong relation with the color sense.

Equipments

Recording. A universal recorder, type 202 made by Sanei Instrument Co., Ltd. was used for recording of E.R.G.. This recorder consisted of a pre-amplifier, main-amplifier and ink-writing oscillograph. The recording paper was run with the speed of 6cm. per min. in the recording.

Light adaptation. In order to observe the course of dark adaptation, attention should be paid first to the state of light adaptation. Considering that in light adaptation by ordinary electric bulb, the eye was weakly adapted to the light of the shorter wave and was strongly adapted to the light of the longer wave, it was adapted to the standard illuminant C for 15 minutes from the distance of 56 cm.. The illumination was 700 lux.

Stimulating light. A slide projector with an incandescent electric bulb of 100V., 1KW. was used as the illuminant, and Mazda's color filters were inserted to make the light chromatic. The filters used were violet (V-V_1), blue (V-B_1), light blue (V-B_2), green (V-G_1), yellow (V-Y_1), orange (V-O), light red (V-R_3), red (V-R_2) and dark red (V-R_1). The transmittance of each of these nine filters is shown in Fig. 1. A shutter was fitted on the front of the slide projector, and the experimented person fixed his eyes on it in the irradiation.

Fig. 1. Transmittance of color filter.

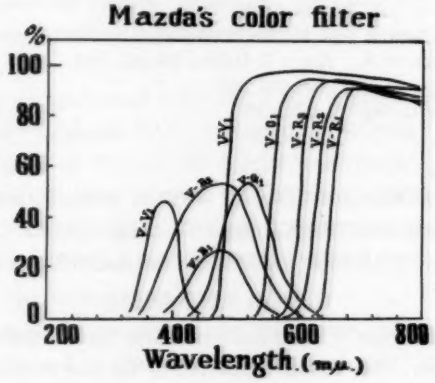

Methods

The experimented person was a 25-year-old man with normal color sense. After dropping anesthesia into the eye, Riggs' contact lens electrode was fitted to it and the other electrode was fixed on the center of the forehead. The eye was adapted to the illuminant C for 15 minutes. Then stimulation was given each for $^1/_{100}$ sec. using the aforementioned chromatic light, 9 seconds after the extinction of the light, then in every 30 seconds till the 5th minute, and in every 1 minute from the 5th to the 30th minute, and the change in the electric potential was recorded.

Results and Discussion

The E.R.G. of the course of dark adaptation to each of the nine filter light is recorded

in Fig. 2. The amplitude of each wave of the E.R.G. is measured and graphed in Figs. 3,4 and 5. The dark adaptation time is shown on the transverse line and the amplitude (μV) of each wave is shown on the longitudinal line.

Fig. 2. The E.R.G. of the course of dark adaptation to each of the filtered light.

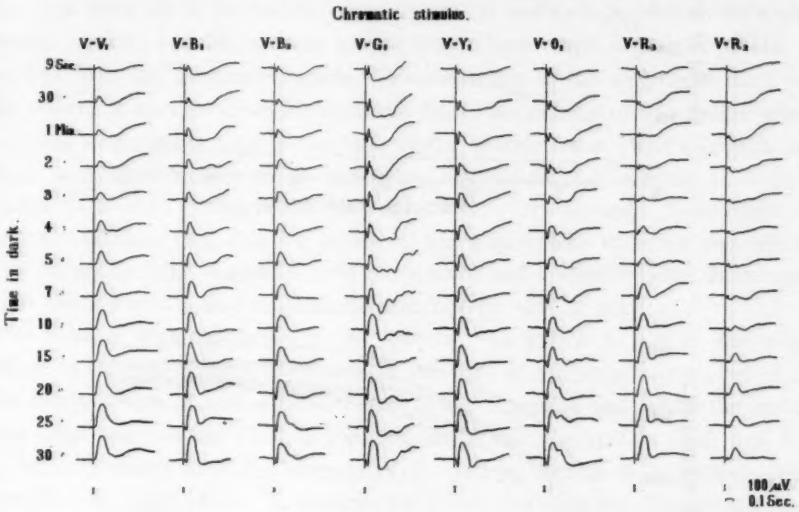

Fig. 3. The curve of dark adaptation of a-wave.

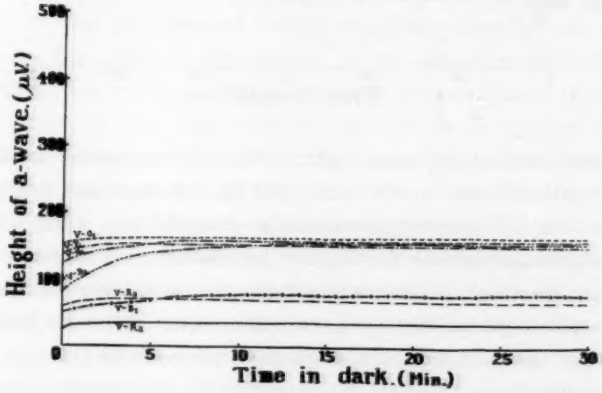

Fig. 4. The curve of dark adaptation of x-wave.

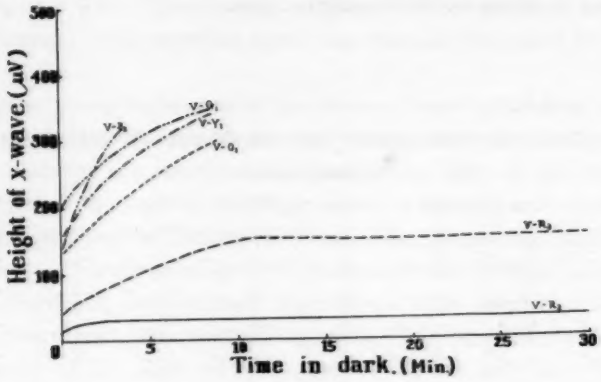

Fig. 5. The curve of dark adaptation of b-wave.

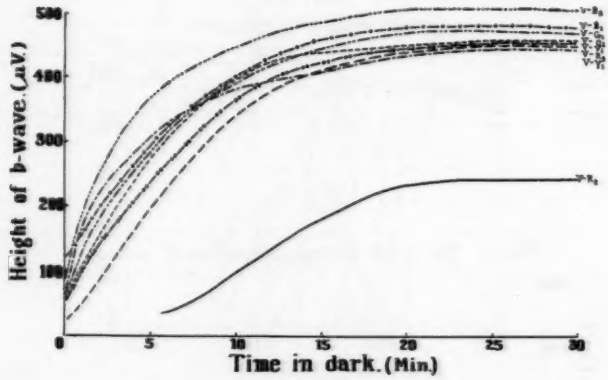

Among the nine kinds of chromatic light, E.R.G. did not appear at all in V-R_1 (dark red). It was considered due to the fact, that the transmittance was low and the light amount was little. In V-V_1 (violet), b-wave was observed but a-and x-waves were not observed. It was perhaps because the light of the shorter wave stimulated the rods mainly and not the cones; therefore, a-and x-waves from the cones were not observed. In V-B_1 (blue), a-and b-waves appeared but x-wave did not. Being different from V-V_1 (violet), V-B_1 (blue) was not the pure light of the shorter wave because although the maximum of its transmittance was 480mμ. (Fig. 1), it transmitted the light between 380 mμ. and 570mμ.. Therefore, the E.R.G. was considered to have appeared in this way too. All of a-, b-and x-waves appeared in all kinds of chromatic light except in these three.

The curve of dark adaptation of the a-wave. The a-wave appeared in seven kinds of chromatic light and did not appear in V-R_1 (dark red) and V-V_1 (violet) (Fig. 3). Being definitely different from the b-wave which reached the maximum in 20–25 minutes of dark adaptation, the a-wave reached the maximum in the initial stage (1–10 minutes) of dark adaptation, and this fact suggested, that the a-wave was photopic. Armington, Johnson, Auerbach, Burian et al. considered that the a-wave contained not only the photopic component but also the scotopic component, and classified it into a_1 and a_2 waves. However, no scotopic a-wave was observed in the present experiment. It was perhaps because the a-wave passed extremely rapidly, and the scotopic a-wave might have been separated if the recording paper had been run extremely rapidly. In comparison of the curves of dark adaptation of the a-wave in various kinds of chromatic light, the maximum was shown sooner in the light of the longer wave than in the light of the shorter wave. The maximum was shown in about 10 minutes in V-B_1 (blue) and V-B_2 (light blue), in 5 minutes in V-G_1 (green), in 2 minutes in V-Y_1 (yellow), and in 1 minute in V-O_1 (orange), V-R_3 (light red) and V-R_2 (red). Such a fact, that the course of the a-wave was different depending on the kind of chromatic light suggested, that the a-wave had a close relation to the color sense just like the x-wave.

The curve of dark adaptation of the x-wave. As shown in Fig. 4, the x-wave was separated to the end of dark adaptation in the light of the longer wave, but in the light of the shorter wave, it was separated only in the beginning and not in the end as it was covered with the b-wave. It was observed for 30 minutes in V-R_2 (red) and V-R_3 (light red), for 9 minutes in V-O_1 (orange), V-Y, (yellow) and in V-G_1 (green), and for $3\,1/2$ minutes in V-B_2 (light blue). It seemed due to the fact that the light of the longer wave stimulated mainly the cones and therefore the x-wave easily appeared and was observed towards the end of the adaptation, but the light of the shorter wave stimulated the rods mainly and the x-wave was hard to be separated being covered with the b-wave. Because of this reason, it was not observed exactly when the curve of dark adaptation reached the maximum in the light of the shorter wave, but it generally tended to reach the maximum comparatively in the earlier stage of the x-wave than of the b-wave. In comparison of the curves of dark adaptation of the x-wave in various kinds of chromatic light, they reached the maximum earlier in the light of the longer wave than in the light of the shorter wave just as in the case of the a-wave. This fact, that the curves of dark adaptation of the a-and x-waves were different depending on the kind of the waves, with Studnitz and Hosoya et al.'s photochemical studies on the decomposition and regeneration of the visual substance of the cones, seemed to suggest, that the visual substance to the light of the longer wave was more quickly regenerated than that to the light of the shorter wave. Furthermore, Studnitz extracted three substances which had an absorptivity of 468mμ, 555mμ, and 655mμ from the retina of the snake which consisted only of the cones, and Hosoya et al. extracted the same substances from the Formosan terrapin, and they clarified that there were three heaps in the absorptive curve. The result of the present

experiment that the curves of dark adaptation were different depending on the kind of chromatic light seemed to support the opinion, that there were several kinds of the visual substance of the cones.

The curve of the dark adaptation of the b-wave. As shown in Fig. 5, the curve of the dark adaptation of the b-wave reached its maximum in 20–25 minutes, slower than in the a-and x-waves. This fact suggested that the b-wave was from the rods. The specific observation that the curve of dark adaptation of the b-wave in every chromatic light except that in V-R_2 (red) had almost the same course, was agreeable with the established opinion, that there was only one kind of rod or rhodopsin being different from the case of the cones. Granit, Adrian and Willmer stated, that the rods had a relation to the sense of blue, but no difference was observed between the curve of the b-wave in the light of the shorter wave and that in the light of the longer wave in the present experiment. However, since not every chromatic light had an equal energy in this experiment, the question whether the rods had a relation to the sense of blue or they controlled only the sense of light brightness and darkness was not clarified by this study. In V-R_2 (red), the b-wave appeared very late and drew a very gentle curve, but it was not known whether it was because of the lowness of the transmittance of the filter and the weakness of the stimulating light, or of the speciality of the chromatic light.

Summary

Succeeding to the former report, aiming to investigate the course of dark adaptation for colour light, after light adaptation for 15 minutes by the illuminant C, using various colour lights as test stimulus produced by Mazda's colour filter, the course of dark adaptation was observed and the curve of dark adaptation was drawn by the measurement of amplitudes of the a, x and b-waves. The results were as follows.

1. At the extreme end of the long wave, red light (longer than 640mμ), ERG did not appear.

2. Blue light (400–560mμ) recorded a and b-waves and violet light (330–440mμ) recorded the b-wave.

3. Other colour lights always recorded a, x and b-waves.

4. The a-wave reached the maximum in the early stage of dark adaptation. The more the length of light wavelengthened, the more it took short time to reach the maximum amplitude.

5. At the short wave, the x-wave was separated only at the early stage of dark adaptation; besides, in long wave, it was seperated at the end stage of dark adaptation.

6. The b-wave reached its maximum at the end stage of dark adaptation. All of the colour-lights showed the same trend on the curve of the b-wave, except red light (longer than 600 mμ).

7. In red light (longer than 600 mμ), the b-wave did not appear at the early stage of dark adaptation and it appeared later than 6 minutes.

(Published in Acta Ophth. Jap. 62:1970. 1958 in Japanese.)

REFERENCES

1) Adrian, F.D.: a) Nature, **154**:361, 1944. b) J. Physiol. **104**:84, 1945. c) J. Physiol. **105**:24, 1946.
2) Armington, J.C., Johnson, E.P., and Riggs, L.A.: J. Physiol. **118**:289, 1952.
3) Armington, J.C., and Schwab, G.J.: Arch. of Ophthalm. **52**:725, 1954.
4) Auerbach, E., and Burian, H.M.: Amer. J. Ophthalm. **40**:42, 1955.
5) Biersdorf, W.R., and Armington, J.C.: J. Opt. Soc. Amer. **47**:208, 1957.
6) Burian, H.M.: Arch. of Ophthalm. **51**:509, 1954.
7) Granit, R.: Sensory Mechanisms of the Retina, Oxford, 1947.
8) Granit, R. and Munsterhjelm, A.: J. Physiol. **88**:436, 1937.
9) Granit, R. and Wrede, C.M.: J. Physiol. **89**:239, 1937.
10) Hasimoto, T.: Acta O. Jap. **60**:151, 1956.
11) Hayashi, A.: Acta O. Jap. **61**:1670, 1957.
12) Hosoya, Y., Okita, T., and Akune, T.: The Tokoku J. Exp. Med. **34**:352, 1938.
13) Motokawa, K., and Mita, T.: The Tohoku J. Exp. Med. **42**:114, 1942.
14) Polyak, S. L.: The Retina, Chicago 1948.
15) Sakanashi, H.: Acta O. Jap. **62**:656, 1958.
16) Sato, K.: Acta O. Jap. **61**:1241, 1957.
17) Studnitz, G.V.: Kl. Mbl. f. Augenh. **109**:1943.
18) Willmer, E.N.: Retinal structure and color vision, Cambridge, 1946.

ABSORPTION OF FATTY SOLUBLE VITAMINS INTO THE OCULAR MELANIN

Koku KOJIMA and Katsuyoshi MIZUNO

Dept. of Ophthalmology, Nagoya University School of Medicine

In the preliminary report, Mizuno[1] observed that melanin granules in the pigment epithelium and choroid absorb a large quantity of thiamine and riboflavin, and that the melanin granules supply them to the outer segment of visual cell, in which they convert to co-carboxylase and flavin adenine mononucleotide. On the other hand, it is supposed, from reports of Wald and V. Stüdnitz, that carotinoid as a visual substance is also preserved in melanin granules in the pigment epithelium and choroid, but its physico-chemical mechanism has not yet been made clear. Difficulty of this resarch may be based upon water insoluble nature of fatty soluble vitamins. In the present study, however, absorptive effect of melanin granules on fatty soluble vitmains is proved.

Materials

To isolate intact, uncontaminated melanin granules from cattle ocular melanin Laxer's method was used, and Mizuno's method was used to activate melanin granules.

Helenien dipalmitate was extracted from Bayer's Adaptinol by chloroform and crystalized with absolute alcohol.

Helenien dipalmitate was next saponified before use by N-KOH in ethanol at 53°C for 15 min. Helenien alcohol was extracted with light petroleum: this solution, after being

washed with water, was evaporated to dryness.

Carotine was prepared from carot by Kühn's method.

Vitamin A palmitate Hoffmann-La Roche) and its alcohol were prepared in the same method as helenien.

In order to confirm the purity of prepared carotine, helenien alcohol, helenien dipalmitate, and vitamin A alcohol, Kisser's method was used; descending paperchromatography was employed with a solvent of top layer of isopropanol: Water= 1 : 1. The Rf of helenien dipalmitate is 0.00; heleninen alcohol 0.72; vitamin A palmitate 0.00; and vitamin A alcohol 1.0.

Fig. 1. Standard curve of helenien.

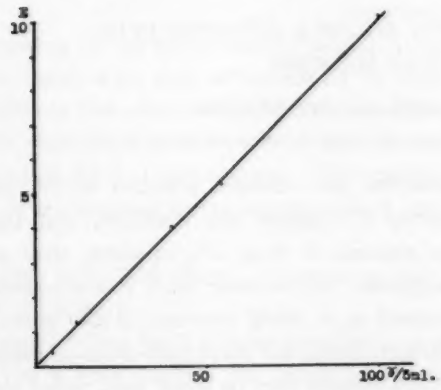

Fig. 2. Absorbed fatty soluble vitamins by melanin granules.

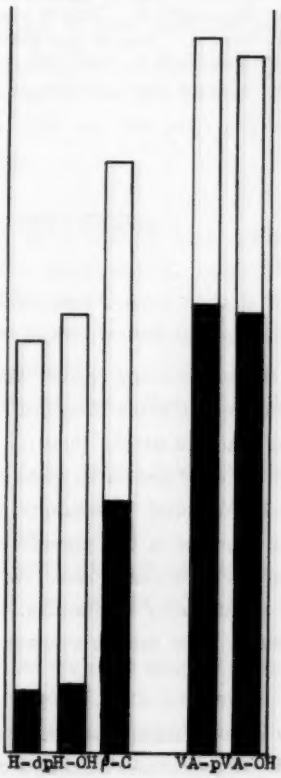

H-dp: Helenien dipalmitate.
H-OH: Helenien alchohol
β-c: β-Carotine
VA-p: Vitamin A palmitate
VA-OH: Vitamin A alcohol

Method

About 20-30γ of β-carotine, helenien dipalmitate and helenien alcohol, and about 40 I.U. of vitamin A palmitate and vitamin A alcohol were first dissolved in 5ml of absolute alcohol and next suspended to 50ml of water. This 6ml of suspension was mixed with 10mg of melanin granules and shaked vigorously, and centrifuged. The 5ml of supernatant was made transparent by adding absolute alcohol, and from this solution fatty soluble vitamins were extracted with light petroleum and their concentrations determined colorimetrically.

To determine the concentration of carotine and vitamin A in reaction mixture the method described by Pett et al. was used, and the concentration of helenien was determined by the standard curve as shown in Fig. 1.

Result

Both vitamin A palmitate and vitamin A alcohol were absorbed in 10mg of melanin granules in the same degree; about 25 I.U. from 40 I.U. as shown in Fig. 2 (a).

Similarly, 3.0γ of helenien dipalmitate and helenien alcohol were absorbed from 20.0γ. and 11.4γ of β-carotine from 27γ.

Comment

Since Wald published his report, it has been observed by many authors that the retina obtains vitamin A and xanthophyl from the blood stream and pigment epithelium. Yamamoto has found that the vitamin A content of retina is larger than that of the pigment epithelium and choroid, and their vitamin A decreases in the first stage of dark adaptaion. It is, therfore, conceivable that the vitamin A is stored in these tissues and supplied to the visual cell for the synthesis of rhodopsin. The mechanism of the storage, however, is still unknown.

Yamamura has found that vitamin A has a good affinity for the melanin pigments which are dispersed in the liver tissue of the dog fish, by staining their frozen section with osmium-glycerol dich-lorohydrin reagents after defatting it moderately by absolute alcohol. This report suggested the idea for our experiment of the absorption of fatty soluble vitamins into melanin granules.

As shown by the above deta, the absorbed volume of vitamin A palmitate in 10 mg of melanin granules was 25.6 I.U. from 40 I.U. and vitamin A alcohol is 25.2 I.U. from 40 I.U.

Collins et al. observed that the rhodopsin content of the eye of piebald rats was more than three times greater than that of albino rats, although albino and piebald rats did not differ in respect of the amount of vitamin A stored in the liver, and moreover, the albinos had extremely low capacity for regenerating rhodopsin. Therefore, their observations have been confirmed the vitamin A absorbing effect of melanin granules.

No agreement was reached on the point of function of xanthophyl in the retina, but it is doubtless that it concerns a photochemical function of the retina directly or indirectly, and helenien alcohol and dipalmitate one of the xanthophyl, were absorbed in some amount

into melanin granule.

Bielig and Busch had observed β-carotine in the pigment epithelium and choroid, but its functional meaning is still obscure, but some amount of it also was absorbed by melanin granules.

As reported in the previous paper, negative charge of melanin granules combines with positive charge of thiamine and riboflavin, so the absorptive effect is based upon the combination between base of the vitamins and acid of melanin. This assumption may be extended to the absobtion of fatty soluble vitamins by melanin granules.

There is no doubt that melanin, one of the high-polymer system, posesses a covalent double bond in its molecule, and that electron may proceed between melanin and carotinoid which also posesses many double bond in its molecule.

It is, therfore, presumable that the electron exchange between the two electron orbitals of these molecules causes melanin granule to combine with fatty soluble vitamins.

Conclusion

Suspensions of vitamin A palmitate, vitamin A alcohol, helenien dipalmitate helenien alcohol and β-carotine, were mixed with melanin granules, and supernatans were measured by colorimetrical methods after extraction with petroleum ether.

Both vitamin A palmitate and vitamin A alcohol were absorbed in 10mg of melanin granule to the same degree; about 25 I.U. from 40 I.U.

Similarly, 3.0γ of helenien dipalmitate and helenien alcohol were absobed (by 3.) from 20.0γ.

And then, 11.4 of β-carotine was absorbed 11.4γ from 27γ.

It is possible that the absorptive effect of melanin granule is related to the π-electron orbitals both in melanin and fatty soluble vitamin.

REFERENCES

1) Brindly et al.: J. Physiol. **116**:350, 1952.
2) Collins et al: Biochem. J. **53**:152, 1953.
3) Kisser: Arch. of Biochem. and Bioph., **63**:118, 1956.
4) Kuhn: Berich. d. Deutsch. Chem. Gesel. **76**: 1, 1951.
5) Kühn: Berich. d. Deutsch. Chem. Gesel. **76**:1, 1951.
5) Mizuno: Clinical Ophth. **6**:256, 1953.
6) Matsushita et al: Clinical Ophth. **10**:1254, 1956.
7) Studnitz: Deutsche Med. Woch. **76**:1, 1951.
8) Yamamoto: Acta Ophth. Jap. **42**:1007 & 2400, 1938.

OPTICAL INVESTIGATION OF LIMIT OF VISUAL ACUITY REPORT 2

Akira YAMAMORI

Department of Ophthalmology, School of Medicine, University of Tokyo

Chapter II

Limit of Acuity of Non-corrected Eyes

7. Distribution of Saturation on the Retina. The test chart for measuring visual acuity usually consists of a number of test types printed in black on white ground. When the subject looks at a test type its image is formed on the macula lutea of the retina. Let the illumination on the macula be Hg when the eye is looking at a blank chart free of test types, and Hi when the whole chart is painted black. Next let the illumination at a point P on the macula be H when the eye looks at an actual test type. A quantity,

$$b=\frac{Hg-H}{Hg-Hi} \tag{2.1}$$

is termed the saturation (or the saturation of blackness) of the test type at the point P (The author). It may be considered as the sum of the intensity of the ray of light reaching the point from each point of the chart. The cases where the phase difference of the light waves must be taken account of, that is, where the role of diffraction is appreciable, will be treated in detail in Chapters III. When the diameter of the pupil is not below 2.5 mm, diffraction has no influence on visual acuity as will be shown later, and discussion will be limited in the present chapter, to the cases where diffraction does not play a significant part.

8. Basic Formula. For convenience' sake let us for the present set aside astigmatism and restrict our discussion to normal, myopic and hyperopic eyes. Let the optical system consisting of the eye and the spectacle lens be represented by A. Let the point P' (Fig. 2.1) be the conjugate of the point P on the retina. The pupil, which functions as a stop, is represented by C.B is a test type and B' its image formed by A. Let B'' be the part of C traversed by the rays coming from B through P'. Since P and P' are conjugate to each other every ray which is to reach P passes through P'. Therefore, among the rays which are to reach P, those and only those that pass through B'' come from B. The saturation of blackness at P when the eye looks at a test type printed in uniform black upon uniformly white ground is given by (2.1). Let the area of C be S and that of B'' be s. Of the light reaching P, suppose a quantity, β passes through each unit area of B'' and another quantity γ through each unit area of C outside B''. Then

$$Hg-H=\gamma S-\{\gamma(S-s)+\beta s\}=(\gamma-\beta)s$$

$$Hg-Hi=\gamma S-\beta S=(\gamma-\beta)S$$

therefore

$$b=\frac{s}{S} \tag{2.2}$$

If an adequately wide area of the chart is entirely black or is completely devoid of

test types and left white, the illumination at every point of the macula lutea is equal. Therefore, though (2.2) is a formula for the saturation at a specified point of the macula, the saturation at two distinct points can be compared by its aid, and it can thus be regarded as a formula representing the distribution of saturation over the macula. This (2.2) is called the basic formula of distribution of saturation, and the distribution of saturation over the retina when the eye is looking at test types of various shapes can be easily derived from it.

Fig. 2.1

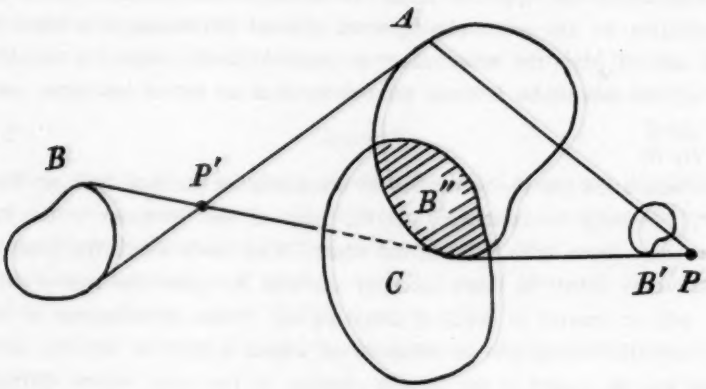

9. A Black and a White Area Separated by a Straight Line. A Test Type of Black Stripes. Let us first consider the case in which the eye looks at a black and a white area having a straight-line boundary between them. Let CD be the projection, from P' on the plane of the pupil, of the boundary. Draw a coordinate axis AA' perpendicular to CD with the center of the pupil as origin, and let the coordinate of the point of intersection E of CD and AA' be p, with the radius of the pupil as unity. Then P can serve as the coordinate of P on the retina. In this case the saturation at P is given by

$$b=\frac{s}{S}=\frac{\text{area of segment } ACD}{\text{area of circle } O}$$

Therefore

$$b=\frac{1}{2}+\frac{1}{\pi}(p\sqrt{1-p^2}+\arcsin p) \qquad (2.3)$$

This is the basic formula for obtaining the saturation of a test type having straight-line boundaries. When $p\leqq -1$ $b=O$ and when $p\geqq -1$ $b=1$.

Helmholz got (2.3) by integrating the illumination on the retina.

Next let us consider a test type consisting of parallel black stripes of a width equal to the space between two adjacent stripes. Let the width (and separation) of the projection of the stripes on the plane of the pupil be ρ times the radius of the pupil. By

Fig. 2.2

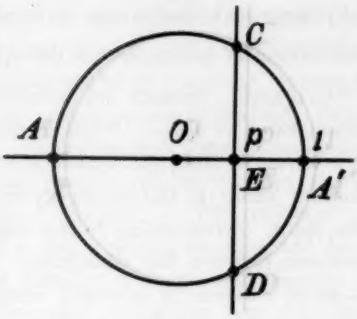

Table 2.1

p \ ρ	1.0	0.8	0.6	0.4	0.2
0	0.392	0.504	0.586	0.462	0.490
0.1	394	508	574	477	500
0.2	406	515	538	500	
0.3	424	511	500		
0.4	455	500			
0.5	500				
Amp	0.216	0.030	0.172	0.076	0.020

Fig. 2.3

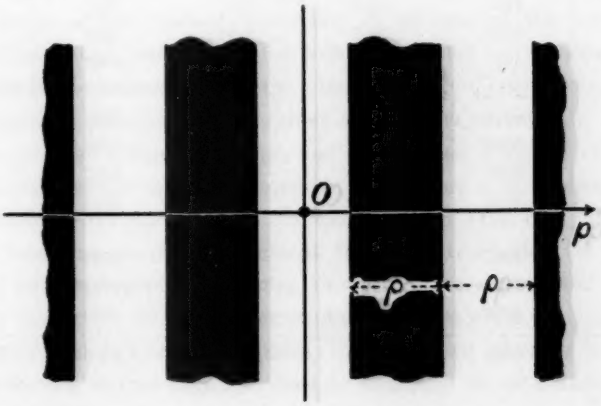

repeated application of (2.3) we can easily get the distribution of saturation. When the number of stripes is sufficiently large, calculation may be carried out only for the region $0 \leq p < \frac{\rho}{2}$ or $0 \geq p \cdot \frac{\rho}{2}$. The distribution of saturation for the values of ρ between 1.0 and 0.2 is given in Table 2.1, in which amp ρ denotes the difference between the maximum valve of b,b_{max} and the minimum value of b,b_{min}. When $\rho=0$,$b=0.5$ all over the retina, of course, and amp $(0)=0$. As is apparent from the table $b(0)=b_{min}$ at $\rho=1.0$ and the distribution of b has the maximum value at the places corresponding to the black stripes and the minimum value at the places corresponding to the white stripes, while at $\rho=0.6$, $b(0)$ becomes b_{max} and the relation between the distribution and the type is reversed. This implies that the black-white relation is reversed when $\rho=0.6$, the white ground appearing dark and the black part light. It is also seen that amp (ρ) has a minimum near $\rho=0.8$ and assumes large values in the neighborhood of $\rho=0.6$. This can be qualitatively confirmed by looking through a convex lens of +6.0 D and moving the test type (in the form of stripes) farther from the eye. Now let us find the exact value of ρ for which amp (ρ) is minimum. Calculalion shows that according as ρ is 0.75, 0.80, 0.81, 0.82, 0.83, 0.85, and 0.90, amp (ρ) is 0.0760, 0.0332, 0.0260, 0.0196, 0.0256, 0.0488, and 0.1060. Therefore guessing the minimum to occur between $\rho=0.82$ and $\rho=0.83$ the values of amp (ρ) for the values of ρ between 0.821 and 0.825 are tabulated in table 2.2, which shows that the minimum occurs near $\rho=0.823$.

Table. 2.2

p \ ρ	0.821	0.822	0.823	0.824	0.825
0	0.5000	0.5000	0.5000	0.5000	0.5000
0.05	4958	4959	4960	4960	4961
0.1	4921	4924	4925	4927	4929
0.15	4906	4908	4912	4915	4918
0.2	4947	4952	4957	4962	4967
0.25	5001	5006	5012	5017	5022
0.3	5040	5046	5051	5057	5062
0.35	5066	5071	5077	5082	5088
0.4	5076	5082	5087	5093	5099
$p/2$	5076	5082	5088	5094	5100
0.12					4920
0.13	4909	4912	4913	4915	4918
0.14	4907	4908	4910	4914	4917
0.16	4908	4911	4914	4918	4921
Amp	0.0188	0.0184	0.0180	0.0188	0.0200

10. Marginal Acuity ; Coefficient of marginal Acuity. In the preceding article it was stated that, if aberration is disregarded the blurring of the retinal image of a test type consisting

of stripes is determined by the ratio between the dimension of the projection of the test type on the plane of the pupil and the radius of the pupil in the case of the myopic and the hyperopic eye. This is true, in fact, with other test types as well, and by its use a formula for the limit of visual acuity of a myopic, hyperopic, or astigmatic eye wearing a lens that does not give full correction can be derived. Before doing that let us define the term marginal acuity. When an eye wearing an incorrect lens recedes from a test type the acuity reckoned from its size and the distance at which it first becomes illegible is called the marginal acuity (Yamamori)……The ordinary "acuity" is determined by the maximum distance at which a test type can be read, and the author's marginal acuity is determined by the minimum distance at which it is illegible.

Let a be the standard dimension of the test type, e.g. the width of a stripe in the striped test type or the width of the opening of the Landolt ring. Let the ratio of the dimension of the projection of a to the radius of the pupil be ρ. As stated in Art. 9, if $\rho>0.823$ a striped test type appears as stripes and the black as black and the white as white. If $\rho=0.823$ the surface appears uniformly gray and no stripes are visible, and if $\rho<0.823$ stripes are visible but with the black and the white reversed. This phenomenon of reversal is most conspicuous in the neighborhood of $\rho=0.6$. As ρ becomes smaller the stripes become less and less distinct and finally invisible as ρ approaches 0. In the case of the Landolt ring, it appears as ring if $\rho>0.8$ and the direction of the opening can be recognized. At $\rho=0.8$ the ring is barely visible as ring and the opening can just be recognized. With some practice, however, one can generally tell the direction of the opening till ρ equals 0.5. In ordinary consulting room practice 0.8 may be regarded as the lower limit of ρ for the direction of the opening to be visible. This limiting value of ρ at which the test type becomes indistinguishable is termed the coefficient of marginal acuity (Yamamori) and denoted by ν. For example, in the Landolt ring ν is 0.8 if the width of the opening is taken as standard dimension, and in the striped test type $\nu=0.823$ with the width of a stripe as the standard dimension. In the case of the 6-6 ring (Fig. 2.4) calculation and observation both give $\nu=0.8$ with one quarter of the diameter of the ring taken as the standard dimension. In the checker pattern $\nu=1.2$ with the side of each square as the standard dimension. It is rather troublesome to calculate from theory the values of ν for a ring or a letter test type, and the process is further complicated by the problem of contrast between contiguous surfaces. Therefore it is necessary to check the result of culculation with experiment. In the ring test type very different values are assumed by ν according to the requirement for visibility whether the ring must be recognized as ring and the opening distinctly as opening or merely the direction of the opening need be detected. We may experimentally find the ν for an unknown test type by placing it beside a known one and viewing them together through a suitable convex lens. In this method a striped type may best be employed as the standard of comparison. If the number of the stripes is sufficiently large the distribution of saturation alone need be considered and there is no need for bothering about contrast. But in actual practice

the number cannot be increased indefinitely and we must be contented a test type with three or four stripes. Then the value of ν may be considered approximately 0.823.

The striped test type is desirable as the standard of comparison in measuring ν be-

Fig. 2.4
6-6 ring for the acuity of 0.3 at 5m.

Fig. 2.5

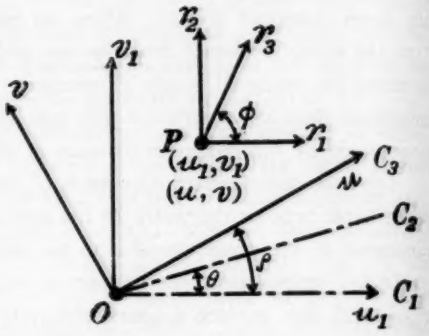

cause the black and the white stripes are seen as such if $\rho > \nu$ and as white and black if $\rho < \nu$, thus facilitating the determination of the point of the marginal visibility. Prepare a set of striped test types of various sizes and post them on the wall. Next place in their midst the test type whose ν is to be measured, e.g. a Landolt ring for $\frac{0.5}{5}$, that is, one with an opening 15 mm in width. The observer's eye is corrected as completely as possible for astigmatism with a cylinder and further a spherical lens ca +4 D stronger than the correct lens for the eye is worn. With the other eye screend the observer views the test types while advancing toward and receding from the wall, stopping at the position where the test type in question just becomes illegible. Find which of the striped types is in the same state. At the distance where a $\frac{0.5}{5}$ Landolt ring can just be recognized as ring the stripe type for the same acuity is approximately in the state of marginal visibility. (A type with stripes 15 mm in width is for $\frac{0.5}{5}$.) Therefore we conclude that the value of ν for the Landolt ring is about 0.8.

The value of ν varies according to the choice of the standard dimension. For example, if we adopt the diameter of the Landolt ring as the standard dimension ν will be five times as large as when the width of the opening is adopted, that is $\nu = 4$. Let the standard dimension of a test type corresponding to the acuity of 1.0 at 5 m be a_0 and call the quantity n, defined by

$$n = \frac{5}{a_0}\nu \qquad (2.4)$$

the absolute coefficient of the marginal acuity, which is a constant characteristic of the particular test type and independent of the choice of the standard dimension. When we want to distinguish ν and n the former is called the relative coefficient. The value of n is 2740 for the striped test type and 2700 for the Landolt ring and the 6-6 ring.

Table. 2.3

θ	$\theta+\varepsilon$	R	V'
−30°	6°49′	14.9	0.122
−15°	21°49′	18.2	0.100
0°	36°49′	23.0	0.079
15°	51°49′	27.5	0.066
30°	66°49′	31.0	0.059
45°	81°49′	32.8	0.055
60°	96°49′	32.9	0.055

11. Combination of two systems each consisting of a spherical and a cylindrical lens. Let us work out the principle governing combination of cylindrical lenses which has a close connection with the marginal acuity of the astigmatic eye. It was demonstrated by Reche (1913) and others that the refraction of a pair of thin cylindrical lenses in close contact having a common optical axis could be represented by a combination of a spherical and a cylindrical lens. But this has been disputed a great deal in connection with existence of bistigmatism proposed by Marquez (1909). Therefore it may not be useless to demonstrate that, if aberration is disregarded, such sphero-cylindrical combination has same antirefraction, inclination and derivative of inclination as a combination of two thin cylindrical lenses even with respect to extra-axial rays.

Let there be two sets of such sphero-cylindrical combinations, the first set consisting of a sphere S_1 and a cylinder C_1 whose powers are S_1 and C_1 diopters respectively ,and the second set, of a sphere S_2 and a cylinder C_2 of powers S_2 and C_2 diopters respectively. Take the axis of C_1 as the u_1 axis of coordinates and draw the v_1 axis perpendicular to it. (Fig 2.5) Let the point where the optical axis passes through the plane of the lens be taken as origin. Suppose the axis of C_2 makes an angle of θ with that of C_1. Let the coordinates of a point P be (u_1, v_1). Draw another set of coordinate axes r_1 and r_3, the angle between r_1 and u_1 being ϕ, and let the coordinates of P with respect to them be $(r_1\ r_3)$. At P let the first combination of lenses have an inclination $I_{1,3}\ (r_1, r_3)$ along r_3 and the second combination an inclination $I_{23}\ (r_1, r_3)$. Then by (1.83)

$$\frac{\partial \cot I_{1,3}\ (r_1, r_3)}{\partial r_3} = C_1 \sin\phi \cos,\ \phi, \frac{\partial \cot I_{2,3}\ (r_1, r_3)}{\partial r_3} = C_2 \sin(\phi-\theta)\cos(\phi-\theta) \quad (2.5)$$

If we call the combination of the two combinations, i.e. the system of all the four lenses, the third combination, the cotangent of the inclination of the third combination at P along r_3 is given by

$$\cot I_{3,3}\ (r_1, r_3) = \cot I_{1,3}\ (r_1, r_3) + \cot I_{2,3}\ (r_1, r_3) \quad (2.6)$$

provided all the lenses are thin and in contact and the whole system can be regarded to lie on a single plane, and provided, moreover, all the inclinations are nearly right angles, which conditions all paraxial rays may be assumed to satisfy.

From (2.6) we get, by (2.5),

$$\frac{\partial \cot I_{3,3}(r_1, r_3)}{\partial r_3} = \frac{1}{2}\{C_1 \sin 2\phi + C_2 \sin 2(\phi - \theta\} \tag{2.7}$$

Let the value of ϕ which makes the left side of the equation vanish be ρ, then

$$C_1 \sin 2\rho + C_2 \sin 2\rho \cos 2\theta = C_2 \cos 2\rho \sin 2\theta \quad \therefore \quad \tan 2\rho = \frac{C_2 \sin 2\theta}{C_1 + C_2 \cos 2\theta} \tag{2.8}$$

The left side of (2.7) will vanish also when $\phi = 0$ or $\phi = \rho + \frac{\pi}{2}$.

The equation (1.86) will thus be valid at P, and by Art. 5 a sphere S_3 and a cylinder C_3 and a point G can be chosen so that G will have same antirefraction, inclination and derivative of inclination with respect to the combination of S_3 and C_3 as the corresponding quantities which P has with respect to the third combinalion. Here the direction of the axis of C_3 is already known from (2.8).

In Fig. 2.5, draw r_1 and r_2 axes through P parallel respectively to u_1 and v_1, and let the antirefraction and inclination at P along r_1 and r_2 with respect to the third combination be $A_{3,1}(r_1, r_2)$, $A_{3,2}(r_1, r_2)$,

$I_{3,1}(r_1, r_2)$ and $I_{3,2}(r_1\ r_2)$ respectively. Then putting $\phi = 0$ and $\phi = \frac{\pi}{2}$ in (2.7) we have

$$\left.\begin{aligned} \frac{\partial \cot I_{3,1}(r_1, r_2)}{\partial r_1} &= -\frac{C_2}{2} \sin \theta \\ \frac{\partial \cot I_{3,2}(r_1, r_2)}{\partial r_2} &= \frac{C_2}{2} \sin 2\theta \end{aligned}\right\} \tag{2.9}$$

which, substituted in (1.22) gives

$$U = -C_2 \sin 2\theta \tag{2.10}$$

Let the antirefraction of the first combination at P along r_1 and r_2 be $A_{1,1}(r_1\ r_2)$ and $A_{1,2}(r_1, r_2)$ respectively and the antirefraction of the second combination be $A_{2,1}(r_1, r_2)$ and $A_{2,2}(r_1, r_2)$ respectively. Then

$$A_{3,1}(r_1, r_2) = A_{1,1}(r_1, r_2) + A_{2,1}(r_1, r_2) \tag{2.11}$$

$$A_{3,2}(r_1, r_2) = A_{1,2}(r_1, r_2) + A_{2,2}(r_1, r_2) \tag{2.12}$$

Putting $\gamma = 0\ ; \frac{\pi}{2}\ ; -\theta$; and $\frac{\pi}{2} - \theta$ in turn in (1.58) and substituting these values in (2.11) and (2.12) we get

$$A_{3,1}(r_1, r_2) = S_1 + S_2 + C_2 \sin^2 \theta \tag{2.13}$$

$$A_{3,2}(r_1, r_2) = S_1 + S_2 + C_1 + C_2 \cos^2 \theta \tag{2.14}$$

and substituting (2.10), (2.13) and (2.14) in (1.69) and (1.76) we get

$$C_3 = \sqrt{C_2^2 \sin^2 2\theta + (C_1 + C_2 \cos 2\theta)^2} = \sqrt{C_1^2 + C_2^2 + 2C_1 C_2 \cos 2\theta} \tag{2.15}$$

$$S_3 = S_1 + S_2 + \frac{1}{2}(C_1 + C_2 - C_3) \tag{2.16}$$

Substitution of the same in (1.71) and (1.74) gives

$$\sin \rho = \frac{1}{\sqrt{2}} \sqrt{1 - \frac{C_1 + C_2 \cos 2\theta}{C_3}}, \quad \cos \rho = \frac{1}{\sqrt{2}} \sqrt{1 + \frac{C_1 + C_2 \cos 2\theta}{C_3}} \tag{2.17}$$

if $C_2 \sin 2\theta \geqq 0$ and

$$\sin \rho = -\frac{1}{\sqrt{2}} \sqrt{1 - \frac{C_1 - C_2 \cos 2\theta}{C_3}}, \quad \cos \rho = \frac{1}{\sqrt{2}} \sqrt{1 + \frac{C_1 + C_2 \cos 2\theta}{C_3}} \tag{2.18}$$

if $C_2 \sin 2\theta \leqq 0$.

Having thus obtained all the elements of the third combination let us see whether G will occupy the same position as P if the optical system to which P belongs is replaced with the other system containing G. First, from (2.17) and (2.18), by (2. 15),

$$\sin 2\rho = \pm \frac{C_2 \sin 2\theta}{C_3} \geqq 0 \tag{2.19}$$

if $C_2 \sin 2\theta \geqq 0$,

and, $$\sin 2\rho = \mp \frac{C_2 \sin 2\theta}{C_3} \leqq 0 \tag{2.20}$$

if $C_2 \sin 2\theta \leqq 0$.

Now $C_3 \geqq 0$ by (2.15). Therefore whatever the sign of $C_2 \sin 2\theta$ may be we have

$$\sin 2\rho = \frac{C_2 \sin 2\theta}{C_3} \tag{2.21}$$

Now take the u axis in the direction of the axis of C_3 and draw the v axis perpendicular to it through 0 (Fig. 2.5). Let the coordinates of G with respect to these axes be (u, v). Then from (1.82)

$$u = \frac{\cot I_{3,1}(r_1, r_2) \sin \rho - \cot I_{3,2}(r_1, r_2) \cos \rho}{S_3} \tag{2.22}$$

$$v = \frac{\cot I_{3,1}(r_1, r_2) \cos \rho + \cot I_{3,2}(r_1, r_2) \sin \rho}{S_3 + C_3} \tag{2.23}$$

Let the inclinations at P along r_1 and r_2 with respect to the first combination alone be respectively $I_{1,1}(r_1, r_2)$ and $I_{1,2}(r_1, r_2)$, let the corresponding quantities with respect to the second combinstion be respectively $I_{1,1}(r_1\ r_2)$ and $I_{2,2}(r_1, r_2)$ then by (1.56) and (1.57) we have

$$\left.\begin{aligned} &\cot I_{1,1}(r_1, r_2) = v_1(S_1 + C_1),\ \cot I_{1,2}(r_1, r_2) = -u_1 S_1, \\ &\cot I_{2,1}(r_1, r_2) = (v_1 \cos\theta - u_1 \sin\theta)(S_2 + C_2)\cos\theta + (u_1 \cos\theta + v_1 \sin\theta) S_2 \sin\theta, \\ &\cot I_{2,2}(r_1, r_2) = (v_1 \cos\theta - u_1 \sin\theta)(S_2 + C_2) \sin\theta - (u_1 \cos\theta + v_1 \sin\theta) S_2 \cos\theta \end{aligned}\right\} \tag{2.24}$$

which, substituted in (2.22),

gives in turn by (2.21), (2.17) and (2.18)

$$u = u_1 \cos\rho + v_1 \sin\rho + \frac{1}{2 S_3 \cos\rho}\left[v_1\{(C_1 + C_3 + C_2 \cos 2\theta)\frac{C_2 \sin 2\theta}{2C_3} - \frac{C_2}{2}\sin 2\theta, \frac{C_1 + C_3 + C_2 \cos 2\theta}{C_3}\right.$$

$$\left. - u_1\{(C_1 - C_3 + C_2 \cos 2\theta)\frac{1}{2}\frac{C_1 + C_3 + C_2 \cos 2\theta}{C_3} + C_2 \sin 2\theta, \frac{1}{2}\frac{C_2 \sin 2\theta}{C_3}\right]$$

Therefore $$u = u_1 \cos\rho + v_1 \sin\rho \tag{2.25}$$

Substituting (2.24) in (2.23) we get

$$v = v_1 \cos\rho - u_1 \sin\rho$$

Thus (2.25) and (2.26) show that G (u, v) and P (u_1, v_1) occupy an identical position, Q.E.D.

In the foregoing proof we assumed $C_3 \geqq 0$, but from the property of a sphero-cylindrical combination it is clearly to be seen that we could have made $C_3 \leqq 0$ and replaced S_3 and α with $S_3 - C_3$ and $\alpha \pm \frac{\pi}{2}$ respectively.

12. Effect of a cylindrical lens whose axis makes an obliques angle with the axis of

astigmatism

Let C_1 be a cylinder which when worn in the usual way, exactly compensates for the astigmatism of an eye. Then the image of a point on the retina formed by the combined system of the eye and the lens will be also a point. If now another cylinder C and a spherical lens L are worn in adition to and in close contact with C_1 the rays coming from a point will pass through a linear image P_1' parallel to the axis of C and another P_2' perpendicular to it. But by Art. 11 the combination of C_1, C and L is equivalent to the combination of a cylinder and a sphere, say, C_2 and L' respectively. Therefore if C_2 and L' are worn instead of the first combination they will form the images of P at P_1' and P_2'. Let the refraction of the eye in the direction of the axis of C_1 be M_1 and therefore that in the direction perpendicular to the axis be M_1+C_1. Let $L_1=M_1+L'$. In Fig. 2.6, OM_1, OL and OL_1 indicate the direction of the axes of C_1, C and C_2 respectively. Let $<M,OL$, be ϕ and $<M,OL$ be α. Here M_1,C_1,L_1,C_2 and ϕ are known quantities and the unknowns C,L and α may be easily obtained as follows:

Fig. 2.6.

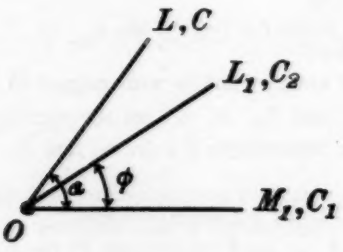

The lens $(M_1,\ C_1)$ and $(L,\ C)$ together are equivalent to the lens $(L_1,\ C_2)$. Now consider a lens whose refraction is$-C_1$ and which is so placed that its axis is parallel to that of C_1, and call it$-C_1$. If the combination $(M_1,\ C_1)$ and $(-M_1,-C_1)$ are superposed the whole will show no refraction at all. Therefore

$(M_1,\ C_1)+(L,C)+(-M_1,-C_1)=(L,C)$ and

$(L_1,\ C_2)+(-M_1,-C_1)=(L,C)$

Now substitute $\phi,-M_1,\ L_1$, and$-C_1$ for θ_1S_1,S_2 and C_1 respectively, leaving C_2 alone and putting $C_3=C,S_3=L,\rho=\alpha$ in (2.15), (2.16) and (2.21) Then we get

$$C=\sqrt{C_1^2+C_2^2-2C_1C_2\cos 2\phi}, \tag{2.27}$$

$$L=L_1-M_1+\frac{1}{2}(-C_1+C_2-C). \tag{2.28}$$

$$\sin 2\alpha=\frac{C_2\sin 2\phi}{C} \tag{2.29}$$

From the last equation we get two values of α between $-\pi$ and$+\pi$, of which, by (2.17) and (2.18) we should adopt the one with the larger absolute value if C_1 is larger than $C_2\cos 2\phi$ and the other if otherwise. It goes without saying that we may make the

cylinder $-C$ and the sphere $L+C$, changing α into $\alpha \pm \frac{\pi}{2}$

Fig. 7.

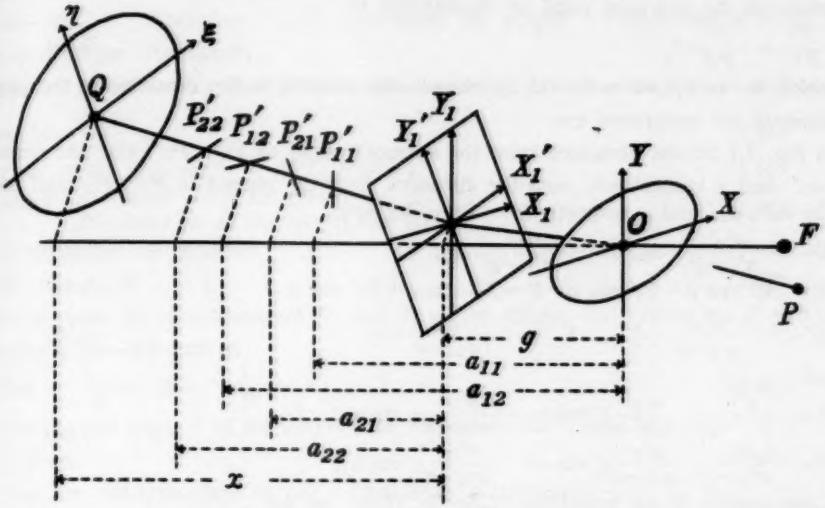

13. Test-type-plane Ellipses. In an astigmatic eye the principal meridians are in general perpendicular to each other, and the defect can be completely corrected by wearing the combination of a spherical and a cylindrical lens. Therefore the refracting system of an astigmatic eye may be regarded to belong to the group having a pair of perpendicular focal lines described in Art. 5. In other words, the image of a point P on the retina formed by an astigmatic system consists of two line segments P'_{11} and P'_{12} perpendicular to each other but not lying on a common plane (Fig. 2.7). Next let us consider the case of an astigmatic eye wearing a combination of a sphere of power L_1D and a cylinder of power C_2D instead of the combination of a sphere (M_1 D) and a cylinder (C_1 D) which are the right lenses for complete correction. Draw X and Y axes on the plane of the entrance pupil and X_1 and Y_1 axes on the plane of the lenses, making X and X_1 parallel to and Y and Y_1 perpendicular to the axis of the cylinder. Draw another set of axes X_1' and Y_1' on the plane of the lenses at the position which the X-Y axes would occupy if they were rotated through an angle equal to α given by (2.29). Draw ξ and η axes on the plane of the test type parallel to X_1' and Y_1' respectively. The origines of all these coordinate axes are to lie on the path of the ray passing through the center of the entrance pupil and the point P. Let P_{11} and P_{12} be the line images, parallel respectively to Y and X, of P formed by the eye, and let P_{21}' and P_{22}' the line images, parallel respectively to Y_1' and X_1', of P formed by the eye with the lenses L_1 and C_2 on.

Since the chief cause of astigmatism is departure of the surface of the cornea from a true sphere, the image of the periphery of the pupil as seen from the front of the

eye does not lie on a plane. But as the distance between the cornea and the pupil is small, the image of the latter may be regarded as coplanar without perceptible error. Wpen the astigmatism is very strong the apparent shape of the pupil becomes an ellipse. Therefore let the entrance pupil be represented by

$$\frac{X^2}{P_1^2}+\frac{Y^2}{P_2^2}=1, \tag{2.30}$$

which is an ellipse with the principal axes parallel to the direction of the principal meridians of the astigmatic eye.

In Fig. 2.7 let the distances from the entrance pupil to P_{11}', P_{12}' and the lenses be a_{11}', a_{12}' and g respectively, and the distances from the glasses to P_{21}', P_{22}' and the test type be a_{21}', a_{22}' and x respectively. Then we have

$$X=\frac{a'_{11}}{a'_{11}-g}X_1,\ Y=\frac{a'_{12}}{a'_{12}-g}Y_1, \tag{2.31}$$

$$X_1=X_1'\cos\alpha-Y_1'\sin\alpha,\ Y_1=X_1'\sin\alpha+Y_1'\cos\alpha, \tag{2.32}$$

$$X_1'=\frac{a'_{21}}{a'_{21}-x}\xi\ ,\quad Y_1'=\frac{a'_{22}}{a'_{22}-x}\eta\ , \tag{2.33}$$

and

$$\left.\begin{aligned} X&=\frac{a'_{11}}{a'_{11}-g}\left(\frac{a'_{21}}{a'_{21}-x}\xi\cos\alpha-\frac{a'_{22}}{a'_{22}-x}\eta\sin\alpha\right),\\ Y&=\frac{a'_{12}}{a'_{12}-g}\left(\frac{a'_{21}}{a'_{21}-x}\xi\sin\alpha+\frac{a'_{22}}{a'_{22}-x}\eta\cos\alpha\right),\end{aligned}\right\} \tag{2.34}$$

Consequently, if we transform (2,30) by (2.34) we get

$$\frac{a^2{}_{11}}{P_1^2\,(a'_{11}-g)^2}\left(\frac{a'_{21}}{a'_{21}-x}\xi\cos\alpha-\frac{a'_{22}}{a'_{22}-x}\eta\sin\alpha\right)^2+\frac{a'^2_{12}}{P_2^2(a'_{12}-g)^2}$$
$$\left(\frac{a'_{21}}{a'_{21}-x}\xi\sin\alpha+\frac{a'_{22}}{a'_{22}-x}\eta\cos\alpha\right)^2=1 \tag{2.35}$$

which is the projection of the entrance pupil on the plane of the test type from the point P. Now there is the following relation between the coefficients:

$$\left.\begin{aligned} &\frac{1}{a'_{11}-g}=-M_1,\ \frac{1}{a'_{12}-g}=-M_2,\ (M_2=M_1+C_1)\\ &\frac{1}{a'_{21}}=L,\ \frac{1}{a'_{22}}=L+C\end{aligned}\right\} \tag{2.36}$$

whence

$$\left.\begin{aligned} &\frac{a'_{11}}{a'_{11}-g}=1-gM_1,\quad \frac{a'_{12}}{a'_{12}-g}=1-gM_2\ ,\\ &\frac{a'_{21}}{a'_{21}-x}=\frac{1}{1-xL},\ \frac{a'_{22}}{a'_{22}-x}=\frac{1}{1-x(L+C)}\end{aligned}\right\} \tag{2.37}$$

Substituting these in (2.35) we get

$$\frac{(1-gM_1)^2}{P_1^2}\left\{\frac{\xi\cos\alpha}{1-xL}-\frac{\eta\sin\alpha}{1-x(L+C)}\right\}^2+\frac{1-gM_2)^2}{P_2^2}\left\{\frac{\xi\sin\alpha}{1-xL}+\frac{\eta\cos\alpha}{1-x(L+C)}\right\}^2=1. \tag{2.38}$$

If we put

$$\left.\begin{aligned} A&=\frac{1}{(1-xL)^2}\left\{\frac{(1-gM_1)^2}{P_1^2}\cos^2\alpha+\frac{1-gM_2)^2}{P_2^2}\sin^2\alpha\right\},\\ B&=\frac{1}{(1-x(L+C))^2}\left\{\frac{1-gM_1)^2}{P_1^2}\sin^2\alpha+\frac{(1-gM_2)^2}{P_2^2}\cos^2\alpha\right\},\\ H&=\frac{\sin\alpha\cos\alpha}{(1-xL)(1-x(L+C))}\left\{-\frac{(1-gM_1)^2}{P_1^2}+\frac{(1-gM_2)^2}{P_2^2}\right\},\end{aligned}\right\} \tag{2.39}$$

in order to simplify calculation, (2.38) becomes

$$A\xi^2+2H\xi\eta+B\eta^2=1. \tag{2.40}$$

Since by (2.40) we have

$$AB-H^2=\frac{(1-gM_1)^2(1-gM_2)^2}{P_1^2P_1^2\ (1-xL)^2\ \{1-x(L+C)\}^2} \tag{2.41}$$

and, in general $(1-gM_1)(1-gM_2)\neq 0$ (2.42)

$AB-H^2>0$. Therefore (2.40) represents an ellipse. This ellipse is called a test-type-plane ellipse (Yamamori).

Revolve ξ and η axes through an angle β and call them ξ' and η', where β is given by

$$\tan 2\beta=\frac{2H}{A-B} \tag{2.43}$$

Then (2.40) becomes $A\xi'^2+B'\eta'^2=1$ (2.44)

where
$$\left.\begin{aligned} A'&=A\cos^2\beta+H\sin 2\beta+B\sin^2\beta \\ B'&=A\sin^2\beta-H\sin 2\beta+B\cos^2\beta \end{aligned}\right\} \tag{2.45}$$

There is also the relation

$$A'=B'=A+B \tag{2.46}$$

From these the semidiameters R_1 and R_2 of the ellipse (244) along the ξ' and η' axes respectively are obtained as

$$R_1=\frac{1}{\sqrt{A'}},\quad R_2=\frac{1}{\sqrt{B'}}\ . \tag{2.47}$$

The position angle ε of the ξ'axis with respect to the x axis is

$$\varepsilon=\alpha+\beta \tag{2.48}$$

Thus the test-type-plane ellipse is completely determined.

14. Extention of the meaning of the basic formula

Let us consider the size of the part of the plane of the entrance pupil traversed by the rays coming from an infinitesimal part of the test type and reaching a point P on the retina. In Fig. 2.8 let

Fig. 2.8

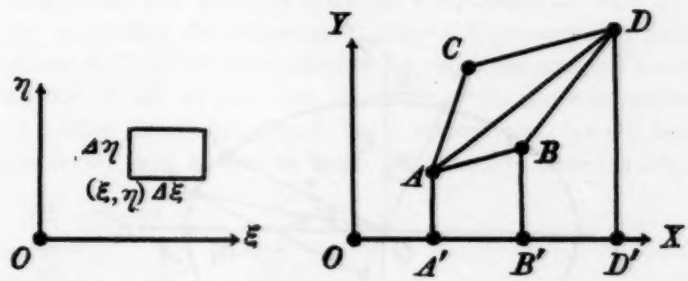

A denote the point $\{X(\xi,\eta),\ Y(\xi,\eta)\}$,

B the point $\{X(\xi+\Delta\xi,\eta),\ Y(\xi+\Delta\xi,\eta)\}$,

C the point $\{X(\xi,\eta+\Delta\eta), Y(\xi,\eta+\Delta\eta)\}$ and

D the point $\{X(\xi+\Delta\xi,\eta+\Delta\eta),\ Y(\xi+\Delta\xi,\eta+\Delta\eta)\}$.

On the plane of the test type, i.e., $\xi\eta$ plane, the area of the infinitesimal rectangle having vertices at (ξ,η), $(\xi+\Delta\xi,\eta)$, $(\xi,\eta+\Delta\eta)$, and $(\xi+\Delta\xi,\eta+\Delta\eta)$ is $\Delta\xi\Delta\eta$. The rays starting from this rectangle and reaching P will pass through the quadrilateral $ABCD$ on

the XY plane. To obtain the area of the triangle ABD draw perpendiculars to the X axis from A,B and D, and let them intersect it at A',B' and D', respectively. Then triangle ABD

$$= \frac{1}{2}[A'B'(DD'-BB')-B'D'(BB'-AA')]=\frac{1}{2}[\{X(\xi+\Delta\xi,\eta)-X(\xi,\eta)\}\{Y(\xi+\Delta\xi,\eta+\Delta\eta)-Y(\xi+\Delta\xi,\eta)\}-\{X(\xi+\Delta\xi,\eta+\Delta\eta)-X(\xi+\Delta\xi,\eta)\}\{Y(\xi+\Delta\xi,\eta)-Y(\xi,\eta)\}]$$

$$=\frac{1}{2}\Delta\xi\cdot\Delta\eta\left(\frac{\partial X}{\partial\xi}\cdot\frac{\partial X}{\partial\eta}-\frac{\partial Y}{\partial\zeta}\right)$$

Similarly,

$$\text{triangle } ACD=\frac{1}{2}\Delta\zeta\cdot\Delta\eta\left(\frac{\partial X}{\partial\xi}\cdot\frac{\partial Y}{\partial\eta}-\frac{\partial X}{\partial\eta}\cdot\frac{\partial Y}{\partial\xi}\right)$$

Therefore

$$\frac{ABCD}{\Delta\xi\cdot\Delta\eta}=\frac{\partial X}{\partial\xi}\cdot\frac{\partial Y}{\partial\eta}-\frac{\partial X}{\partial\eta}\cdot\frac{\partial Y}{\partial\xi} \tag{2.49}$$

whence, by (2.34)

$$\frac{ABCD}{\Delta\xi\Delta\eta}=\frac{a'_{11}a'_{12}a'_{21}a'_{22}}{(a'_{11}-g)(a'_{12}-g)(a'_{21}-x)(a'_{22}-x)} \tag{2.50}$$

The left side of the equation is a constant independent of X,Y,ξ and η. Therefore (2.2) has a meaning on the test plane as well as on the plane of the entrance pupil. In other words, if S is the area of the test-type-plane ellipse and s, the area of the test type included in it, then (2.2) represents the degree of saturation of the test type at P. If the test-type-plane ellipse becomes a segment of a straight line as a limiting case of an ellipse (2.2) must be calculated from (2.3).

Fig. 2.9

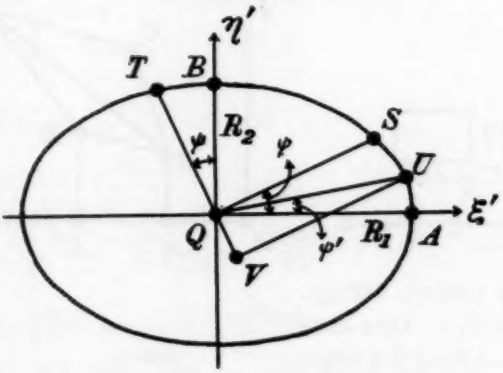

15. Formula for marginal acuity. Let a_0 be the standard dimension [See Art. 10] in meter of the test type for an eye of acuity 1.0 to be used at a distance of 5 meters. For example, a_0 is equal to 0.0015 for the Landolt ring. Suppose a test type whose standard dimension is a m. is at the threshold of illegibility [See Art. 10.] when placed at a distance of x m. from the eye being tested. Then the marginal acuity V' is given by

$$V' \frac{x}{5} \cdot \frac{a_0}{a} \tag{2.51}$$

If the test-type-plane ellipse is a circle of radius R the coefficient of marginal acuity ν is given by

$$\frac{a}{R} = \nu \tag{2.52}$$

From the above two we get

$$V' = \frac{a_0 x}{5\nu R} \tag{2.53}$$

The test-type-plane ellipse becomes a circle when a myopic or hypermetropic eye wears a spherical lens and when an astigmatic eye is corrected by a suitable lens for the astigmatism only. This simple case will be treated in Art. 17.

The ring test type, of which the subject is required to tell the direction of the opening in the ring, gives very different values of acuity according to the direction of the opening when used for an astigmatic eye. Two letter test types may give a consistent value of the acuity of a simple myopic eye while giving unequal values for an astigmatic eye. This is because an astigmatic eye has different acuity for different directions. For the purpose of measuring with the greatest accuracy the acuity which varies with directions the striped test type is the best. It may be considered to give the acuity in the direction perpendicular to the length of the stripes.

With the ξ' η' coordinate axes the test-type-plane ellipse is represented by (2.44). Let Q be the origin (Fig. 2. 9) and draw a line QS which makes an angle of ψ with the ξ' axis and let it intersect the ellipse at S. Draw QT perpendicular to QS and let it intersect the ellipse at T. If QS is the direction for which the marginal acuity is wanted QT is the direction of the stripes. Let A and B be the points of intersection of the ellipse with the positive part of the axes, ξ' and η' respectively. Let QU be the semidiameter conjugate to QT and denote the angle UQA by ψ'. Since $QA = R_1$ and $QB = R_2$

$$\left.\begin{aligned} &\tan\left(\psi + \frac{\pi}{2}\right) \tan\psi' = -\frac{R_2^2}{R_1^2} \\ &\text{whence} \quad \frac{\sin\psi'}{\cos\psi'} = \frac{R_2^2}{R_1^2} \cdot \frac{\sin\psi}{\cos\psi} \\ &\text{Therefore} \quad \sin^2\psi' = \frac{R_2^4 \sin^2\psi}{R_1^4\cos^2\psi + R_2^4\sin^2\psi} \\ &\qquad\qquad \cos^2\psi' = \frac{R_1^4\cos^2\psi}{R_1^4\cos^2\psi + R_2^4\sin^2\psi} \end{aligned}\right\} \tag{2.54}$$

If we respresent the test-type-plane ellipse in polar coordinates with Q as pole and ξ' as initial line and let QU be r, we have

$$r^2 = \frac{R_1^2 R_2^2}{R_1^2\sin^2\psi' + R_2^2\cos^2\psi'} \tag{2.55}$$

Draw UV perpendicular to QT and let their intersection be V, and let UV be R. Then

$$R=r\cos(\psi-\psi')=r(\cos\psi\cos\psi'+\sin\psi\sin\psi') \tag{2.56}$$

Let us consider the ratio of the width of each stripe to R. Since the ellipse is symmetrical with respect to ξ' and η' axes we have to consider only the part of the domain of ψ and ψ' in which $0\leq\psi\leq\frac{\pi}{2}$ and $0\leq\psi'\leq\frac{\pi}{2}$. Therefore we get from (2.54)

$$\left.\begin{aligned}\sin\psi'&=\frac{R_2^2\sin\psi}{\sqrt{R_1^4\cos^2\psi+R_2^4\sin^2\psi}}\\ \cos\psi'&=\frac{R_1^2\cos\psi}{\sqrt{R_1^4\cos^2\psi+R_2^4\sin^2\psi}}\end{aligned}\right\} \tag{2.57}$$

and from (2.56) by (2.54), (2.55) and (2.57)

$$R=\frac{R_1R_2\sqrt{R_1^4\cos^2\psi+R_2^4\sin^2\psi}}{\sqrt{R_1^2R_2^4\sin^2\psi+R_1^4R_2^2\cos^2\psi}}\cdot\frac{R_1^2\cos^2\psi+R_2^2\sin^2\psi}{\sqrt{R_1^4\cos^2\psi+R_2^4\sin^2\psi}}$$

Therefore we heve

$$R=\sqrt{R_1^2\cos^2\psi+R_2^2\sin^2\psi} \tag{2.58}$$

If ρ is the ratio of the width of each strip to R the reasoning of Art. 9 stands here as well. Therefore $\nu=0.823$, too, and the marginal acuity V' is given by (2.53), that is,

(2.59)

Here ψ is the angular distance of the line in whose direction the marginal acuity is to be measured from the ξ' axis. If, however, we denote by θ its angular distance from the X axis, we have by (2.48)

$$\theta=\psi+\varepsilon \tag{2.61}$$

that is, $$\psi=\theta-\varepsilon \tag{2.60}$$

We can get V' by substituting (2.61) in (2.59). There is one thing to be remembered here. The direction of the axis of a cylindrical lens is generally indicated by the international system, that is, the angle is measured in the counterclockwise direction by the operator looking at the subject's eye. But in the present study the angle is measured in the counterclockwise direction as seen by the subject looking at the test type. Therefore if one is to adopt the international system, the sign of the angles must be reversed before performing the calculation.

The acuity V' is given by (2.59) and (2.61) as

$$V'=\frac{a_0x}{5\nu R},\quad R=\sqrt{R_1^2\cos^2(\theta-\varepsilon)+R_2^2\sin^2(\theta-\varepsilon)} \tag{2.62}$$

where θ is the angular distance from the X axis of the direction for which the acuity is being measured. If we employ, instead of ν, the coefficient of absolute marginal acuity n, (2.62) becomes by (2.4)

$$V'=\frac{x}{nR},\quad R=\sqrt{R_1^2\cos^2(\theta-\varepsilon)+R_2^2\sin^2(\theta-\varepsilon)} \tag{2.63}$$

All the lengths, x, a_0, P_1, P_2, and g are measured in meters.

As an illustration let us perform the calculation about the practical case of equipping the author's left eye with a circular hole 4.15 mm in diameter, a cylindrical lens C_2 and aspherical lens L_1. Here $M_1=-0.75$ D, $C_1=0.5$ D, $M_2=-0.25$ D, $P_1=P_2=2.075$ mm, $L_1=1.0$ D, $C_2=2.0$ D, $\phi=-30°$ (The angle of the cylindrical lens is 30° if measured by the international system),

$x=5$ m, and $g=8$ mm.

By (2.27), (2.28) and (2.29) we get

$C=1.80278$ D, $L=1.59861$ D, $\alpha=-36°57'$.

Substituting these values in (2.39) we get

$A=0.00478$, $B=0.000914$, $H=0.00000937$.

Substituting these in (2.43) we get $\tan 2\beta=0.00484$, whence

$\beta=0°8'$ or $-89°52'$.

Let us adopt the first value, and by substitution in (2.45) get

$A'=0.00478$, $B'=0.000914$

Substituting these in (2.47) we get

$R_1=14.5$ mm, $R_2=33.1$ mm.

The position angle ε of R_1 measured from the X axis is by (2.48)

$\varepsilon=-36°57'+8'=-36°49'$.

The test-type-plane ellipse has been completely determined now. Putting $a_0=1.5$ mm and $\nu=0.823$ in (2.62) we get the values V' of the marginal acuity corresponding to various values of θ as shown in table 2.3, which closely agree with the observed values obtained from the experiment with the author's left eye.

16. Formula for marginal acuity: Axis of astigmatism parallel to axis of cylindrical lens worn

In this article let us discuss the cases when $\phi=0$.

If $C_2\geqq C_1$ we have by (2.27), (2.28) and (2.29)

$$C=C_2-C_1,\quad L=L_1-M_1, \tag{2.64}$$

$$\alpha=0 \text{ or } \frac{\pi}{2}.$$

Here we have,

$$\alpha=0, \tag{2.65}$$

since $-C_1+C_2\cos 2\phi=C_2-C_1\geqq 0$.

Substitution of (2.64) and (2.65) in (2.39) gives

$$\left.\begin{aligned} A&=\frac{1}{\{x(L_1-M_1)-1\}^2}\cdot\frac{(1-g\,M_1)^2}{p_1^2}\\ B&=\frac{1}{\{x(L_1-M_1-C_1+C_2)-1\}^2}\cdot\frac{(1-g\,M_2)^2}{p_2^2}\\ H&=0 \qquad (M_2=M_1+C_1)\end{aligned}\right\} \tag{2.66}$$

From (2.47) and (2.66) we get

$$R_1=\left[\frac{p_1\{x(L_1-M_1)-1\}}{1-g\,M_1}\right],\quad R_2=\left[\frac{p_2\{x(L_1-M_1-C_1+C_2)-1\}}{1-g\,(M_1+C_1)}\right] \tag{2.67}$$

Also $\varepsilon=0$ by (2.48) because $\alpha=\beta=0$.

Therefore by (2.62)

$$V'=\frac{v_0 x}{5\nu R},\quad R=\sqrt{R_1^2\cos^2\theta+R_2^2\sin^2\theta} \tag{2.68}$$

where R_1 and R_2 are the quantities given by (2.67).

If, however, $C_2\leqq C_1$,

$$C=C_1-C_2,\quad L=L_1-M_1-C_1+C_2 \tag{2.69}$$

since $-C_1+C_2\cos 2\phi=C_2-C_1\leqq 0$, we have

$$\alpha=\frac{\pi}{2} \tag{2.70}$$

substituting (2.69) and (2.70) ih (2.39) we get

$$\left.\begin{aligned} A &= \frac{1}{\{x(L_1-M_1-C_1+C_2)-1\}^2}\cdot\frac{(1-g\,M_2)^2}{p_2^2} \\ B &\equiv \frac{1}{\{x(L_1-M_1)-1\}^2}\cdot\frac{(1-g\,M_1)^2}{p_1^2}\,,\quad H=0 \end{aligned}\right\} \qquad (2.70)$$

If we calculate R_1 and R_2 from (2.71) the result will be the reverse of that from (2.67). But in the present case $\alpha=\frac{\pi}{2}$, that is, $\varepsilon=\frac{\pi}{2}$, and the coordinate axes are interchanged. Therefore we see that (2.67) and (2.68) are applicable to the case where $C_2 \leqq C_1$. In other words (2.68) gives the marginal acuity V' regardless of the relative magnitudes of C_1 and C_2. Experiment shows good agreement of the calculated and observed values.

17. Marginal acuity of a myopic or hypermetropic eye wearing a spherical lens

Put $C_1=C_2=0$, $p_1=p_2=p$, $M_1=M$, $L_1=L$ in (2.67)

Then we have

$$R_1=R_2=\left[\frac{p\{x(L-M)-1\}}{1-g\,M}\right] \qquad (2.72)$$

Substituting this in (2.68) we have

$$V'=\left[\frac{a_0x(1-gM)}{5\nu p\{x(L-M)-1\}}\right] \qquad (2.73)$$

This is the formula for the marginal acuity of a myopic or hypermetropic eye wearing a lens of power L D instead of one of power M D which would exactly compensate the defective refraction when worn at a distance g from the entrance pupil. Here p is the radius of the entrance pupil. If we use instead of ν the coefficient of absolute marginal acuity, n, (2.73) becomes

$$V'=\left[\frac{x(1-gM)}{np\{x(L-M)-1\}}\right] \qquad (2.74)$$

It must be noted here that M represents the actual refraction with which the subject eye is functioning while its acuity is being measured. If there is no accommodation M is the degree of myopia or hypermetropia, but if the eye is exercising accommodation M is so much more myopic than the eye itself. For example, a normal eye exercising accomodation of A D will have $-A$ for the value of M.

Marginal acuity below γ 0.1

For testing an eye whose acuity if less than 0.1 the usual practice is to use the test type for 0.1 at distances less than the normal 5 meters, and calculate the acuity from the maximum distance at which the type can be identified. Therefore if the threshold of illegibility [See Art. 10.] is reached at a distance of x m

$$V'=0.1\,\frac{x}{5} \qquad \text{that is, } x=50\ V' \qquad (2.75)$$

Substituting this in (2.73) we can get V'. Before that, however, we must pay attention to the sign of the quantity inside the absolute value symbols. In the left side of (2.73), a_0, x, ν and p are all positive. About the numerator, g may be considered to lie between zero and 0.03, because it is the distance from the entrance pupil to the lens worn. M, the refraction of the eys, can never be as high as +30 D, even if it is

a highly hypermetropic eye and its crystalline lens has been surgically removed. Therefore $1-gM$ is positive, and all we have to consider is the term $x(L-M)-1$ in the denominator. Since the marginal acuity is less than 0.1 when measured at 5 m, $5(L-M)-1$ is not zero and $x(L-M)-1$ is a continuous function of x. Therefore if x is reduced continuously from 5 m and $x(L-M)-1$ changes its sign in the process, it must pass through zero at some point in the way. Then V' becomes infinite. Consequently V' will become greater than 0.1 before that. This means that when x is reduced from 5 m the test type for 0.1 must reach the threshold of illegibility before $x(L-M)-1$ becomes zero. Suppose this occurs at a distance of x_0. Then $x_0(L-M)-1$ and $5(L-m)-1$ must be of the same sign. Hence we can get the marginal acuity by solving either of the following equations:

I. When $L-M>1/5$

$$V'=\frac{a_0\cdot 50V'(1-gM)}{5\nu p\{50V'(L-M)-1\}} \tag{2.76}$$

II. When $L-M<1/5$

$$V'=-\frac{a_0\cdot 50V'(1-gM)}{5\nu p\{50V'(L-M)-1\}} \tag{2.77}$$

From (2.76) we get

$$V'=\frac{\nu p+10a_0(1-gM)}{50\nu p\ (L-M)}\ ,\ \left[\ L-M>\frac{1}{5}\ ,\ V'<0.1\ \right] \tag{2.78}$$

and frcm (2.77)

$$V'\|\ \frac{\nu p-10a_0(1-gM)}{50\nu p\ (L-M)}\ ,\ \left[\ L-M>\frac{1}{5}\ ,\ V'>0.1\ \right] \tag{2.79}$$

Thus (2.78) and (2.79) give the marginal acuity from the distance at which the 0.1 test type reaches the threshold of illegibility for an eye whose acuity is less than 0.1.

Experiments carried out with a large number of eyes have given values well agreeing with the calculation, not only for the stripe test type but for the Landolt ring and the 6-6 ring.

18 Relation between visual acuity and the formula for marginal acuity

We have derived (2.62) as the general formula for marginal acuity, and (2.68), (2.73), (2.78) and (2.79) as the formulae for special cases. These formulae give the limits of the naked or corrected eye deduced by geometrical optics. Fig. 2. 10 shows diagrammatically the curve (*EFGHI*) of observed acuity and the curve (*KHI*) given by the formula for marginal acuity. As is evident from the definition of marginal acuity (Art. 10) the acuity ought to be smaller in value theoretically than marginal acuity. But experiments with a large number of eyes show that the two may be regarded as practically equal when the marginal acuity is 0.5 or less. In other words, when V' is less than 0.5 it may be regarded as expressing the actual acuity. (The portion between H and I in the figure). When the acuity exceeds 0.5 the test type shows some flickering and makes it difficult to judge whether it is in the threshold of illegibility. This flickering is considered to be due to the dimension of the cells of the macula lutea and the

phenomenon of excursion of the eye in the state of fixation. Besides, diffraction of light due to its undulatory nature and the aberration of the refracting system are thought to contribute to the indistinctness of the retinal image. As the refractive power L of the lens worn approaches $M+\frac{1}{x}$ the acuity increases, but the difference between it and the marginal acuity calculated with the formula also increases. (*HG*) When L becomes equal to $M+\frac{1}{x}$ the calculated marginal acuity becomes infinite, and the observed acuity reaches a maximum, which is usually between 1.5 and 2.0. This maximum is maintained even when L becomes less than $M+\frac{1}{x}$ as long as the subject eye exercises accommodation and keeps the retinal image sharp (*GF*). But when L becomes too small for the power of accommodation the acuity falls. (*FE*)

19. Summary

Let g be the distance between the lens and the entrance pupil of the eye, and x the distance between the lens and the test type. Draw X and Y axes on the plane of the entrance pupil parallel to the principal meridians. Let the equation of the entrance pupil be

$$\frac{X^2}{p_1^2}+\frac{Y^2}{p_2^2} \tag{2.30}$$

Suppose the eye would be completely correeted for its ametropia with a combination of a spherical lens M_1 of power M_1 and a cylindrical lens C_1 of power C_1.

We are going to deal with the cases in which these two lenses are replaced with a spherical lens L_1 of power L_1 and a cylindrical lens C_2 of power C_2. Let the axis of C_2 lie at an angular distance ϕ from the axis of C_1, and calculate the following three quantities:

$$C=\sqrt{C_1^2+C_2^2-2C_1C_2\cos 2\phi}\ , \tag{2.27}$$

$$L=L_1-M_1+\frac{1}{2}\left(-C_1+C_2-C\right), \tag{2.28}$$

$$\sin 2\alpha=\frac{C_2\sin 2\phi}{C} \tag{2.29}$$

(2.29) will give two values of α between $\pm\pi$. Call them α_1 and α_2 so that $|\alpha_1|<|\alpha_2|$. Adopt α_1 or α_2 for the value of α according as C_1 is smaller than or larger than $C_2\cos 2\phi$.

Put

$$\left.\begin{aligned} M_2&=M_1+C_1\\ A&=\frac{1}{(1-xL)^2}\left\{\frac{(1-gM_1)^2}{p_1^2}\cos^2\alpha+\frac{(1-gM_2)^2}{p_2^2}\sin^2\alpha\right\}\\ B&=\frac{1}{\{1-x(L+C)\}^2}\left\{\frac{(1-gM_1)^2}{p_1^2}\sin^2\alpha+\frac{(1-gM_2)_2}{p_2^2}\cos^2\alpha\right\}\\ H&=\frac{\sin\alpha\cos\alpha}{(1-xL)\{1-x(L+C)\}}\left\{-\frac{(1-gM_1)^2}{p_1^2}+\frac{(1-gM_2)^2}{p_2^2}\right\} \end{aligned}\right\} \tag{2.39}$$

and calculate A, B and H. Then obtain β which will satisfy

$$\tan 2\beta=\frac{2H}{A-B} \tag{2.43}$$

and calculate

$$\left.\begin{aligned} A' &= A\cos^2\beta + H\sin 2\beta + B\sin^2\beta \\ B' &= A\sin^2\beta - H\sin 2\beta + B\cos^2\beta \end{aligned}\right\} \tag{2.45}$$

Put

$$R_1 = \frac{1}{\sqrt{A'}}\ ,\ R_2 = \frac{1}{\sqrt{B'}} \tag{2.47}$$

$$\varepsilon = \alpha + \beta \tag{2.48}$$

Then the required marginal acuity V' in given by

$$V' = \frac{a_0 x}{5\nu R}\ ,\ R = \sqrt{R_1^2\cos^2(\theta-\varepsilon) + R_2^2\sin^2(\theta-\varepsilon)} \tag{2.62}$$

Here ϕ is the angular distance, from the X axis, of the line along which the marginal acuity is to be measured, and a_0 is the standard dimension of the test type for the acuity 1.0 at five meters, and ν is a constant characteristic of the test type called its coefficient of marginal acuity.

Fig. 10.

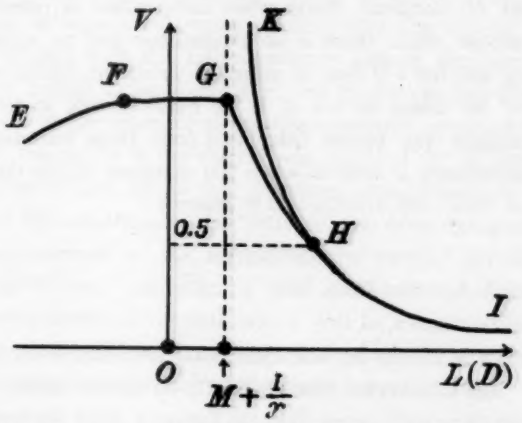

A test type consisting of uniform parallel black stripes with adjacent stripes separated by a space equal to the stripe in width is suitable for measuring the acuity in the direction perpendicular to the length of the stripes. With this test type having stripes 1.5 mm in width an eye is rated to have the acuity of 1.0 when it can just perceive it as stripes at a distance of 5 meters. In other words, $a_0 = 0.0015$ when ν assumes the theoretical value, 0.823. The values given by (2.62) agree very closely with experimentally observed values.

If we put $\phi = 0$ we get the formulae for the marginal acuity for the case in which one of the axes of astigmatism and the axis of the cylindrical lens worn are parallel with each other as follows:

$$R_1 = \left[\frac{p_1\{x(L_1M_1-)-1\}}{1-gM}\right],\ R_2 = \left[\frac{p_2\{x(L_1-M_1+C_2)-1\}}{1-g\ (M_1+C_2)}\right] \tag{2.67}$$

$$V' = \frac{a_0 x}{5\nu R}\ ,\ R = \sqrt{R_1^2\cos^2\theta + R_2^2\sin^2\theta} \tag{2.68}$$

Again, if we put $C_1=C_2=0$, $P_1=P_2=P$, $M_1=M$ and $L_1=L$, we get the formula for the marginal acuity for a myopic or hypermetropic eye wearing a spherical lens.

$$V'=\left[\frac{a_0x\ (1-gM)}{5\nu p\{x(L-M)-1\}}\right] \tag{2.73}$$

If the subject's acuity is less than 0.1 when tested at five meters, the usual practice is to let him approach approach a test type for 0.1 (5 m) till he can identify it. Here the marginal acuity is given by

$$V'=\frac{\nu p+10a_0(1-gM)}{50\nu p\ (L-M)}\ ,\ \left[L-M>\frac{1}{5}\ ,\ V'<0.1\ \right] \tag{2.78}$$

or

$$V'=\frac{\nu p-10a_0(1-gM)}{50\nu p\ (L-M)}\ ,\ \left[L-M<\frac{1}{5}\ ,\ V'<0.1\ \right] \tag{2.79}$$

The striped test type is suitable for rational measurement of marginal acuity whether astigmatism is present or not, and has $a_0=0.0015$ and $\nu=0.823$. On the other hand the Landolt ring and the 6-6 ring as well as letter test types are unsatisfactory for the rational measurement of marginal acuity when astigmatism is present, though they can be used for the purpose when there is no astigmatism and no cylindrical lens is used. With the Landolt ring and the 6-6 ring of standard dimension 0.0015, ν is usually 0.8, and with practice ν may be taken as 0.5 if it is required only to tell the position of the ring. When we compare the values calculated from these formulae with experimental results almost no discrepancy is noticed when the marginal acuity does not exceed 0.5.

(Published in Acta Ophth. Jap. 62:2313, 1958 in Japanese.)

REFERENCE

Helmholtz, H.: H.B. d. physiol. Optik, 1910.

STUDIES ON MYOPIA BY ESTIMATING ANISEIKONIA AND THE REFRACTIVE COMPONENTS OF BOTH EYES

Tomihisa SUGATA

Department of Ophthalmology, Tokyo Medical and Dental University

There has been consideration distpute among ophthalmologists about the genesis of myopia: Tikashi Sato (1941, 1942) stressed that the myopia is in majority of cases due to the increase of refractive power of the lens. On the other hand, Jin Otsuka has published, with his coworkers, a series of many works on myopia since 1943, and advocated (1951) that the elongation of the axial length of the eye is the principal cause of the genesis and progress of myopia, although the increase of the refractive power of the lens may participate to a lesser extent in it.

Their conclusion was, however, drawn from the data obtained without any consideration to the side of the eye, namely right or left, and their data would have seemingly contained some individual variation, which should be avoided if an unequivocal conclusion is to be obtained.

In this investigation, therefore, the axial length was measured for both eyes by means of X-ray Vision, and all other refractive components were also obtained for both eyes. The difference of refractive components of both eyes was calculated, and the mutual relation among them was examined chiefly using the difference, in order to eliminate individual variation; then it was studied from the statistical point of view which refractive component plays the most predominating role in the progress of myopia.

Material and Method

The axial length was measured for both eyes of 121 subjects by X-ray Vision: X-ray tube was attached to the apparatus for the measurement, so that the distance between the focus and narrow slit through which the eye of subject was irradiated, became about 49 cm. The slit was placed at the distance of about 7 mm. from the skin of lateral orbit of the subject. The face of the subject who has been dark adapted was fixed, and X-ray was irradiated under the condition of tube current of 3 mA. and voltage of 130 K.V., when narrow beam of X-ray meets the retina at equatorial region, bluish-white ring can be seen. As the slit moves back-ward in parallel with the antero-posterior axis of the eye, the ring became smaller, then fused into a small bluish-white disk, and finally the disk disappeared suddenly. The position of the slit at the moment of its disappearance corresponds to the posterior pole of the eye. Next, the appex of the cornea was checked by a plate equipped in the apparatus. The distance of both points was measured with accuracy of 1/10 mm. using the scale with vernier and the axial length was obtained, the error being within 0.1038 mm..

The routine measurements of the refraction, the corneal curvature, the degree of exophthalmos were carried out. Aniseikonia was measured by means of A.O. space eikonometer and Otsuka-Hosaka's method which will be mentioned in detail later. The refractive power of the lens and the total refractive power of the eye were computed from measrured value using constants of Gullstrand's schematic eye. All the values of these refractive components were obtained for both eyes. By correlation analysis of these values, the mutual relation among refractive components was studied.

Result

(1) The role of the axial length in the manifestation of the anisometropia

A significant correlation between the degree of refraction and the axial length was ascertained (Correlation index $r = 0.7018$) even when it was calculated without any consideration about the side of the eye; this result is in good accordance with that of Stenström, Sorsby, Otsuka, and Ohno. However, closer correlation was found when the difference between the components concerning both eyes were taken (Correlation index $r = 0.8806$). On the other hand, the difference of the degree of the refraction of both eyes had only a slightly significant correlation with the difference of the refractive power of the lens (Correlation index $r = 0.3196$) and the difference of the total refractive power of both eyes (Correlation index $r = 0.2252$). These results cleary indicate that the difference of

axial length is the principal cause of the manifestiation of anisometropia.

(2) The role of the axial length in low grade myopia

According to the statistical examination by the Ministry of Education of Japan, the percentage of myopia in Japanese students changed evidently before and after the World War II: There were 67% in 1937, 14% in 1949, 20% in 1955 of high school students. This variation in percentage of myopes was refered to the influence of environment. In spite of decrease and the increase of myopes, the percentage of high grade myopes in students remained constant. Therefore the low grade myopia was regarded to be different in nature from high grade myopia which is also called the congenital myopia. Nevertheless, as these assumption has been supported by no analytical examination of refractive components, the following study performed:

For the sake of convenience of analysis, 178 cases of myopic eye were divided into two groups, i.e. low grade myopia (from-0.25 to-3.00 dptr.) and high grade myopia (higher than-3.25 dptr.). Mutual relations among the refractive components were studied for these two groups; and it was found that even in low grade myopia the correlation between the degree of refraction and the axial length of the eye was significant (Correlation index $r=0.2274$). On the contrary, the refractive power of the lens revealed no significant correlation with the degree of refraction.

Judging from these results, it can be postulated that, even in low grade myopia, the elongation of the axial length plays the most important role in the manifestiation of myopia.

(3) The exophthalmos in myopia

Ishida (1934) imagined that the difference of the degree of exophthalmos of both eyes may increase according as the difference of the degree of refraction becomes higher, but he could not obtain accurate statistical data. Therefore correlation analysis of the relation between exophthalmos and the degree of myopia was carried out. The degree of exophthalmos of both eyes was measured with Hertel's exophthalmometer and the difference of both eyes was calculated.

The correlation of this difference with the difference of refraction of both eyes was examined, and a significant correlation was obtained. However, when the relation of exophthalmos with the degree of refraction and the axial length was examined for measured value only instead of the difference, no significant correlation was obtained.

From these results, it was concluded that the difference of degree of exophthalmos of both eyes in myopes indicates the degree of anisometropia and can be regarded to represent the axial length to some extent in myopic cases.

(4) The role of axial length in aniseikonia

Aniseikonia in horizontal and vertical meridians were measured in 108 out of 121 subjects mentioned above. A.O. space eikonometer was used so far as the patient had high stereoscopic acuity which is required for this method. For the subject having low stereoscopic acuity, Otsuka-Hosaka's method was used. This is a method to compare

directly the size of images which are brought into sensation, by using modified Maddox rod and tangent scale for distance of 5 metres in dark room.

On each arm of tangent scale, a small white lamp is placed at the distance of 35 cm from the centre where a bright light for fixation is placed. When the patient stands at the distance of 5 metres wearing Maddox rod on one eye, he can see three red lines through it, one corresponding to the fixation lamp and two with less brightness corresponding to small white lamps. (When measurement is performed for horizontal meridian, small lamps on vertical arms of tangent scale are extinguished.) As an auxillary lamp, a small green lamp can be slid along the rale scaled each 1 cm.. The patient looks at the fixation lamp at the centre with the fellow eye not wearing Maddox rod and follows the movement of green lamp. The points where green lamps coincide the lines corresponding to small lamps seen through Maddox rod is checked. The difference between the distance of white lamps and that of green lamps corresponds to the difference of images of both eyes. Therefore the per cent change can be calcuated by the following equation: The per cent change of images

$$= \frac{\text{Distance between two green lamps in cm} \sim 70\,\text{cm}}{70\,\text{cm (Distance between two white lamps)}} \times 100\%$$

(mean value of 3 measurements)

This procedure was performed using horizontal and vertical arms of tangent scale, and the per cent change of images for horizontal and vertical meridian was obtained.

By the correlation analysis, definite correlation was found between aniseikonia and refractive components for horizontal meridian. On the contray, for vertical meridian no definite correlation was obtained. The results for horizontal meridian will be given below.

A significant plus correlation was obtained between the per cent magnification of images and the difference of the refraction of both eyes (Correlation index $r=0.4351$). The difference of the axial length (Correlation index $r=0.3714$), difference of the degree of the refraction without astigmatism (Correlation index $r=0.4356$), and the difference of the refractive power of the lens (Correlation index $r=0.2898$) between both eyes had also significant correlation with the per cent change of images. A significant minus correlation was found between the per cent change of images and the difference of corneal refractive power of both eyes (Correlation index $r=0.2416$). On the other hand, no significant correlation was obtained between the per cent change of images and the difference of the total refractive power of both eyes.

According to the theory of aniseikonia put forward by Ogle, the per cent change in the magnification of the retinal images is approximately 1.4 per cent per dptr. of myopia changes in uncorrected axial myopia. On the other hand, if the ametropia is caused by the change in the refractive power of the eye, the per cent change is about-0.3 per cent per dptr. of myopia; this value is negligible compared with the former value. In view of this theoretical consideration, the present results indicate that the aniseikonia is, for the most part, of axial origin. A slightly significant correlation between the per cent magni-

fication of images and the difference of degree of the refractive power of lens was also recognized. This result indicated that the refractive power of the lens can take part to a lesser extent in the manifestiation of aniseikonia. From these reasults it is reasonable to conclude that the refractive error is for the most part due to the change of the axial length.

This conclusion is also supported by the study of the distribution curve of aniseikonia: In figure, interrupted line indicates the ditribution curve of per cent change of images actually measured for the present material. Dotted line shows the distribution curve of per cent of retinal images calculated under the assumption that the ametropia of present material is purely of refractive origin. On the other hand solid line is derived under the assumption that the ametropia is purelly of axial origin. As readily seen in the figure, the greater part of of aniseikonia in the present material that the refractive errors are in majority of cases due to the change of axial length.

It is extremely difficult to find any reason of the fact that the definite conclusion was not obtained for vertical meridian, unlike the horizontal. However, the following assumption seems to serve for the explanation of this fact: (1) So-called basic (anatomical) aniseikonia in vertical meridian would have disturbed to get definite conclssion. (2) Deviation of actually obtained value of refractive components from optical constants of schematic eye in vertical meridian would have been larger than in horizontal meridian, and this may be also an explanation of the present results.

Fig. 1. Frequency distribution of aniseikonia for horizontal meridian.

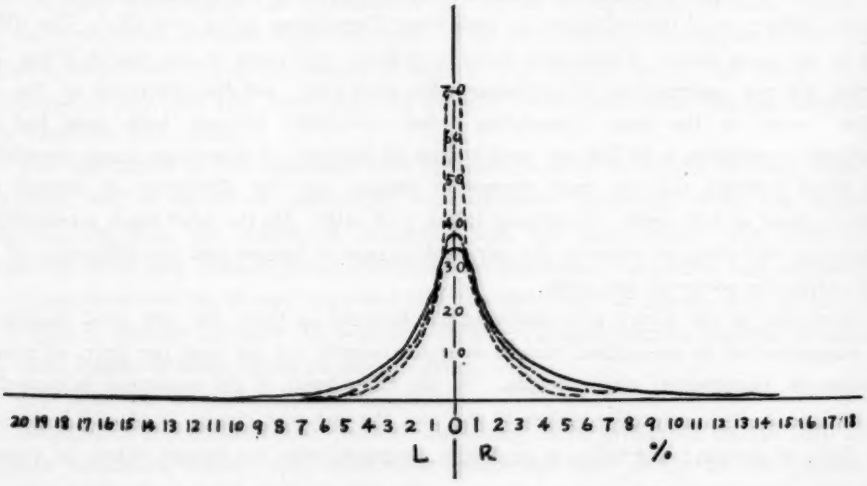

Fig. 2. Frequency distribution of aniseikonia for verltical meridian.

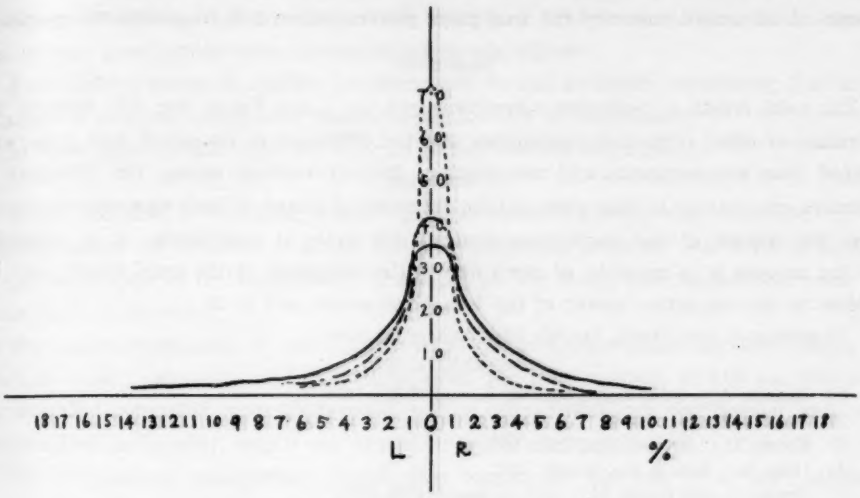

—·—·— Frequency curve of the present material.
·····Frequency curve to be expected when refraciive error of the present material is entirely refractive.
————Frequency curve to be expected when refractive error of the present material is entirely axial.

Discussion

Some cases of myopia are indeed, when studied case by case, due to the elongation of the axial length, and other cases may be due to the increase of refractive power of the eye. However many authors such as Stenström, Sorsby, Otsuka, and Ohno agreed that the myopia when as a whole is in majority of cases due to the elongation of axial length. However, the conclusion of these authors were drawn from studies on refractive components which obscure more or less the conclusion must have been included in their data. In order to reach an unequivocal conclusion about the problem, it is of prime importance to avoid such errors due to individual variation. Therefore the author examined correlation among refractive components with special regard to the difference of both eyes each subjects, and arrived at the conclusion that the elongation of axial length plays the most important role in genesis of myopia.

From the point of view of aniseikonia, this conclusion is also found to be warranted. The significant plus correlation between per cent change of images and difference of degree of refraction of both eyes indicates that the aniseikonia in myopia is for the most part axial origin. In addition the distribution curve of aniseikonia also indicated the axial origin of aniseikonia. All these results clearly show the elongation of the axial length to be the most important cause of myopia. Therefore it is said that Otsuka's theory of

genesis of myopia has noted that all these results are against Sato's opinion that the increase of refractive power of the lens plays predominating role in genesis of myopia.

Summary

The axial length of both eyes were measured by X-ray Vision for 121 subjects and the values of other refractive components and the difference of images of both eyes were obtained from measurements and calculations. Mutual relations among the difference of refractive components of both eyes and the difference of images of both eyes were examined. From the results of the correlation analysis and study of aniseikonia, it is concluded that the myopia is in majority of cases due to the elongation of the axial length, and the increase of the refractive power of the lens plays small part in it.

(Published in Acta Ophth. Jap. 62: 1841, 1958 in Japanese.)

REFERENCES

1) Hosaka, A.: Ochanomizu medical journal, 3:325, 1955.
2) Hosaka, A., and Sugata, T.: Folia ophthalm. 53:14, 1959.
3) Kondo, M.: Acta o. Jap. 57:58, 1953.
4) Ohno, S.: Acta o. Jap. 10:460, 1957.
5) Otsuka, J. and Kondo, M.: Acta o. Jap. 55:100, 1951.
6) Otsuka, J. and Kondo, M.: Folia ophthalm. Jap. 3:35, 1952.
7) Otsuka, J. and Kondo, M.: Acta o. Jap. 56:477, 1952.
8) Sugata, T.: Acta o. Jap. 62:2618, 1958.
9) Sugata, T.: Acta o. Jap. 62:2618, 1958.

THE PERIODICITY IN THE ELECTROMYOGRAPH OF HUMAN EXTRAOCULAR MUSCLES

Tetsuya KUBOKI

Department of Ophthalmology, School of Medicine, Hirosaki University

Since 1952, electromyographical studies of human extraocular muscles have been reported by Björk (1952) and other researchers. The works of these workers are divided into three groups:

a) Observations of the action potentials of a single unit or of a whole muscle as superimposed potentials (Björk, 1953; Breinin, 1955 and Kamo-uchi, 1955 et al.).

b) Studies on discharge intervals of a single unit (Kuboki, 1954 and Sakatani, 1956).

c) Investigations on kinesiology by observing the integrated potentials of a muscle (Breinin, 1958 and Momose, 1958).

These works have introduced new informations to the ophthalmological field, but they are not yet so powerful as to solve many still existing problems.

It seems to be ascribed to some reasons which exist in this field of research. The first reason is the difficulty of separating the firing of a single motor unit, and at the same

time, the low rate of happening of abnormal spike discharges in these muscles. Secondly, kinesiology which must be the most usefull method in the ophthalmological field, does not offer us any quantitative value for statistical investigations.

From these reasons the author has attempted to find a method expressing the action potentials of a whole extraocular muscle quantitatively or statistically.

In these experiments, only the internal rectus was investigated.

Methods

As an electrode, a monopolar needle electrode made of a steel wire was used. It was insulated except 0.5 to 1.0 m.m. at the tip. The indifferent electrode was fixed on the nose (in the early stage of the experiment, it was on the ear lobe), and the earth electrode was on the back of the hand.

The action potentials of the muscle was fed to a differential amplifier, which has selectable time constants. In this experiment the time constant of 0.05 sec was used. The amplified potentials were displayed to a dual beam cathod-ray oscilloscope and were photographed on a paper, which was drawn 50 or 100 c.m. per second.

The influence of polarisation, which may happen by the use of a steel electrode was negligible in virtue of 2MΩ interelectrode resistance. By making use of square current pulses, it was ascertained, that no deformation of the pulse waves occured. However, when a silver silver-chloride needle electrode (insulated except the tip) and a naked steel electrode were put into Ringer solution being connected to the input of the amplifier, spontaneous discharge on account of the resolution of steel happened (Fig. 1,A). It was eliminated by insulating the needle except the tip, and with the use of a time constant of 0.05 sec. (Fig. 1,B).

Fig. 1. A. Spontaneous discharge of a naked steel electrode in Ringer solution (time constant: 0.3 sec). B. Ditto, with the same electrode insulated except the tip (time constant: 0.05 sec). C. Examination on the interference of brain waves and the potentials of the other muscles: the needle electrode was inserted into the orbital tissue, and the indifferent electrode was fixed on the nose (time constant: 0.05 sec.). D. Ditto, the indifferent electrode being fixed on the ear lobe (time constant: 0.05 sec.).

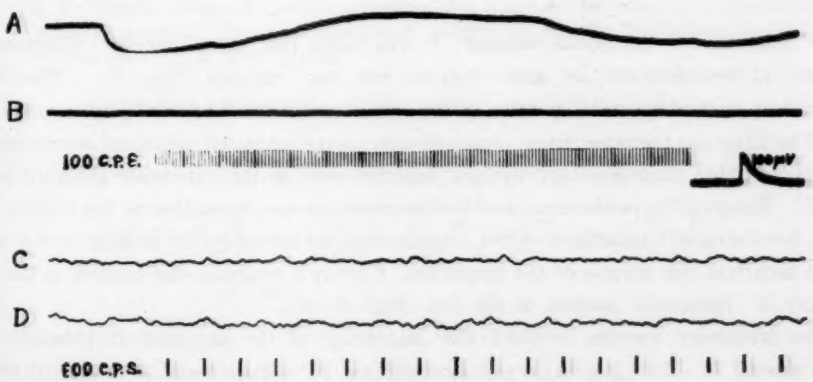

Furthermore, when the needle electrode was inserted into the orbital tissue having some distance from the internal rectus, neither interference of brain waves nor of other muscles was observed (Fig. 1,C and D). It seemed to be preferable to fix the indifferent electrode rather on the nose than on the ear lobe.

If the needle electrode was inserted exactly into the muscle belly, the waves presented only the superimposed spike discharges of each motor unit. However, when the needle was put at some distance from the muscle, the waves presented periodic vibrations (Fig. 2).

Fig. 2. Superimposed potentials of internals of the internal rectus at the primary position of the eye. A. The needle was inserted exactly into the muscle belly. B. The needle was put some distance aside from the muscle.

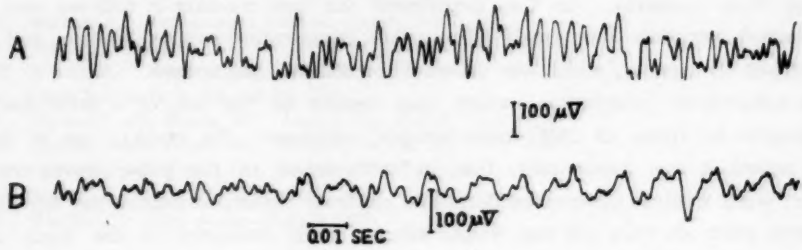

The experiments were made on 12 adult subjects being in their supine position.

A perimeter having a diameter of 60 c.m. was set before the eye, and the other eye was covered. A white object of 1.0 c.m. in diameter was set on the perimeter.

The experiments were performed on horizontal positions of the eye.

Results

By inspection of the waves obtained, it was found that these periodic vibrations are composed of two elements, i.e. slow rhythm and fast rhythm (Fig. 3). The former appeared on every horizontal position of the eye, except on the abducted positions over about 30°. The latter, on the other hand, appeared only on the adducted positions over about 30°. So it follows, that there are two rhythms superimposed on the extremely adducted position (Fig. 4). The relative predominance of the two rhythms was dependent on the position of the needle, however, the frequency of either rhythm was not varied by the position of the needle.

To ascertain the results of the inspection, Fourier's analysis was applied to the waves on every 20° horizontal position of the eye (Figs. 5~11).

The frequency spectra revealed the maximum of the amplitude distribution at the region around 75~120 c.p.s. on the primary position, 20° adducted and 20° abducted position.

On the other hand, on the frequency spectra of 40° or of the extremely adducted position, two maxima of the amplitude distribution were seen. One of them was at the region around 75~120 c.p.s., and the other at the region around 120~200 c.p.s.

Fig. 3. Periodic waves of the internal rectus of a man aged 35 years at every 10° horizontal position of the eye.

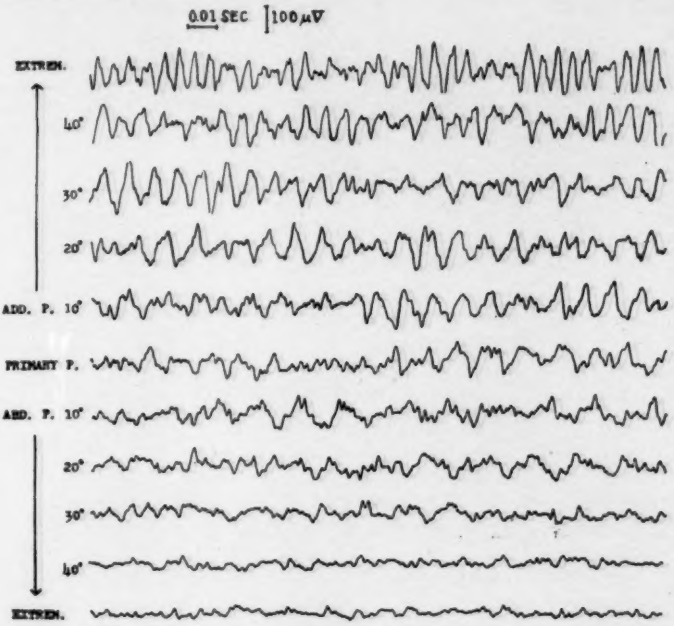

Fig. 4. Periodic waves of the internal rectus of a man aged 36 years at the extremely adducted position. The three traces were recorded by different positions of the needle. S: slow rhythm. F. fast rhythm.

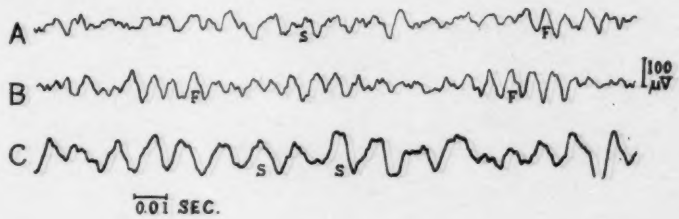

Figs. 5—11. Frequency spectra of the periodic waves of the internal rectus of a man aged 25 years.

Fig. 5. Frequency spectra at the primary position.

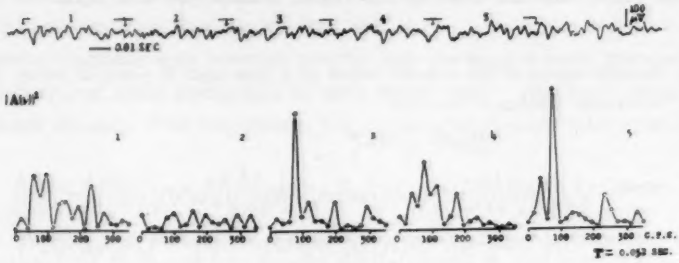

Fig. 6. Frequency srectra at 20° adducted position.

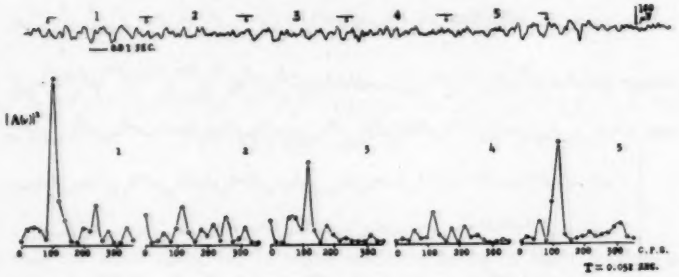

Fig. 7. Frequency spectra at 40° adducted position.

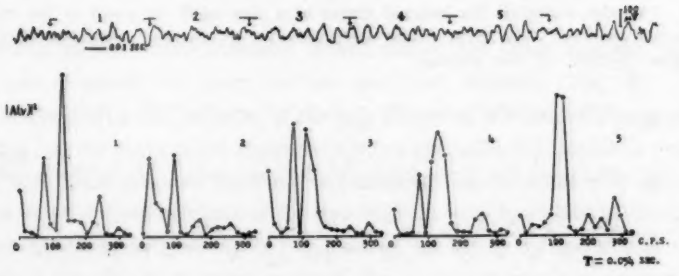

Fig. 8. Frequency spectra at the extremely adducted position.

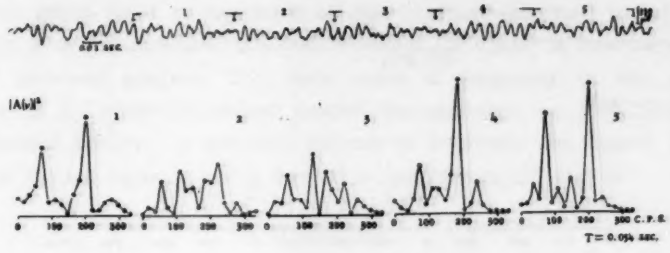

Fig. 9. Frequency spectra at 20° abducted posititon.

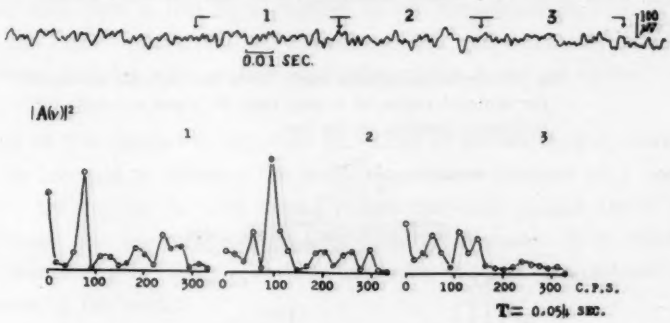

Fig. 10. Frequency spectra at 40° abducted position.

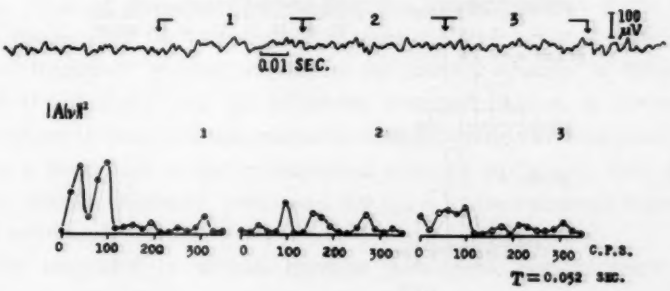

Fig. 11. Frequency spectra at the extremely abducted position.

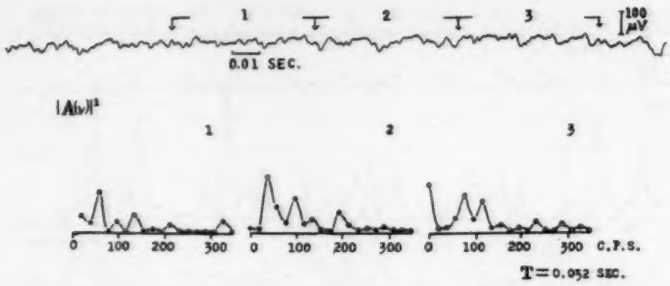

Furthermore, to determine the mode value of frequency of each rhythm, period histograms by measuring each periodic vibration were made from the waves of comparatively longer recording time (Fig. 12). Each histogram contains 150~200 values, except on the abducted positions.

Fig. 12. Periodhistograms made from the periodic wavesof the internal rectus of a man aged 35 years, at every 10° horizontal position of the eye.

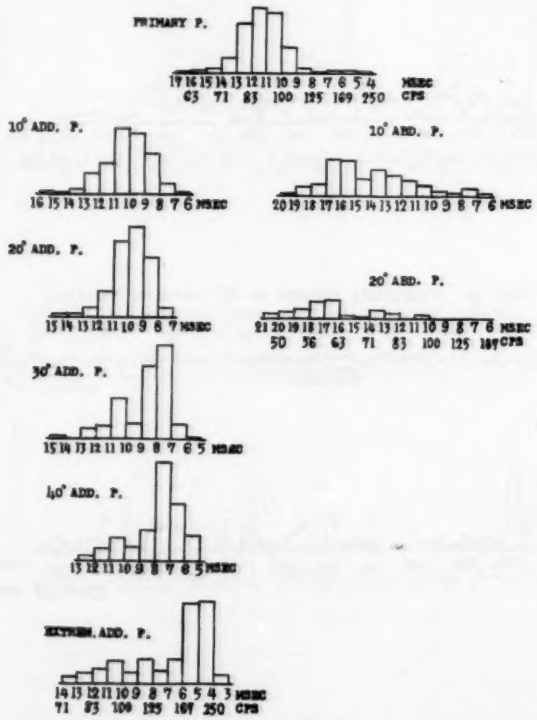

On the histograms are represented the mode values of period or frequency of the rhythms. The mode value of frequency of slow rhythum increased with the degree of adduction, but it never exceeded the limit of about 120 c.p.s. It decreased to about 60 c.p.s. at 20° abducted position, The mode value of frequency of fast rhythm was 125~143 c.p.s. at 30° adducted position, reached its maximum, i.e. 200~250 c.p.s. at the extremely adducted position. It was very difficult to determine the degree of adduction where the fast rhythm appears, but it seemed to be between 20° and 30°.

Discussion

Piper[4] (1912) found in his famous experiment, that the action potentials of skeletal muscles induced with two surface electrodes reveal periodic vibrations, i.e. so called Piper-rhythm, which has the frequency of about 50 c.p.s..

The author attempted to find Piper-rhythm on the extraocular muscles which had not been studied by Piper. However, on account of the great difficulty of taking out the potentials of these muscles with surface electrodes, above described method was thought out.

The success of this method is supposed to be due to the anatomical characteristics of the extrinsic eye muscles as follows: the nerve insertion is localized at a posterior point of the muscle; the muscle is very closely constructed with muscle fibers; each muscle fiber runs through the muscle from its origin to the insertion. So it seems to happen, that a needle electrode acts like a surface electrode through the muscle sheath and connective tissues in the orbita.

The periodic vibrations were not always observed, because their happening was not only dependent on the position of the needle, but also on the individuality of the subject. What elements in the subject were related to the generation of the periodicity was not clear.

The mode value of frequency of the rhythms on each position of the eye must be determined in future after the observations on more subjects, but it is presumed, that the mode value of frequency of slow rhythm at the primary position is between 70~100 c.p.s. and that of fast rhythm at the extremely adducted position is between 150~250 c.p.s.. Both values of frequency are respectively approaching the maximum frequencies of discharge of a single unit at the corresponding positions of the eye: they are 70 c.p.s. at the primary position (Kuboki[3], 1954), and 200 c.p.s. at the extremely adducted position (Björk[1], 1953 and Suzuki[6], 1959).

It has been advocated by several Japanese researchers, that the motor units in the skeletal muscles are divided into two groups, i.e. tonic units and kinetic ones (Tokizane[7], 1955: Jinnai[2], 1958 et al.). The same fact has been asserted on the extraocular muscles (Kuboki[3], 1954 and Sakatani[5], 1956). The author presumes that the slow rhythm and the fast one represent the activities of tonic units and kinetic ones respectively.

Summary

Superimposed potentials of the internal rectus were induced with a monopolar needle electrode by a special technique, and the vibrations on the waves were observed and analysed by means of harmonic analysis. The results were as follows:

1. With a monopolar needle electrode superimposed potentials of the internal rectus muscle could be induced, as periodic vibrations which resemble the Piper-rhythm.

2. As the results of inspection and analysis of the waves on horizontal positions of the eye, two elementary vibrations were presumed, i.e. slow rhythm and fast rhythm.

3. The slow rhythm appeared in the region from about 30° abducted to the extremely adducted position of the eye, and its frequency was 60 to 120 c.p.s., getting an increase with the adducting movement.

4. The fast rhythm appeared only at the adducted positions over about 30°, being superimposed on the slow rhythm. Its frequency was 120 to 250 c.p.s..

These rhythmical waves were observed not on the whole, but on the majority of normal subjects.

(Publisheed in Acta Ophthalm. Jap. 62:2361, 1958 in Japanese.)

REFERENCE

1) Bjork, A & Kugelberk, E.: E.E.G. & Clin. Neurophysiol, 5:271, 1953.
2) Jinnai, D.: Proceedings of the VIIth Annual Meeting of the Japan E.E.G. Society and of the XIth Meeting of the Japan E.M.G. Society. Dept. of Neurosurgery, Univ. of Tokyo, 1958.
3) Kuboki, T.: Acta O. Jap. 58:874, 1954.
4) Piper, H.: Elektrophysiologie der Menschlicher Muskeln, Julius Springer, Berlin, 1912.
5) Sakatani, S.: Acta O. Jap. 60:1080, 1956.
6) Suzuki, S.: Sapporo City Hospital Med. Journal, 19:42, 1959.
7) Tokizane, T.: Kwagaku, 25:22, 1955.

DEVELOPMENT OF LACRIMAL APPARATI IN JAPANESE FETUS

Takayuki SEO

Department of Ophthalmology, Nippon Medical College

Embryological studies of lacrimal apparati, especially the lacrimal passage, of the European fetus have been made by Born (1877) and others. Thus various theories have been proposed as to their early development. On Japanese fetus, however, information is quite insufficient: only the works by Iwata (1927), Nishi (1933) and Fukamizu (1931, on lacrimal canaliculi) on early and late development are available at present. Development of the accessory lacrimal gland was studied by Falchi (1905), Contino (1908) and Ask (1908) and, in this country, by Tawara (1932), Sanada (1939), Yokoyama (1956) and others. On the developmental course of the lacrimal gland studies were made by Ewetzky (1879)

and speciale-Cirincione (1908). However, they did not deal with the latter half of the development. In this country this field has been left untouched. Extensive studies on the lacrimal apparati in general and on their developmental correlations are quite rare in this country as well as in others. The present author examined the lacrimal apparati, namely lacrimal passage, lacrimal gland and accessory lacrimal gland, of the Japanese fetus and attempted to obtain developmental relationship between them.

Materials and Methods

The materials of this study were 31 fetuses, from 2 months (S.S.L.: 18 mm.) to the end of the 10th month (body length: 49.5 cm). (2 months, 2; 3 months, 8; 4 months, 8; 5 months, 5; 6 months, 3, 7 months, 2; 8 months, 1; 9 months, 1; 10 months, 1), and 46 sides of the lacrimal apparati. All materials were fixed with 10% formol. Those from fetuses older than 5 months were decalcified with 5% trichloracetic acid and embedded in paraffin or celloidin. Two to thirty micron thick horizontal and sometimes sagittal and frontal serial preperations from the upper margin of the orbita to the palate, including the bulbus and whole lacrimal apparati, were prepared. Microscopic examinations were performed after H. E. stain.

Results

Lacrimal passage

In 18 mm (S.S.L.) fetuses the cellular cord was already observable which was the origin of the nasal duct with bifurcating upper and lower lacrimal canaliculi (Figs. 1 and 2). Formation of theearly lumen of the nasal duct was observed in 30 mm fetuses and that of the lacrimal canaliculus in those in the middle of the 3rd month. In fetuses at the end of the 3rd month the vertical and horizontal portions of the lacrimal canaliculi were clearly differentiated and the lower end of the nasal duct was close to the mucous membrane of the nasal cavity.

In the beginning of the 4th month the opening to the lacrimal sac of the upper and lower lacrimal canaliculi was clearly observable. In the middle of the 5th month openings of the upper and lower lacrimal points could be observed (Fig. 5). At the same time, the lumen of the lacrimal passage was completely communicated to the lower end of the nasal duct, the communication with the nasal cavity remaining.

At the end of the 6th month the communication of the nasal duct with the nasal cavity was still closed. At the end of the 7th month opening of the lower nasal duct to the nasal cavity was first observed, though only on one side (right). At the same time, the lacrimal passage was completed morphologically (Fig. 6). Namely, the epithelium of the lacrimal canaliculi took the appearance of a stratified flat epithelium and the lacrimal sac and nasal duct were greatly enlarged.

In the 8th month and thereafter, development of the lacrimal passage was slow. The stratified cylinder epithelium of the lacrimal sac and nasal cavity was completed in the 8th month fetus.

The opening of the lower nasal duct to the nasal cavity was found without exception

in fetuses older than 8 months. As the boundary between the lacrimal sac and nasal duct, an extremely narrow portion was first observed in the 9 month fetus. This boundary was obscure in younger fetuses.

The lower part of the nasal duct, after it had been unified combined or: with the nasal cavity, was still extended caudal, forming the so-called Bochdalek diverticulum.

The presence of the diverticulum of the nasal passage was observed from the beginning of the 3rd month.

Regarding the appearance of lymph tissue in the lacrimal passage, lymphocyte aggregates of various sizes were first observed near the openings of the lacrimal canaliculi to the lacrimal sac in the 9 month fetus. In the 10 month fetus no lymph tissue was observed clearly.

The ossifical nasal duct was nearly completed at the end of the 7th month and a perfect bony tube was observed in the 8 month fetus.

In the fetus in the end of the 10th month, near the center of the nasal duct, a small serous gland was found which was presumably communicated to the duct. The palpebral fissure was completely formed in the beginning of the 7th month.

Lacrimal gland

The lacrimal gland was formed as the bud-like or rod-shaped premordium in 35mm S.S.L. fetuses (Fig. 3). It developed from the conjunctival sac to the cranial lateral of the bulbus and bifurcation of the duct was first observed in the end of the 3rd month. However, the lumens of the gland tube were obscure (Fig. 4).

Toward the end of the 4th month the opening of the duct to the conjunctival sac became clear. In the end of the 5th month the gland was separated into two groups (palpebral and orbital lacrimal glands) by a fiber bundle of connective tissue, presumably the orbital fascia. In the end of the 6th month lobule formation of the lacrimal gland became marked. After the 7th month, as age of embryo increased, development and differentiation of the lacrimal gland became clearer. The glandular structure was complicated and "Schaltstück" and duct could be differentiated. In the end of the 10th month development of the lacrimal gland was maximum and presented the so-called first, namely morphological, accomplishment. The protoplasma of the glandular cell was filled with fine basic granules, presumably presenting initiation of the secretary function. The duct underwent multiple branching and meandered strongly.

Accessory lacrimal gland

The cell group, which was supposed to be the premordium of Krause's gland, was observable from the beginning of the 4th month. The contact (communication) with the conjunctival sac was completed in the middle of the 5th month and branching of the terminal portion of the gland and the duct were formed in the middle of the 6th month. The development and differentiation proceeded further after the 7th month. However, it was much more inferior to the development of Wolfring's gland.

The cell group, which is supposed to be the premordium of Wolfring's gland, appeared

at the beginning of the 6th month, somewhat later than that of Krause's gland and opened towards the conjunctival sac. It developed rapidly at the end of the 7th month and exceeded the development of Krause's gland. It extended from the upper border of the tarsus into the Meibom's gland and further posterior to it. In the 9th month the shape of a compound tubular gland was acquired. However, its development continued till the end of the 10th month.

Furthermore, the development of both glands in the lower palpebra was relatively poor in both extent and degree. No secretary granules could be observed in the glandular cell even at the end of the 10th month. The development of the accessory lacrimal gland was not uniform and, in some places glands with young shape were observed. This tendency was especially marked in Krause's gland of the lower palpebra.

So far description was made on the development of the lacrimal passage, lacrimal gland and accessory lacrimal gland. Of various lacrimal apparati, the nasal duct and lacrimal canaliculi developed first. The development of the lacrimal gland was more delayed and in the beginning of the 3rd month. Krause's gland appeared in the beginning of the 4th month and Wolfring's gland in the beginning of the 6th month. In the middle of the 4th month the duct of the lacrimal gland opened towards the conjunctival sac. The lacrimal points of the upper and lower lacrimal canaliculi opened in the middle of the 5th month. At the beginning of the 7th month the palpebral fissure was completed. At the end of the 7th month the opening of the lower part of the nasal duct to the nasal cavity was observed and the shape of the lacrimal passage was accomplished and lacrimal excretion was awaited. However, though the lacrimal gland showed a histological picture, which was presumably the initiation of the secreting function, completion of development was postponed until after the birth. The development and differentiation of the accessory lacrimal gland was especially imperfect, it did not parallel the development of the lacrimal passage and was to be completed after birth, like the lacrimal gland.

Conclusions

1. In a 18 mm S.S.L. fetus, the cellular cord, which was the premordium of the nasal duct with bifurcation formation of the upper and lower lacrimal canaliculi, was already observable.

2. The early lumen formation of the nasal canal was observed in a 30 mm S.S.L. fetus and that of the lacrimal canaliculi in the fetus in the middle of the 3rd month.

3. Opening of the upper and lower lacrimal points were observed in the middle of the 5th month. The lumen of the lacrimal passage were prepared, except the contact to the nasal cavity.

4. In a fetus at the end of the 7th month, on the right side, the opening of the lower nasal canal towards the nasal cavity was first observed and the shape of the lacrimal passage was formed.

5. The premordium of the lacrimal gland was first observed in a 35 mm S.S.L. fetus.

Branching of the duct was observed at the end of the 3rd month and the opening of the duct to the conjunctival sac was at the end of the 4th month.

6. In an 8 month fetus the shape of compound tubular serous gland was almost completed. At the end of the 10th month histological pictures, presumably the initiation of the secretary function, was found.

7. The premordium of Krause's gland was observed in the beginning of the 4th month and that of Wolfring's gland in the beginning of the 6th month.

(Published in Acta Ophthalm. Jap. 62:1747, 1958 in Japanese.)

Fig. 1. Premordium of the left lacrimal canaliculus. A 18 mm S.S.L. fetus (horizontal section)

Fig. 2. Caudal end (arrow) of premordium of the bilateral nasal canals. An 18 mm S.S.L. fetus (horizontal section)

Fig. 3. Right nasal canal (upper arrow) and premordium of the lacrimal gland (lower arrow). A 35 mm S.S.L. fetus (horizontal section)

Fig. 4. Left lacrimal gland. End of the 3rd month (horizontal section

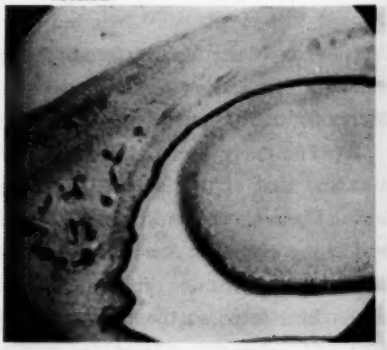

Fig. 5. Opening of right upper lacrimal point. Middle of the 5th month (horizontal section)

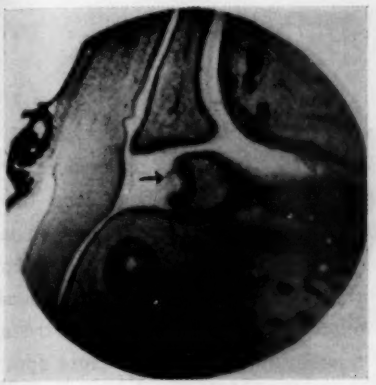

Fig. 6. Opening of lower part of the right nasal canal to the nasal cavity. End of 7th month (frontal section)

REFERENCES

1) Ask, F.: Anat. Hefte, 40:1910,
2) Born, G.: Morphol. Jahrbuch, 2:1876.
3) Born, G.: Morphol. Jahrbuch, 5:1879.
4) Contino, A.: Graefe's Arch. f. Ophth. 66:1908.
5) Ewetsky, Th.: Arch. f. Augenheilk. 8:1879.
6) Fukamizu, J.: Acta O. Jap. 35:1931.
7) Iwata, N.: Folia Anatomica Jap. 5:1927.
8) Nishi, S.: Kumamoto Igakukai-zasshi. 9:1931.
9) Speciale-Cirincione: Arch. f. Ophth. 69:1908.
10) Sanada, Y.: Acta O. Jap. 43:1939.
11) Tawara, T.: Kaibogaku-zassi, 5:1932.
12) Yokoyama, S.: Nagasaki Igakukai-zasshi, 31:1956.

STUDIES ON THE INITIAL GROWTH OF THE EXTRA-OCULAR MUSCLES OF JAPANESE

Tsuneto IWASAKI

Ophthalmological Department, Nagasaki University Medical School

Introduction

There are many literatures seen on comparative studies of growth of ocular muscles but almost no literatures is seen, in the east or west, on studies of growth of human ocular muscles. Therefore a systematic study on the growth of human ocular muscles were planned.

Materials and Methods

Thirty seven embryos, sitting height of 5.5 mm to body length of 45 cm, were obtained for the studies. (Table 1.) Embryos which were of less than 3 months gestation were decalcified, embedded in celloidin, serially sectioned in 10-30μ and were studied microscopically in hematoxylin eosin stain or van Gieson's stain.

Results

The base of oculomotor muscles grow at the posterior and slightly inner side of the bulbus in embryos of 7-7.5 mm.. In embryos of 7 mm length there is an area in larynx height extending to the posterior part of the upper margin of the bulbus along the innerside of the lower margin of the trigemenius ganglion, outside of the carotid and inner side of the jugular vein. The lower part of this area appears to joint the cell-group of the posterior wall of the larynx in the anterior wall of the mesencephalon surrounding the carotid and extending in a tape-form from the external side of the carotid to the inner side respectively. In the embryo of 7.5 mm the area is the same but is more apparent as a group of cells. The length is about 600μ. The upper and lower parts are thin and the middle part, the area near the lower pole of the bulbus (Fig. 1), is large and the stump is almost round. The lower part of the base (Fig. 2) ends as a small group of cells caught between the carotid and jugular vein and is differentiated distinctly from the surrounding area. In a 11 mm length embryo, from the relation with the increased growth of the bulbus, it moves to inner lower part of the bulbus and the group of cells is more dense. In a 13 mm length embryo, it is what it almost differentiable into the upper part of the common base of M. rectus superior and M. levator palpebrae and the lower part of the common base of M. rectus medialis, inferior and M. obliquus inferior. Off

Table 1.

Embryo number	1	2	3	4	5	6	7	8	5	10	11	12	13	14	15	16	17
body length (mm)	5.5	7.0	7.2	7.5	7.5	9.0	10.0	11.0		11.0	13.0	14.0	13.0	15.0	16.0	15.0	16.0
Haase's gestation-month	1	1	1	1	1	1	1	2		2	2	2	2	2	2	2	2
Kunitomo's gestation-week				3-5	3-5	3-5	3-5	3-5	30	3-5	6	6	6	6	6	6	6

18	19	20	21	22	23	24	25	26	27	28	29	30	31	32	33	34	35	36	37
19.0	16.5	18.0	17.3			32.0		24.0	25.5	27.0	28.0	36.0	53.0	120	260	300	310	390	450
2	2	2	2	2	2	2	2	2	2	2	2	2	3	4	6	6	7	8	10
6	6	6	6	6	6	9	10	10	10	10	10	10	10	15	22	25	26	32	37

Fig. 1. Embryos of 7.5mm length (middle part of the base of oculomotor muscles).

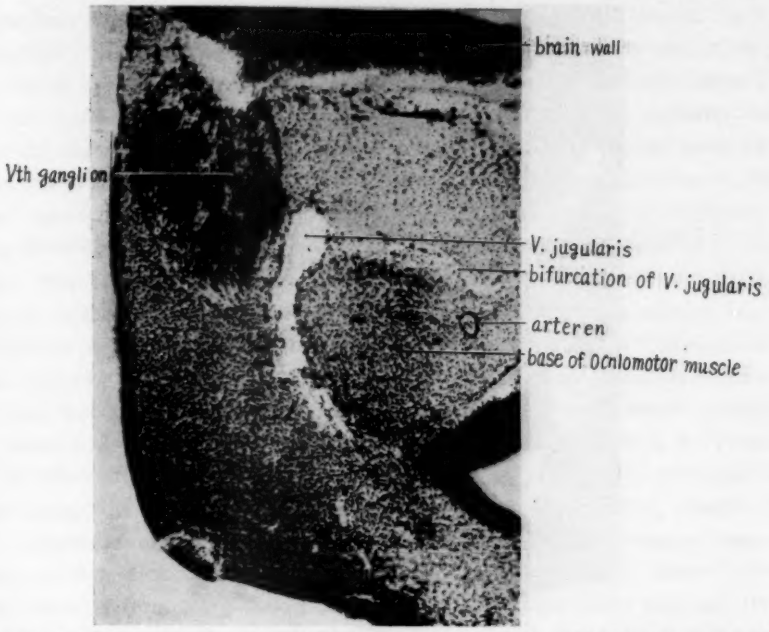

Fig. 2. Embryos of 7.5mm length (inferior part of the base of oculomotor muscles).

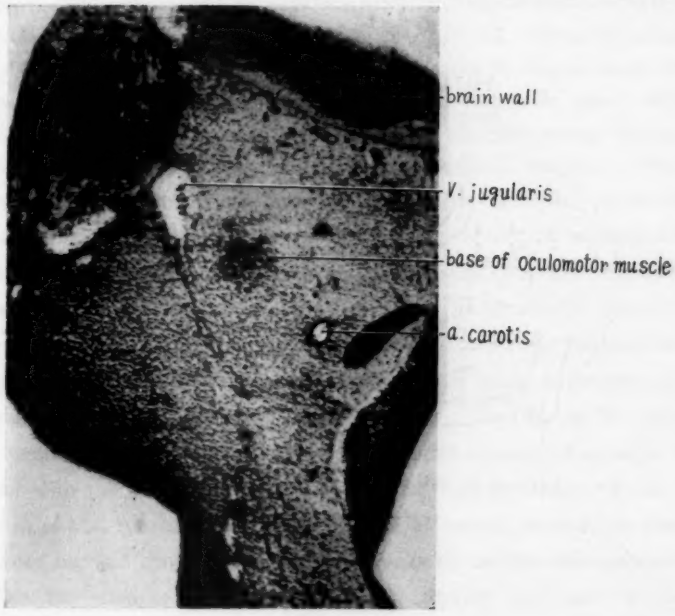

Fig. 3. Embryos of 7.5mm length.

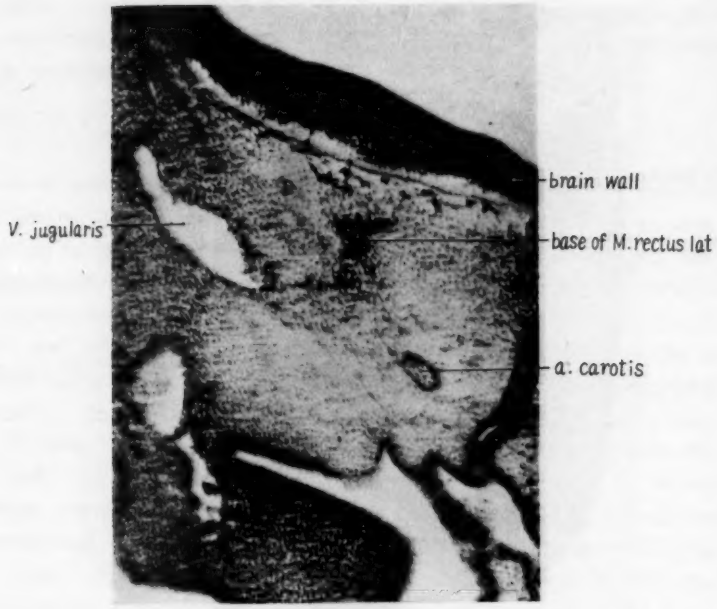

Fig. 4. Embryos of 16.5mm length.

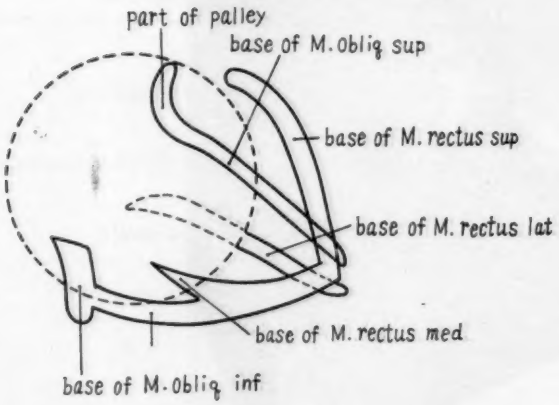

course the unclear part in the former can be pointed out as a narrow part in the dorsal side of the bulb in the upper part of the base of the oculomotor muscle in a 7.5 mm length embryo. The base of M. rectus superior begins in the upper end of the base of muscles which are under control of the oculomotor nerve and is noticed along the inner side of the ocular nerve on the dorsal side of the bulbus from the posterior side. In a 15 mm length embryo it apppears in crescent shape, extending from the posterior part of the lower pole of the bulbus passing over the upper part of the junction of the frontal nerve and nasolacrimal nerve and also the lower end of the base of M. obliquus superior is slightly more up than the upper end of the base of M. rectus superior. The lower part of the base of M. rectus superior ends at the height of the lower pole of the bulbus and conjunct to the common base of M. rectus medialis and M. rectus inferior. In a 16.5 mm length embryo it is already taking a particular position (Fig. 4). Distinct M. levator palpebrae superior is noticed along the inner side of origin of M. rectus superior and is noticed along the upper side of M. rectus superior in a 120 mm. length embryo. The common base of M. rectus medialis, lateralis and M. obliquus inferior in a 14 mm length embryo is closer to the lower end of the bulbus and extends forward, but the diffe- rentiation of the base of M. rectus medialis, M. rectus inferior and M. obliquus inferior is unclear. In a 15 mm length embryo the common base of those three present, in a stick shape, close to the inner side of the lower edge of the bulbus and its direction is from the posterior-external side to anterior-inner side and it's length is about 1000μ. The extending point is enlarged in an oval shape which is the base of M. obliquus inferior. The major axis of M. obliquus inferior in this period coincides with the major axis of M. rectus medialis and inferior. The base of M. obliquus inferior gradually develops to the external-anterior side and makes almost a 90 degree angle with the major axis of M. rectus in a 16.5 mm. length embryo. The length is about 560μ, the width about 270μ in the maximum part and shows almost a complete wedge shaped muscle. In a 25.5 mm. embryo it completely separates from M. rectus inferior. The base of M. rectus medialis in a 16.5 mm length embryo, the anterior half part makes the same angle with M. rectus inferior and separates slightly over the M. rectus inferior but the posterior half side, which constitutes the majority of the muscle, does not separate and stays as common base of M. rectus inferior and medialis. As gradually growth advances, it separates and moves, to the upper part and becomes completely independent in a 23 mm length embryo. The M. rectus medialis in this period is weak in general and lacks in good developed muscle cells compared with other muscles. The base of M. rectus inferior in a 16.5 mm. length embryo points to the anterior-inner side almost straight from its start and conjuncts, with the base of M. obliquus inferior, but the shape of the muscle in a 23 mm. embryo is also the same and the length of M. rectus inferior is about 900μ, but it is remarkably big and contains many more developed muscle cells compared with other muscles. With the advance of development, the anterior half part of the M. rectus

inferior gradually moves to the external-inferior side and in a 25.5 mm length embryo the whole shape is slightly bended and shows its peculiar figure. The base of the oculomotor nerve in a 7.5 mm embryo, begins from the middle of the anterior wall of the mesencephalon respectively, then runs to the inferior-external side and comes close about 300μ, to the upper end of the base of the oculomotor muscle in the inner side of the upper end of the trigeminus ganglion. In a 9 mm length embryo the nerve apparently goes out of the cerebral parenchym as many small fasiculas of fibers and gathers into one big nerve trunk (size about 40μ). The end penetrates into the base of the oculomotor muscle. It gets to the lower-ventral area of the base of the muscle in a 10 mm embryo. In a 11 mm embryo the ganglion cells in the origin become distinct and the nerve trunk also increase in size (the diameter is about 60μ in both eyes) remarkably. The course is also the same in a 14 mm embryo and runs along the inner side of the artery and gets to the dorsal side of the bulbus and then further runs downward and penetrates into the inferior base, getting close to the base of M. rectus superior. The branch of M. rectus superior is not yet seen. The branches of M. rectus superior, medialis, inferior and M. obliquus inferior become apparent in a 16.5 mm length embryo. In a 13,14 mm length embryo, the base of M. obliquus superior is seen on the upper-external side of the upper end of the base of the oculomotor muscle (base of M. rectus superior). It indicates a transverse elliptic shape (size about 1/5 of the bulbus) extending to the anterior-external side in the external side of the upper edge of the bulbus and ventral-ocular side of the upper edge of the frontal nerve. In a 15 mm embryo it extends to the ventral side in tape form with a width of about 150μ and length of about 520μ. The major axis makes an acute angle with the median plane and extends from the inferior-external side to the superior-internal side. The lower end of M. obliquus superior locates over the caput of M. rectus superior also in this embryo. In a 16.5 mm length embryo the lower end of the base gets to the inner side of the optic nerve and begins from the same part with M. rectus superior. The base of the trochlear part and tendon (reflected portion) is already seen (Fig. 4). The trochlear nerve is noticed in a 9-10 mm. length embryo. It begins from the dorsal side of the mesencephalon in the area slightly lower than the area where the oculomotor nerve begins and gets near to the upper edge of the bulbus, running anterior-interior as a weak fas icula of fibers (compared with M. oculomotor of this period). The size is about 26μ in both left and right. The course is also the same in a 11 mm. length embryo (the size of the nerve trunk is about 34μ). It descends along the vein and disappears almost in the middle area of the bulbus. A dense stained cell group is noticed near the end, but it cannot be decided whether this is the base of M. obliquus superior. The course in a 13 mm, 14 mm length embryo is also the same as in a 11 mm length embryo, but the apparent period, when the nerves penetrate into the muscle base is in a 14.15 mm size embryo. The time from the appearance of the trochlear nerve till the time when the nerve penetrates into the muscle base, is relatively long. In a 7.5 mm. length embryo, the base of M. rectus lateralis present independently near the ruhmboid

brain wall (Fig 3) inferio-posterior to the lower edge of oculomotor nerve. In a 9,10 mm length embryo, it persists together with the lower part of oculomotor muscle and the majority of the cell group, which extends inferior to M. rectus lateralis, faces to the dorsal side. In a 13 mm length embryo it becomes more thin and its upper and extends upward and gets slightly to the external side of the lower pole of the bulbus. In this period, inspite of no development of blasmomuscles in the other muscle bases, one can notice the obscure blasmomuscle in the lower part of the base of M. rectus lateralis. With the advance of development the whole muscle moves upward and locates on the external side of the bulbus. In a 16.5 mm length embryo it almost locate in the peculiar position of M. rectus lateralis. In a 9 mm length embryo, the base of the abducens nerve is noticed for the first time, running anterior-superior along the ventral side of the ruhmboid brain but does not to the base of M. rectus lateralis yet. In a 10 mm length embryo it gets ot the muscle base for the first time (the size of abducens nerve is 34μ on the right and 43μ on the left). In a 13 mm embryo it penetrates into the muscle base as a few fasiculas of fibers and one can notice an obscure blasmomuscle in the muscle base of the penetrated area. In general, the blasmomuscles of the respective muscle base first appear and develops near the penetrating areas of the controling nerves and extend and develop to posterior and anterior side. The oculomotor nerve is the biggest, compared with other ocular nerves and the abducens nerve is the second. The trochlear nerve is the thinnest. The respective nerves become large just before penetrating and penetrate into the muscle separating in fasiculas of nerve fibers like roots and branches of a tree. The size of the nerve in the penetrating area is bigger than the thickness of the respective muscle base at first but the respective muscle bases increase markedly and the ratio is in the reverse after the embryo's length of 25 mm..

The shape of the respective muscles in a 27 mm length embryo coincides with that of the adult.

The insertion line of the respective muscles in a 36 mm. length embryo presents itself as a simple cell group but becomes distinct in a 53 mm length embryo. The muscle fibers are noticed slightly in a part from the center of the muscle to the posterior area in a 27 and 28 mm length embryo and are noticed on the whole muscle in a 36 mm length embryo. In a 53 mm length embryo the number of muscle fibers increase remarkably together with the individual size (size 4-5μ). The nucleus of the muscle occupies the whole width of the muscle fiber in a 120 mm length embryo and gradually moves to the lateral side and is omnipresent in the lateral side in a 26 mm embryo. The transversal crest of the muscle appears for the first time in a respective muscle in a 30 cm, 31 cm length embryo and generally the muscle fibers which developed the transversal crest are bigger than those which did not develop. In this period the transversal crest is only present in few muscle fibers near the penetrating area of the controling nerve or its origin but develops generally into a whole muscle in a 39-45 cm size embryo. Further in this period, the muscle fibers are big in the middle (about 10μ) thin in the origin and

insertion line (about 4μ), and the whole muscle is in spindle form. In general the histological findings are similar to that of the adult.

Discussion

It is said that the base of the oculomotor muscle in low vertebrates develops from the 1st scolex (or premandibular condensation) connecting the lateral side of the prechordal plate and is also called Plechordal plate 〔acanthias, domestic fowls (Adelmann), turtle (Johnson), domestic fowl (Furuichi), Interepithelial cell mass (gull (Rex)), Praeorales Darmrudiment (dog (Bonnet) 〕etc.. Edgeworth also studied dog's embryo and obtained similar results as Bonnet.

In our specimen, no apparent prechordal plate was noticed, but in a 7.0–7.5 mm length embryo, on the upper-external side from the terminal part of the chorda there is a group of cells close to the laryngeal wall and its upper end extends to the dorsal side of the base of the hypophysis. This group of cells is slightly obscure, but considering from the point that it contacts to base of the oculomotor muscle present in its lateral side it may be permitted to be considered as a cell group of the prechordal plate. Therefore the base of the oculomotor nerve of the human embryo develops on the external side of the prechordal plate similar to other animals.

Concernig the relation between the base of the ocular muscle, and the head cavity, there is a 1st, 2nd and 3rd head cavity in acanthias (Lamb), gull (Rex), turtle (Johnson), snake (de Beer) etc.. The base of the oculomotor muscle, M. obliquus superior, M. rectus lateralis develops from the lateral wall respectively. It is said, that the head cavity is only in the base of the ocular muscle in amia (de Beer), domestic fowl (Adelmann, Furuichi) and lacks in the guinea pig, rabbit, dog (Leser), rabbit (Edgeworth, Bonnet), dog (Bonnet) and the human (Lewis). It also lacked in the human embryo in this study.

With respect to the shape of the base of the ocular muscles Reuter said, it presents the shape of a tall wine cup (6 mm. pig embryo) and Lewis said it presents a lens shape (7 mm. human embrpo).

In a 7–7.5 mm human embryo obtained for this study, the upper and lower (dorsal and ventral) end is thin, middle slightly big, and the horizontal section was almost round.

Concerning the development number of the base of extra-ocular muscles it is said, that they develop from 1) Only one base in the 〔gull (Rex), pig(Reuter, Keil), guinea pig, rabbit, dog (Leser), human (Lewis)〕etc..

2) Two independent bases 〔ammocoete (Kupffer), domestic fowl (Adelmann, Furuichi)〕etc. 3) Three independent bases 〔acanthias (Marschall, Wijhe, Lamb, Adelmann), amia (de Beer), turtle (Johnson), snakes (de Beer), rabbit (Edgeworth)〕. It is open to doubt to say whether the base of the ocular muscles is one (Leser) or three (Edgeworth) in the same animal (rabbit). In the human embryo in this study the respective ocular muscle developed from three independent bases of M. oculomotorius, M.

obliquus superior and M. rectus lateralis. There are Leser (guinea pig, rabbit, dog), Lewis (human), Reuter, Keil (pig) etc, who mention, that the M. obliquus superior and M. rectus lateralis develop from one common base. From this study in human embryo the base of M. obliquus superior is noticed as a short elliptic shape of a cell group size of about 1/5 of the bulbus, on the posterior external upper side of the bulbus in a 13-14 mm size embryo. The frontal nerve is seen just on the external side. The base of the M. rectus lateralis is noticed in a 7.5 mm embryo and both are completely independant. Lewis has recognized one base as the common base of the whole ocular muscles in the human embryo and it is probably the base of the oculomotor muscle and has missed the base of M. rectus lateralis and M. obliquus superior.

Conclusion

1 The base of the oculomotor muscles grows at the posterior, superior and external side of the bulbus in a 7-7.5 mm length embryo. It is divided into 2 parts. One is a common base of the M. rectus superior and M. levator palpebrae superior. The other is the common base of the M. rectus medialis, M. rectus inferior and M. obliquus inferior.

2. The base of M. rectus superior is discriminated in a 7.5 mm length embryo. In a 16.5 mm length embryo, it already occupies a particular position of the muscle. The base of M. levator palpebrae superior is clearly observed inside of M. rectus superior in a 53 mm length embryo and in a superior part in a 120 mm length embryo.

3. M. rectus medialis begins to separate from M. rectus inferior in a 16.5 mm length embryo. It shifts gradually to the superior part and separates completely from M. rectus inferior in a 23 mm length embryo, then, occupies a particular position of the muscle. M. obliquus inferior is observed on the thickened part at the anterior and medial edge of the base of M. rectus inferior in a 15 mm length embryo and gradually develops to the anterior-external side. In a 25.5 mm length embryo, it occupies a particular position of the muscle.

4. The base of the oculomotor nerve is observed at the superior part of the base of the oculomoton muscles in a 7.5 mm length embryo. It reaches the base of the muscles in a 9 mm length embryo. In a 16.5 mm length embryo, the branches of nerves are clearly observed, advancing into M. rectus superior, medialis and inferior.

5. The base of M. obliquus superior grows at the posterior and superior part of the bulbus in a 13-14 mm length embryo. It becomes slender in a 15 mm length embryo. In a 16.5 mm length embryo, the direct portion, reflected portion and trochlea are observed. And the form of the muscle is almost accomplished.

6. The base of the trochlear nerve is observed in a 9 mm length embryo. It reaches to M. obliquus superior in a 15 mm length embryo.

7. The base of M. rectus lateralis grows at the adjacent part of the cerebral wall of the ruhmboid brain, inferior to the base of the oculomotor muscles. The muscle shifts to the external side of the bulbus with growth. In a 16.5 mm length embryo, it occupies

a particular position of the muscle.

8. N. abducens closely approaches M. rectus lateralis in a 9 mm. length embryo. It reaches the muscle in a 10 mm length embryo.

9. Annulus tendneus communis at the beginning of the oculomotor muscles is observed at first in a 16.5 mm length embryo. It is observed clearly in a 27 mm length embryo. The insertion line becomes clear in a 35 mm length embryo.

10. The blastomuscle of extra-ocular muscles appears most fastly in M. rectus lateralis (14 mm length embryo). Shortly after, they appear in all other extra-oculomotor muscles (15 mm. length embryo). The fibers of the muscle appear at first in a 27 mm length embryo. Transversal crests of muscle are observed in embryos grown more than to 300 mm length.

11. The cavity of the head seen in the lower vertebrates lacks in human embryo. Extra-ocular muscles grow as 3 independent bases, bases of oculomotor muscles, the base of M. obliquus superior and the base of M. rectus lateralis. Therefore, if the discription which has been reported up to now is right, from the view of numbers of bases of extra-ocular muscles the human does not belong to the high vertebrates (pig, spermophile, dog etc) but belonges to low vertebrates (acanthias, amia, chylydra, hetrodont etc).

(Published in Acta Ophthalm. Jap. 62:2584, 1958 in Japanese.)

REFERENCES

1) Adelmann, H.B.: Am. J. Anat. 31:55-101, 1922.
2) de Beer, G.R.: Quart. J. Mic. Sci. 68:17, 1924.
3) Bonnet, R.: Anat. Heft, 1 abt, Heft, 51, 16 Bd. 231-332, 1901.
4) Edgeworth, F.H.: Quart. J. Mic. Sci. 56:167, 1911.
5) Edgeworth, F.H.: Quart. J. Mic. Sci. 56:511, 1907.
6) Furuichi, G.: Igaku-Kenkyuu 22:146, 1952.
7) Johnson, C.E.: Am. J. Anat. 14:119, 1913.
8) Keil, R.: Anat. Heft, 1 Abt, 96 Heft. Bd. 32, 1-87, 1907.
9) Lamb, A.B.: Am. J. Anat. 1:185, 1902.
10) Leser, O.: Brit. J. Ophth. 6:111, 1925.
11) Reuter, K.: Anat. Heft. Bd. 9, 365-387, 1897.

Foremost Pharmaceutical Manufacturer in Japan

SANKYO CO., LTD.

Established in 1913

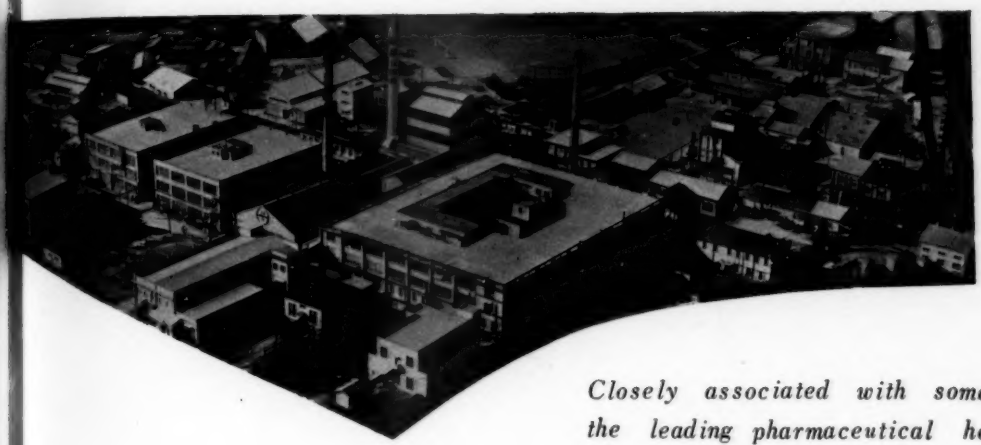

Closely associated with some of the leading pharmaceutical houses in America and Europe.

SANKYO

The products include:

- ★ ANTIBIOTICS
- ★ VITAMINS
- ★ HORMONES
- ★ SULFA DRUGS
- ★ ANTITUBERCULOUS AGENTS and MANY OTHER DRUGS and PHARMACEUTICALS
- ★ AGRICULTURAL CHEMICALS

Head Office; No. 1 Ginza 2-Chome, Chuo-ku, Tokyo.
Branches; Principal cities in Japan